



**UNIVERSITÀ DEGLI STUDI DI PARMA**

Dipartimento di Chimica ed Organica Industriale

Ph.D. in Science and Technology of Innovative  
Materials XXIII Cycle

**Cavitand receptors for  
chiral recognition and  
fluorescent sensing**

Francesca Maffei

Coordinator: **Prof. Anna Painelli**

Supervisor: **Prof. Enrico Dalcanale**

Author: **Francesca Maffei**

# Contents

## CHAPTER 1

### **General Introduction: cavitand based supramolecular sensors**

1.1. Chemical sensors.....	1
1.2. Cavitand as supramolecular receptors.....	4
1.2.1. Phosphonate bridged cavitands.....	5
1.2.2. Quinoxaline bridged cavitands.....	7
1.3. Quartz crystal microbalance transducers.....	8
1.4. Fluorescent chemical sensors.....	11
1.5. References.....	15

## CHAPTER 2

### **Highly selective chemical vapour sensing via molecular recognition: specific C<sub>1</sub>-C<sub>4</sub> alcohols detection with a fluorescent phosphonate cavitand**

2.1. Introduction.....	17
2.2. Design and synthesis of the target fluorescent receptor .....	18
2.3. Fluorescent measurements .....	25
2.4. Conclusions.....	28
2.5. Acknowledgements.....	29
2.6. Experimental section.....	29
2.7. References.....	36

## CHAPTER 3

### **Selective methanol detection: synthesis of a new sterically hindered fluorescent cavitand**

3.1. Introduction.....	37
3.2. Synthesis of the new target fluorescent cavitand.....	38
3.3. Fluorescent measurements in solution.....	41
3.4. Sensor measurements.....	43
3.5. Conclusions.....	45
3.6. Acknowledgements.....	45
3.7. Experimental section.....	45
3.8. References.....	51

## CHAPTER 4

### **Inherently chiral phosphonate cavitands as enantioselective receptors for chiral alcohols and L-amino acids**

4.1. Introduction.....	53
4.2. Synthesis of the receptor .....	56
4.3. Evaluation of (AB) <sub>2</sub> PO <sub>ii</sub> 1PS <sub>i</sub> Me enantioselective recognition properties in the solid state .....	61
4.4. Synthesis of a new target receptor.....	64
4.5. Evaluation of (AB) <sub>2</sub> PO <sub>ii</sub> 1PS <sub>i</sub> Me enantioselective recognition properties in solution toward N-methyl amino acids.....	68
4.6. Conclusions.....	71
4.7. Acknowledgements.....	72
4.8. Experimental section.....	72
4.9. References.....	79

## CHAPTER 5

### **Quinoxaline bridged cavitand as molecular receptors for nitroaromatic explosives**

5.1. Introduction.....	81
5.2. Quinoxaline bridged cavitands.....	83
5.3. Extraction capabilities of 3QxCOOH cavitands towards nitroaromatic compounds.....	88
5.4. Conclusions.....	92
5.5. Acknowledgements.....	92
5.6. Experimental section.....	93
5.7. References.....	100

## CHAPTER 6

### **Active metal template synthesis of hard-to-access mechanically interlocked molecules**

6.1. Introduction.....	103
6.2. Active metal template synthesis of interlocked molecules .....	105
6.3. Introduction to hydrocarbon interlocked molecules.....	107
6.4. Design and synthesis of a hydrocarbon [2]rotaxane.....	109
6.5. Synthesis of the target hydrocarbon [2]rotaxane.....	118
6.6. Conclusions.....	121
6.7. Acknowledgements.....	121
6.8 Experimental section.....	121
6.9. References.....	129

## **APPENDIX A**

Materials and Methods.....	143
----------------------------	-----

## **APPENDIX B**

X-Ray Data Analysis .....	144
---------------------------	-----

<b>The author</b> .....	159
-------------------------	-----

# General introduction: cavitand based supramolecular sensors

1

## *1.1 Chemical sensors*

In the last few years there has been a huge demand to monitor different chemical environments, such as for example urban indoor and outdoor atmospheres, food aromas, explosives, etc. Chemical sensors are among the most promising devices to be exploited for these applications because they have the great advantage to allow an online measure suitable to remote control.<sup>1</sup>

Following the definition given by IUPAC, a chemical sensor is a device that transforms chemical information, ranging from the concentration of a specific sample component to total composition analysis, into an analytically useful signal.<sup>2</sup>

Chemical sensing is part of an acquisition process in which some informations on the chemical composition of a system are obtained in real time. The acquisition process consists of two distinct steps: *recognition* and *amplification*. On this basis the structure of a generic chemical sensor can be ideally divided in two subunits: the sensing material and the transducer. The sensing material, responsible for *recognition*, interacts with target analyte, while the transducer, responsible for *amplification*, transforms these recognition process in a readable signal (Figure 1.1).

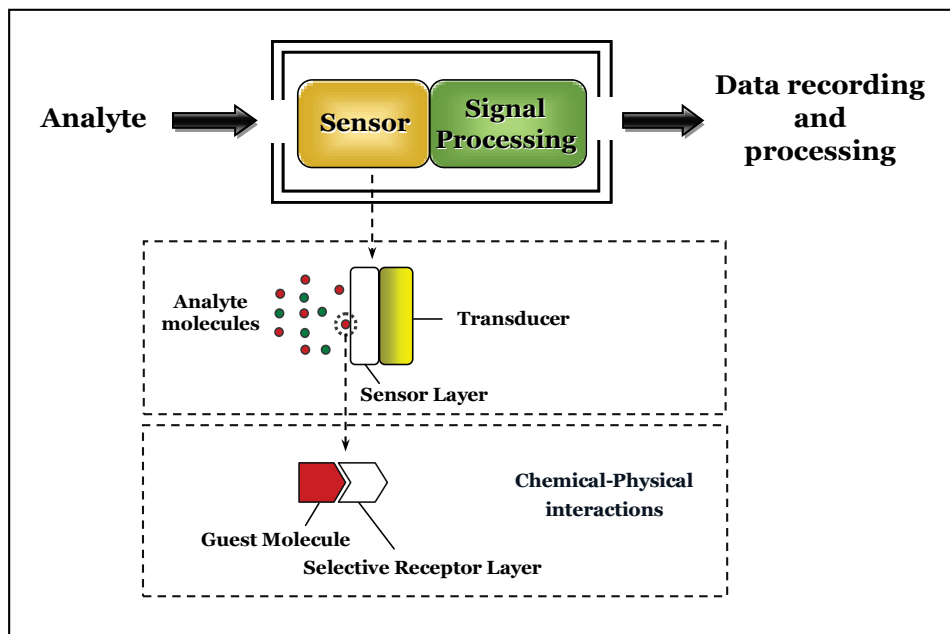


**Figure 1.1.** The chemical sensing process.

The ideal chemical sensor should have the following properties: high *sensitivity*, high *selectivity* or, even better, specificity to a target analyte, low *cross-sensitivity* to interferences and perfect reversibility.<sup>3</sup>

*Sensitivity* can be generally defined as the slope of the analytical calibration curve, that is correlated with the magnitude of the change in the sensor signal upon a certain change in the analyte concentration.<sup>4</sup> “Cross sensitivity” hence refers to the contributions of other than the desired compound to the overall sensor response.

*Selectivity* is instead the ability of a sensor to respond primarily to only one chemical species in the presence of other species (usually denoted interferences).

The quest for better selectivity remains the cornerstone of the chemical sensing research:<sup>5</sup> it can be achieved by using biosensors (e.g. biologically derived selectivity by appropriate enzymes, structure-binding relationship in antibody-antigen complexes,) or by synthesizing materials containing specific binding sites.



*Reversibility* describes the sensor's ability to return to its initial state after it has been exposed to chemical species. The reversibility requires the involvement of weak interactions, since the formation of covalent or ionic bonds would result in an irreversible saturation of the layer.<sup>6</sup>

Sensor sensitivity, selectivity, speed of response, and reversibility are determined by the thermodynamics and kinetics of sensor material/analyte interactions. In particular, high sensitivity and specificity on the one hand and perfect reversibility on the other hand impose contradictory constraints on the sensor design: high sensitivity and selectivity are typically associated with strong interactions, whereas perfect reversibility requires weak interactions, being the limit of reversibility at room temperature in the 80 kJ mol<sup>-1</sup> range.<sup>6</sup> Consequently, it is necessary to find a compromise, and, in most cases, sensors showing partial selectivity to only some of the detected species are used to ensure reversibility.

Conventional approaches for selective chemical sensors have traditionally made using a “lock-and-key” design (a steric fit concept enunciated for the first time by Emil Fischer in 1894),<sup>7</sup> wherein a specific receptor is synthesized in order to bind selectively the analyte of interest.<sup>8</sup> Indeed, to achieve this specificity, biological systems exploit molecular recognition between two species that complement one another in size, shape and functionality. As for biological systems, the concepts of shape recognition and binding site complementarity are central for effective molecular recognition in artificial host-guest systems. This selectivity mechanism is particularly useful in the development of chemical sensors, whereas the recognition process can be translated into an analytical signal.

The “lock and key” approach, so successful in the liquid phase, cannot be automatically transferred to vapour and gas sensing due to two major hurdles:

- in moving from the vapour to the condensed phase the analyte experiences a dramatic increase in nonspecific dispersion interactions, negligible in liquid to solid transfer;<sup>9</sup>
- the entropic cost for binding to the receptor is not alleviated by solvent release in the bulk liquid phase.<sup>10</sup>

For these reasons achieving effective molecular recognition at the gas-solid interface is a demanding task, which requires a fresh approach, both in terms of receptor design and characterization tools.

## 1.2 Cavitant as supramolecular receptors

Supramolecular chemistry may be defined as “chemistry beyond the molecule” bearing on the organized entities of higher complexity that result from the association of two or more chemical species held together by intermolecular forces. Its development requires the use of all resources of molecular chemistry combined with the designed manipulation of noncovalent interactions.<sup>11</sup>

The selective binding of a neutral substrate by a molecular receptor to form a complex involves molecular recognition, which is based on shape complementarity and the presence of specific weak interactions such as hydrogen bonding,<sup>12</sup>  $\pi$ - $\pi$  stacking,<sup>13</sup> and CH- $\pi$  interactions.<sup>14</sup>

Cavitants defined as synthetic organic compounds having enforced cavities of molecular dimensions are particularly interesting and versatile molecular receptors.<sup>15</sup> The complexation properties of these molecule have been extensively studied in the solid state,<sup>16</sup> in solution,<sup>17</sup> and in the gas phase.<sup>18</sup>

In the design of cavitants (Figure 1.2) the choice of the bridging groups connecting the phenolic hydroxyls of the resorcinarene scaffold is pivotal, since it determines shape, dimensions and complexation properties of the resulting cavity.

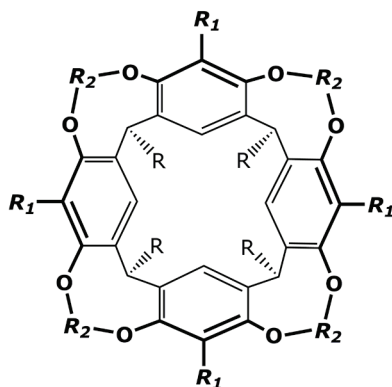


**Figure 1.2.** General structure of a cavitant receptor.

### 1.2.1 Phosphonate-bridged cavitands

Phosphorous groups play an important role in host-guest chemistry and the properties of the phosphoryl (P=O) and thiophosphoryl (P=S) moieties to bind neutral and cationic species have been investigated. Because of their binding capabilities, these groups have been included in preorganized structures to enhance the complexation properties of cavitands.

In particular, much attention is currently devoted to the phosphorous derivative of resorcin[4]arenes, which have opened the route to promising preorganized hosts.<sup>19</sup> The main specific interactions responsible for recognition evidenced by these studies are H-bonding, CH- $\pi$ , and cation-dipole interactions.

Phosphonate cavitands,<sup>20</sup> presenting one to four H-bonding acceptor P=O groups at the upper rim of the cavity, are particularly appealing for the complexation of molecules capable of H-bonding.

The presence of P(V) stereocenters brings configurational properties into play, since the relative orientation of the P=O groups with respect to the cavity determines the number of possible stereoisomers. In the case of tetrabridged phosphonate cavitands the presence of four stereogenic centers gives rise to six possible diastomeric cavitands. The inward (i) and outward (o) configurations are defined relative to the different orientation of the P=O moieties. A clear and exhaustive nomenclature for P(V) bridged cavitands has been proposed by our group.<sup>20</sup> It summarizes in a single acronym number and relative position of P(V) bridges, their stereochemistry, type of substituents respectively at the lower rim, at the apical positions and on the phosphorus bridges. Figure 1.3 reports a survey of all structures discussed in this thesis with their acronym below. The first capital letters define number and position of bridges, the second lower case letters define the in-out stereochemistry at each P(V) center, R<sub>1</sub>, R<sub>2</sub> and R<sub>3</sub> in brackets define respectively the substituents at the lower rim, in the apical positions and on the P(V) stereocenters.

To ensure strong binding, the cavity should contain binding sites preorganized for interaction with guest, and the all inward stereoisomer appears to have a prerequisite for good recognition properties toward cationic and neutral species.

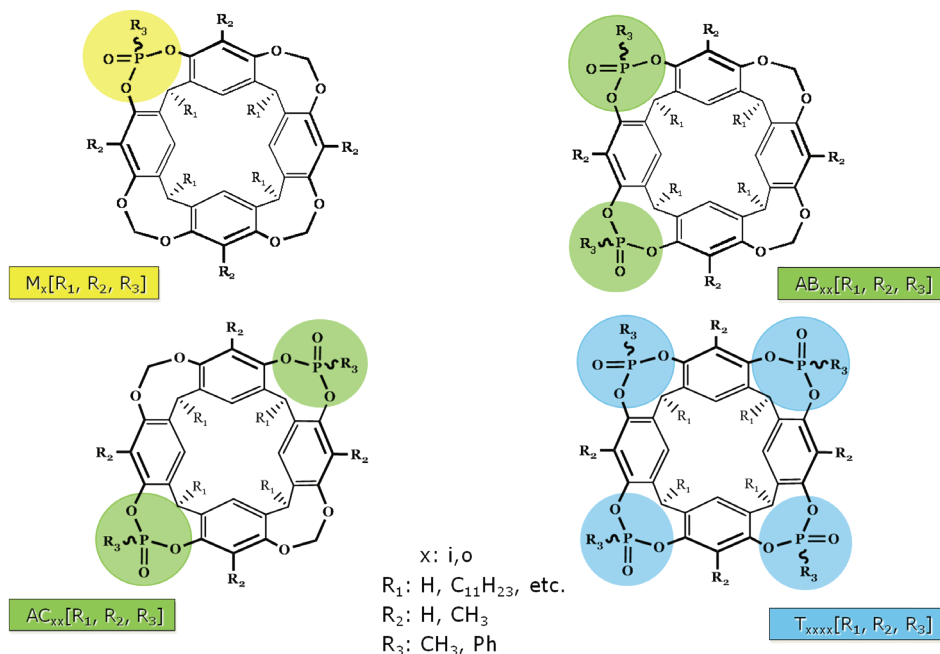
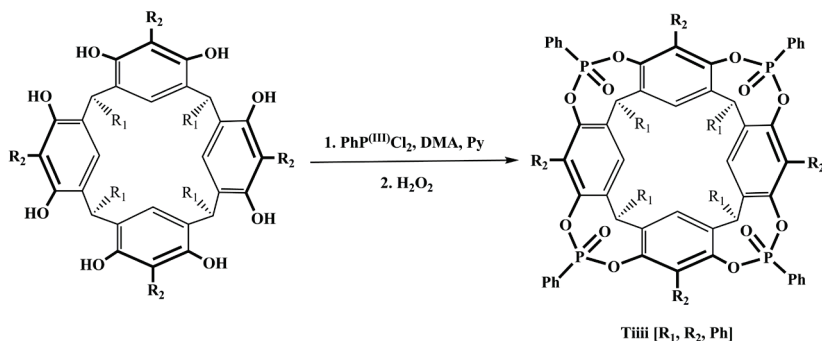


**Figure 1.3.** Phosphonate cavitands nomenclature.

Our group has recently performed a new method to achieve only pure  $T_{iiii}$  with high yields.<sup>21</sup> Reaction of resorcin[4]arene with dichlorophenylphosphine in the presence of pyridine afford exclusively the  $4P^{(III)}$ iiii cavitand. Its subsequent *in situ* oxidation with  $H_2O_2$ , proceeds with retention of configuration at the phosphorous centre and leads to the  $T_{iiii}$  isomer in only one step, without need of purification (Scheme 1.1).



**Scheme 1.1.** Synthesis of tetraphosphonate cavitands.

### 1.2.2 Quinoxaline-bridged cavitands

The cavity of resorcinarenes can be largely extended by bridging phenolic hydroxyl groups with aromatic spacers.<sup>22</sup> Tetraquinoxaline cavitands result from nucleophilic aromatic substitution with 2,3-dichloroquinoxaline on the phenolic oxydryl moieties of a resorcin[4]arene.

A particularly interesting properties of these systems is the reversible switching between a closed “vase” conformation with a deep cavity for guest complexation, and an open “kite” conformation with a flat extended surface.<sup>23</sup> Indeed the quinoxaline spacers can occupy either axial (a) or equatorial (e) positions (Figure 1.4). In the “vase” (aaaa) conformer, the spacers touch each other via their  $\alpha$ -hydrogens while forming a box like cavity with  $C_{4v}$  symmetry which is approximately 7 Å wide and 8 Å deep.<sup>24</sup> The cavity is open at the top and closed at the bottom by the cavitand itself. In the “kite” (eeee) conformer, the spacers are more or less in the same plane ( $C_{2v}$  symmetry). Conformational switching can be reversibly induced by temperature or pH changes, with the “kite” conformation being preferred at low temperatures and low pH values, or by metal-ion addition.

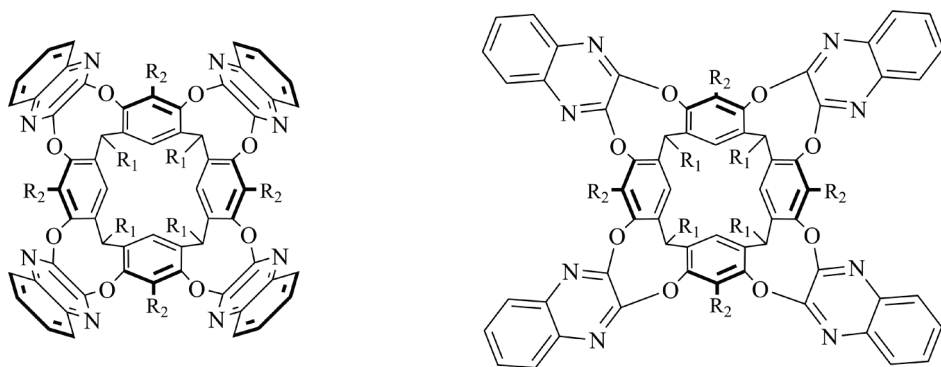


**Figure 1.4.** Structure of quinoxaline cavitand aaaa conformer (left) and eeee conformer (right).

In contrast, in mixed-bridged cavitands with one of the four quinoxaline wings displaced by a different bridge, the thermal vase-to-kite interconversion is switched off by substantially decreasing the solvation of the kite form. Mixed-

bridged cavitands can only adopt the kite conformation by protonation of the quinoxaline nitrogen atoms with an acid such as TFA, as a result of the developing Coulombic repulsion in the vase geometry.

Tetraquinoxaline cavitand, in the vase conformation, forms inclusion complexes in the solid state with neutral molecules like acetone and dichloromethane, but preferentially binds aromatic guests, with binding constants up to  $200 \text{ M}^{-1}$  for 4-(dimethylamino)nitrobenzene in acetone. This value is considerably higher than those observed for other aromatic guests, like benzene and toluene, because of strong dipole-dipole interaction between host and opposite-directed guest in addition to  $\pi$ - $\pi$  interaction.

### ***1.3 Quartz Crystal Microbalance transducers***

Acoustic wave (AW) transducers are the workhorse of supramolecular sensing of gases, because they do not require receptor derivatization for their operation modes, like fluorescent probes for optical sensing. They measure the mass uptake of a sensing layer when exposed to vapours. Usually AW sensors consist of a piezoelectric quartz crystal with electrodes affixed to each side of the plate. When an oscillating potential is applied at a frequency near the resonant frequency of the piezoelectric crystal, a stable oscillating circuit is formed. The key feature of AW sensors is that the frequency and the amplitude of the acoustic wave is affected by a mass change of the system. The Sauerbrey equation describes the resonant frequency shift of an acoustic resonator upon mass increase on its surface.<sup>8</sup>

$$\Delta f = -2f_0^2 \cdot \Delta m \cdot A^{-1} \cdot \sqrt{c/\rho}$$

In the equation  $f_0$  (Hz) is the fundamental frequency of the quartz crystal,  $\Delta f$  (Hz) is the frequency shift proportional to the deposited mass  $\Delta m$  (g),  $A$  ( $\text{m}^2$ ) is the area of quartz plate or electrode surface,  $c$  ( $\text{s}^2\text{m/g}$ ) is the elastic coefficient of the system and  $\rho$  ( $\text{g/m}^3$ ) represents the crystal density.

The Sauerbrey Equation expresses in an adequate manner the real trend for a material in which the frequency shift induced by the coating deposition is lower than 3% of the quartz crystal fundamental frequency. Moreover, it does not

work for thick films, viscous liquid, elastic solids and viscoelastic bodies for which special theoretical models have to be applied to account for the observed frequency shift and impedance spectra.<sup>25</sup>

On the other hand, it implies the assumption that the deposited coating film has an uniform thickness across the entire active region of the resonator and that the frequency shift, resulting from a mass deposited at some radial distance from the centre of the crystal, will be the same regardless of the radial distance.

The more widely applied mass sensors based on this principle are quartz crystal microbalance (QCM) resonators (Figure 1.5). In QCM, the acoustic wave propagates through the bulk of the system in a direction normal to the surface. Therefore thickness and permeability of the layer are critical features. The higher the frequency of the resonator, the less coating must be applied to avoid a quenching of the oscillation: in this sense a resonant frequency of 20 MHz is usually the limit for a typical QCM resonator. The maximum layer thickness depends on the transducer design, the operating frequency of the device, the applied analyte concentrations and the coating nature. As a rule of thumb, the upper limit for the thickness,  $d$ , of viscoelastic acoustically thin films was given as  $d \ll (G/f \nu \rho)$  where  $G$  is the shear modulus of the coating layer,  $\nu$  is the SAW velocity (3.16 Km/s for quartz material),  $\rho$  is the film density and  $f$  is the fundamental oscillation frequency.<sup>26</sup>

The acoustic wave produces surface particle displacements that are parallel to the surface.

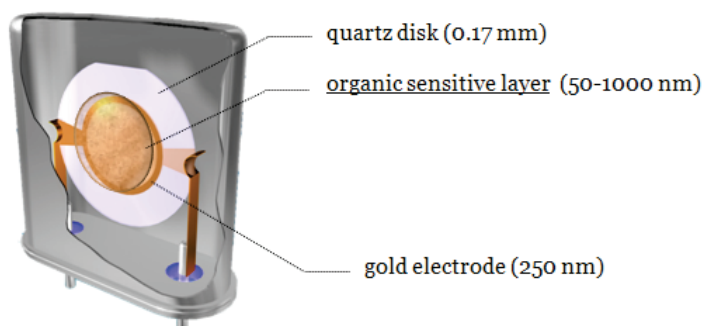


**Figure 1.5.** QCM transducers.

By integrating a QCM measurement platform with a selective sensing layer, a chemical sensor is constructed, in which molecular recognition events are converted into an electric signal.

It must be emphasized that the QCM transducer is totally unspecific, since it does not make any difference whether the interaction takes place in the molecular recognition site or elsewhere in the layer. The key issue of assessing specific host-guest interactions versus non specific adsorption in solid receptor layers has been addressed using adsorption isotherms. Linear adsorption isotherms are typical of non specific physisorption processes, following Henry's law (Figure 1.6, black trace); Langmuir-type isotherms, which deviate significantly from linearity, indicate specific analyte/layer interactions, particularly at low concentrations (Figure 1.6, red trace). At higher concentrations, when the available receptor sites are saturated, the isotherms flattens out returning to the non specific regime. The overall trend for a truly selective layer in a wide analyte concentration range is shown in Figure 1.6, blue trace.<sup>27</sup>

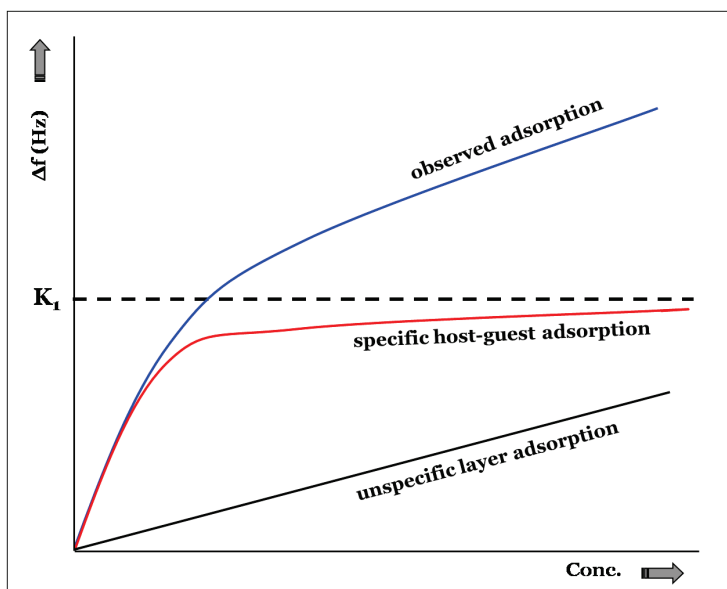


**Figure 1.6.** Theoretical isotherms for specific and non specific analyte adsorption on solid receptor layer in mass sensors.



Reliable measurements require the comparison of the acquired isotherms with the ones relative to those of known non specific layers in the presence of the same analytes and/or with those relative to the same receptor layer exposed to unsuitable guests.

### ***1.4 Fluorescent chemical sensors***

The main issue in the design of any effective chemosensor is the association of a selective molecular recognition event with a physical signal highly sensitive to its occurrence.

Among the different chemical sensors, fluorescent based ones present many advantages: fluorescence measurements are usually very sensitive (even single molecule detection is possible, although only under special condition), of low cost, easily performed, and versatile.<sup>28</sup> The versatility of fluorescence-based sensors originates also from the wide number of parameters that can be tuned in order to optimize the convenient signal. Even very complex analytical problems can be indeed overcome by controlling the excitation and emission wavelengths, the time window of signal collection, and the polarization of the excitation beam or the emitted light. In most cases luminescence intensity changes represent the most directly detectable response to target recognition; more recently, however, other proprieties such as excited state lifetime and fluorescent anisotropy have also been chosen as diagnostic parameters, since they are less affected by the environmental and experimental conditions.<sup>29</sup>

In these sensors the receptor is required for selective binding of the substrate, while the fluorophore provides the means of signaling this binding, whether by fluorescent enhancement or inhibition. In the simplest cases, emission of a photon, fluorescence, follows HOMO to LUMO excitation of an electron in a molecule. Where this emission is efficient, the molecule may be termed a fluorophore. Vibrational deactivation of the excited state prior to emission usually gives rise to a “Stokes shift” in that the wavelength of the emitted radiation is less than that of the exciting radiation. Various other interactions may also modify the emission process, and these are of considerable importance in regard to analytical applications of fluorescence.<sup>30</sup>

Mechanisms which control the response of a fluorophore to substrate binding include photoinduced electron transfer (PET),<sup>31</sup> photoinduced charge transfer (PCT),<sup>30</sup> Fluorescence (Förster) resonance energy transfer (FRET),<sup>30</sup> and excimer/exciple formation or extinction.<sup>30</sup>

In a PET sensor, upon excitation of the fluorophore, one of its electron in the highest occupied molecular orbital (HOMO) is promoted to the lowest unoccupied molecular orbital (LUMO). This promotion enables photoinduced electron transfer from the HOMO of the donor to that of the fluorophore and causes fluorescent quenching of the latter. Upon analyte binding the relevant HOMO of the donor becomes lower in energy than that of the fluorophore.

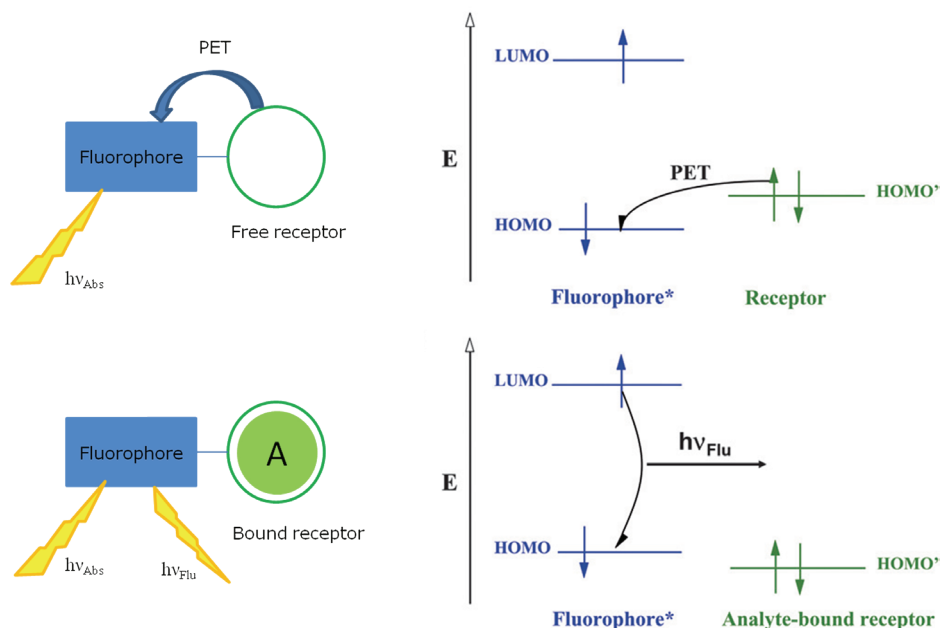


**Figure 1.7.** Mechanism for PET

Consequently PET is not possible anymore and fluorescent quenching is suppressed, in other words, fluorescent intensity is enhanced upon analyte binding (Figure 1.7).<sup>31</sup>

In a PCT (Figure 1.8) sensor the fluorophore contains an electron- donating group such as an amino group, conjugated to an electron-withdrawing one.

Electronic excitation necessarily involves some degree of charge transfer, but in fluorophores containing both electron-withdrawing and electron-donating substituents, this charge transfer may occur over long distances and be associated with major dipole moment changes, making the process particularly sensitive to the microenvironment of the fluorophore. Thus, it can be expected that analytes in close interaction with the donor or the acceptor moiety will change the photophysical properties of the fluorophore.<sup>30</sup>

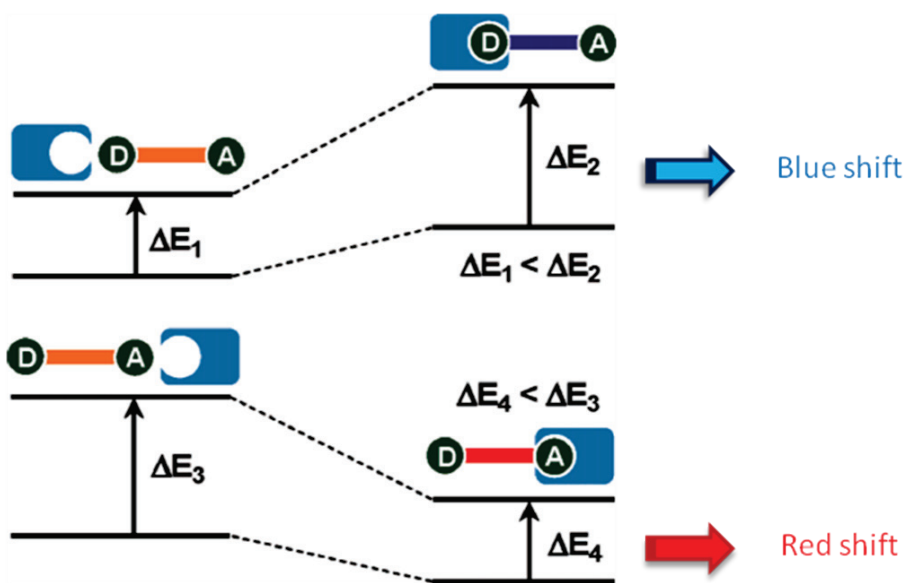


*Figure 1.8. PCT process*

Upon, for example, analyte complexation of an electron donor group within a fluorophore, the electron-donating character of the donor group will be reduced. The resulting reduction of conjugation causes a blue shift of the absorption spectrum together with a decrease of the molar absorptivity. In contrast, analyte binding to the acceptor group enhances its electron withdrawing character, and the absorption spectrum is thus red-shifted with an increase in molar absorptivity. The fluorescence spectra should be shifted in the same direction as the absorption spectra, and in addition to these shifts, changes in the quantum yields and lifetimes can be observed.

All this photophysical effects are obviously dependent on the characteristics of the analyte, and therefore, an higher selectivity is expected compared to QCM transducers.

---

## 1.5 References

- <sup>1</sup> W. Göpel, K.D. Schierbaum, *Sensors*; Eds.: W. Göpel, T.A. Jones, M. Kleitz, J. Lundstrom, T. Seiyama, Wiley-VCH: Weinheim, **1991**; Vol. 2.
- <sup>2</sup> A. Hulanicki, S. Glab, and F. Ingman, *Pure Appl. Chem.* **1991**, *63*, 1247.
- <sup>3</sup> H. Hierlemann, R. Gutierrez-Osuna, *Chem. Rev.* **2008**, *108*, 563 and references cited therein.
- <sup>4</sup> A. D'Amico, C. Di Natale, *IEEE Sensors Journal*, **2001**, *1*, 183.
- <sup>5</sup> J. Janata, M. Josowicz, *Anal. Chem.* **1998**, *70*, 179.
- <sup>6</sup> A. Hierlemann, A.J. Ricco, K. Bodenhöfer, W. Göpel, *Anal. Chem.* **1999**, *71*, 3022.
- <sup>7</sup> E. Fischer, *Ber. Dtsch. Chem. Ges.* **1894**, *27*, 2985.
- <sup>8</sup> R. Elghanian, J.J. Storhoff, R.C. Mucic, R.L. Letsinger, C.A. Mirkin, *Science*, **1997**, *277*, 1078.
- <sup>9</sup> J.W. Grate, G.C. Frye, *Sensors Update*, (Eds. H. Baltes, W. Göpel and J. Hesse), WILEY VCH, Weinheim, **1996**, Vol. 2, 37.
- <sup>10</sup> J. Janata, *Principles of Chemical Sensors*, Plenum press, New York, USA, **1989**.
- <sup>11</sup> J.M. Lehn, *Angew. Chem. Int. Ed. Engl.* **1988**, *27*, 90 [Nobel Lecture].
- <sup>12</sup> J. Rebek, *Angew. Chem. Int. Ed. Engl.* **1990**, *29*, 245.
- <sup>13</sup> C.H. Hunter, K.R. Lawson, J. Perkins, C.J. Urch, *J. Chem. Soc., Perkin Trans. 2*, **2001**, 651.
- <sup>14</sup> M. Nishio, M. Hirota, Y. Umezawa, *The CH- $\pi$  Interactions*, Wiley-VCH, New York, **1998**.
- <sup>15</sup> D.J. Cram, J.M. Cram, *Container Molecules and Their Guests* (ED.:J. F. Stoddart) The Royal Society of Chemistry, Cambridge, **1994**, Chapter 5.
- <sup>16</sup> D.J. Cram, S. Karbach, H.-E. Kim, C.B. Knobler, E.F. Maverick, J.L. Ericson, R.C. Helgeson, *J. Am. Chem. Soc.* **1988**, *110*, 2229.
- <sup>17</sup> a) J.A. Tucker, C.B. Knobler, K.N. Trueblood, D.J. Cram, *J. Am. Chem. Soc.* **1989**, *111*, 3688; b) P. Soncini, S. Bonsignore, E. Dalcanale, F. Ugozzoli, *J. Org. Chem.* **1992**, *57*, 4608; d) T. Haino, D.M. Rudkevich, A. Shivanyuk, K. Rissanen, J. Rebek, Jr., *Chem. Eur. J.* **2000**, *6*, 3797; e) K. Paek, J. Cho, *Tetrahedron Lett.* **2001**, *42*, 1927.
- <sup>18</sup> a) M. Vincenti, E. Dalcanale, P. Soncini, G. Guglielmetti, *J. Am. Chem. Soc.* **1990**, *112*, 445; b) M. Vincenti, E. Pelizzetti, E. Dalcanale, P. Soncini, *Pure Appl. Chem.* **1993**, *65*, 1507.
- <sup>19</sup> a) P. Timmerman, W. Verboom, D.N. Reinhoudt, *Tetrahedron*, **1996**, *52*, 2663; b) D.M. Rudkevich, J.Rebek, Jr., *Eur. J. Org. Chem.* **1999**, 1991.

- <sup>20</sup> R. Pinalli, M. Suman, E. Dalcanale, *Eur. J. Org. Chem.* **2004**, 3, 451.
- <sup>21</sup> R.M. Yebeuthou, F. Tancini, N. Demitri, S. Geremia, R. Mendichi, E. Dalcanale, *Angew. Chem. Int. Ed. Engl.* **2008**, 47, 4504.
- <sup>22</sup> a) J.R. Moran, S. Karbach, D.J. Cram *J. Am. Chem. Soc.* **1982**, 104, 5826; b) J.A. Bryant, J.L. Ericson, D.J. Cram *J. Am. Chem. Soc.* **1990**, 112, 1255; c) D.J. Cram, H.-J. Choi, J.A. Bryant, C.B. Knobler, *J. Am. Chem. Soc.* **1992**, 114, 7748.
- <sup>23</sup> P. Roncucci, L. Pirondini, G. Paderni, C. Massera, E. Dalcanale, V.A. Azov, F. Diederich, *Chem. Eur. J.* **2006**, 12, 4775.
- <sup>24</sup> E. Dalcanale, P. Soncini, G. Bacchilega, F. Ugozzoli, *J. Chem. Soc. Chem., Chem. Commun.* **1989**, 500.
- <sup>25</sup> H.L. Bandey, S.J. Martin, R. Cernosek, *Anal. Chem.* **1999**, 71, 2205.
- <sup>26</sup> A. Ricco, *J. Electrochem. Soc. Interface*, **1994**, 3, 38.
- <sup>27</sup> K. Bodenhöfer, A. Hierlemann, M. Juza, V. Schurig, W. Göpel, *Anal. Chem.* **1997**, 69, 4017.
- <sup>28</sup> L. Prodi, *New J. Chem.* **2005**, 29, 20.
- <sup>29</sup> J.R. Lakowicz, *Principles of Fluorescent Spectroscopy*, 2<sup>nd</sup> Eds, Kluwer Academic/Plenum Publisher, New York, **1999**.
- <sup>30</sup> J.S. Kim, D.T. Quang; *Chem. Rev.* **2007**, 107, 3780.
- <sup>31</sup> A. Prasanna de Silva, T.S. Moody, G.D. Wright, *Analyst*, **2009**, 134, 2385.

# Highly selective chemical vapour sensing via molecular recognition: specific $C_1$ - $C_4$ alcohols detection with a fluorescent phosphonate cavitand

2

## *2.1 Introduction*

In the last few years there has been a huge demand to monitor different chemical species in the gas phase, such as indoor and outdoor pollutants, food aromas, explosives, etc.<sup>1</sup> Chemical vapour sensors are among the most promising devices to be exploited for these applications, because they have the great advantage to allow an online measure suitable to remote control.<sup>2</sup> The need to develop sensors specific for different classes of analytes is well recognized and confirmed by the considerable research efforts spent for the preparation of more and more efficient devices.<sup>3</sup> The crucial parameter to define the success of a given sensor is therefore selectivity,<sup>4</sup> and for this reason the strategy to prepare the sensing material following the principle of supramolecular chemistry has quickly gained increasing importance.<sup>5</sup> However, the realization of selective chemical vapor sensors requires particular attention since they operate at the gas-solid interface. Any given analyte, upon moving

from the vapor to the solid phase, experiences a dramatic increase in non specific dispersion interactions, which tend to override any specific complexation event responsible of the selective responses.<sup>6</sup> As a result, the sensor selectivity drops and false positive/false negative responses soar. A possible solution to this general problem relies on transduction modes activated exclusively by the molecular recognition event.

Following this approach, we report here a new solid state fluorescent sensor based on phosphonate cavitand **Mi**[C<sub>2</sub>H<sub>5</sub>, H, fluorophore] (Figure 2.1), to be used to detect exclusively short chain alcohols in the gas phase. Phosphonate cavitands are molecular receptor presenting one or more P<sup>V</sup> moieties as bridging units.<sup>7</sup> In previous studies we have shown that two are the key factors affecting the sensing performances of mono,<sup>8</sup> di<sup>9</sup> and tetra<sup>10</sup> phosphonate cavitands toward alcohols: (1) the simultaneous presence of hydrogen bonding with one of the P=O groups and CH- $\pi$  interactions with the  $\pi$ -basic cavity, which require an inward (i) orientation of the P=O bridges; (2) a cavity that provides a permanent free volume for the analyte around the inward P=O groups, pivotal for effective hydrogen bonding.<sup>5c,10</sup> Increasing the number of inward facing P=O groups enhances the sensor responses through the entropic stabilization of host-guest complexes, but does not change the observed selectivity trend.

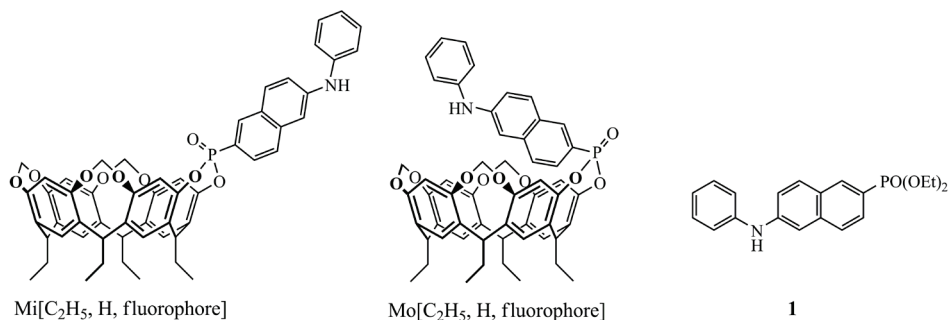


**Figure 2.1.** Fluorescent phosphonate cavitands **Mi** and **Mo**, fluorescent model compound **1**

## 2.2 Design and synthesis of the target fluorescent receptor

At first, a systematic study was undertaken to assess the complexation properties of phosphonate cavitands towards alcohols in the solid state. The



compact tetrakisphosphonate cavitand **Tiiii[H, CH<sub>3</sub>, CH<sub>3</sub>]** was chosen as host for its tendency to crystallize. Crystallization trials of this cavitand were performed using trifluoroethanol (TFE) as solvent. The addition of a short chain alcohol, through vapour diffusion in the mother solution, allowed the easy and fast growth of monoclinic crystals of the corresponding complexes. A whole series of crystal structures of C<sub>1</sub>-C<sub>4</sub> alcohol-cavitand complexes were obtained, displaying the same unit cell dimensions and symmetry in all cases (Figure 2.2). All six complexes present the same interaction pattern: an H-bond between the alcoholic OH and one of the P=O units and CH- $\pi$  contacts between the  $\pi$ -rich cavity and one methyl residue of the alkyl chain. The fitting is optimal for all alcohols up to 2-butanol. In the case of 1-butanol, the contemporary onset of both interactions with the cavitand requires the weakening of the H-bond (a P=O...O distance 2.83 Å versus an average of 2.76 Å for the other alcohols). Over that chain length, the presence of a single additional methylene unit is sufficient to completely suppress complexation in the solid state, as observed in the case of 1-pentanol (Figure 2.3). The solid state study clearly indicates that the two interactions responsible of the high selectivity of phosphonate cavitands towards alcohols occur simultaneously only in the C<sub>1</sub>-C<sub>4</sub> alcohol series. Taken alone, none of them is sufficient to bind alcohols in the solid state. This result can be extended to the case of mono and di-phosphonate cavitands, since their interaction mode with alcohols in the solid state is the same.<sup>5c</sup>

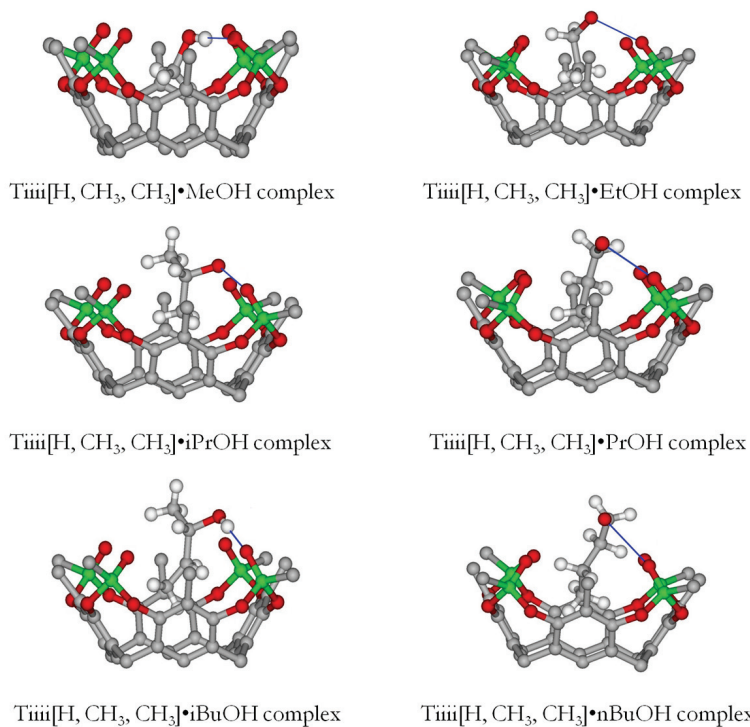


**Figure 2.2.** X-Ray structures of the  $Ti^{III}[H, CH_3, CH_3] \cdot Alcohol$  complexes.

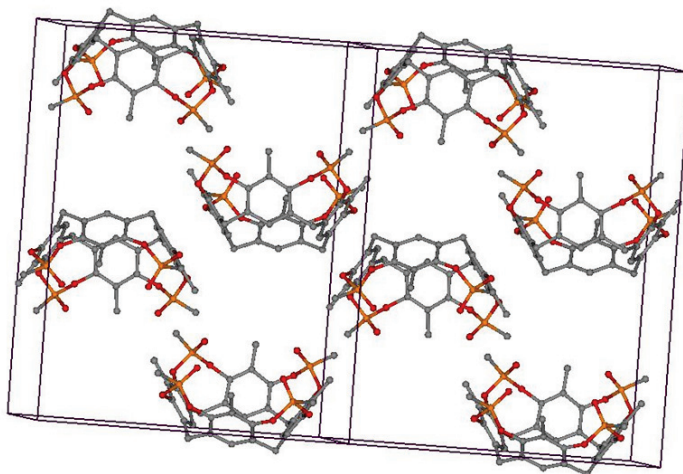
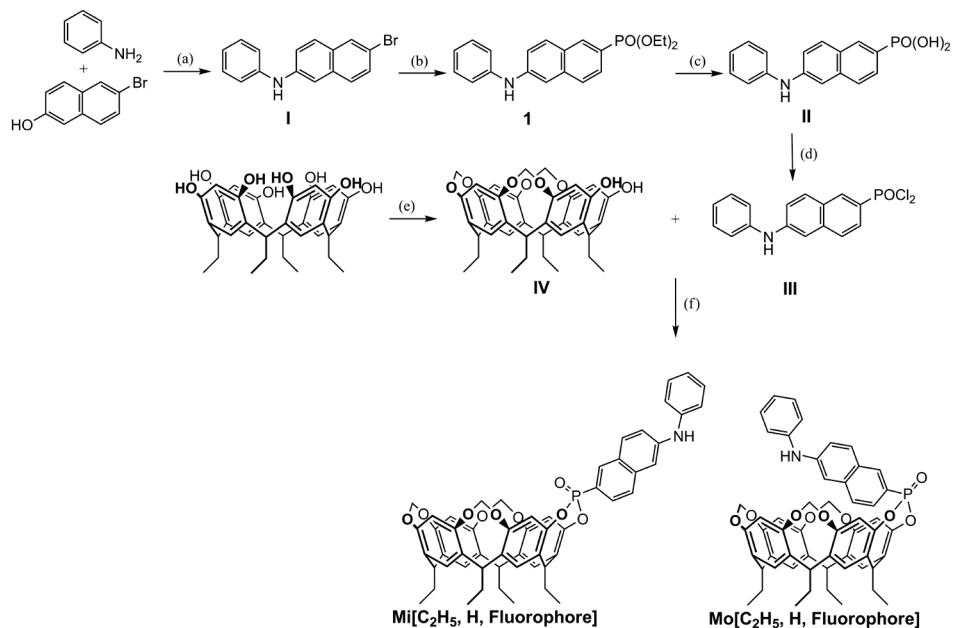


**Figure 2.3.** X-Ray structures of the  $Ti^{III}[H, CH_3, CH_3]$  in the presence of *n*-pentanol.

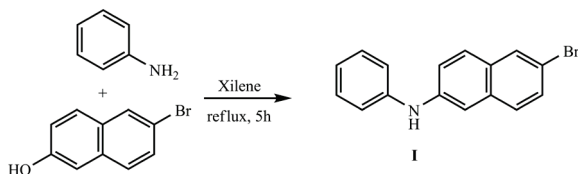
The next step was the selection of a transduction mechanism activated exclusively by this specific complexation mode, to suppress the contribution of dispersion interactions to the overall response registered by QCM transducers.<sup>6b</sup> It is well known that, among the different sensors, those based on luminescence present many advantages, such as high sensitivity, low cost, ease of operation, and versatility.<sup>11</sup> The introduction of a fluorescent moiety on the receptor was necessary because the absorbance and fluorescence of the phosphonate cavitand family is too far in the UV region to be used for practical applications.<sup>12</sup> The choice to introduce at the phosphonate site a fluorophore, similar to the commercial 2-anilino-naphthalene-6-sulfonic acid (2,6-ANS), was due to its excited state with a charge-transfer character. The rationale of this design was based on the belief that the formation of the hydrogen bond between the P=O and the alcoholic OH could decrease the electronic density on the P atom to a such an extent to modify the energy of excited state of the fluorophore. Since in the excited state of 2,6-ANS a charge transfer from the aniline to the naphthalene moiety occurs, the formation of the hydrogen bond was expected to make the charge transfer easier leading to a red-shift of the emission band. This design was also conceived to offer an high specificity, since only the formation of an hydrogen bond could cause such a spectral shift. A single P=O unit was introduced on the cavitand to funnel the H-bond perturbation on a single site, in order to maximize the desired red-shift.<sup>13</sup>

The target cavitand **Mi**[C<sub>2</sub>H<sub>5</sub>, **H**, **fluorophore**] from now onward **Mi** (Figure 2.1), which present at the upper rim one inward-facing fluorescent phosphonate unit and three methylene bridges, was synthesized following a six steps process visualized in Scheme 2.1:



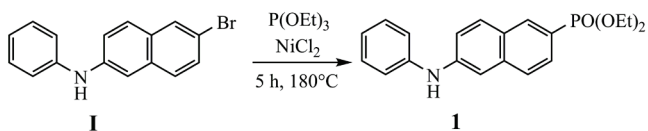
**Scheme 2.1.** (a) *TsOH*, Xylene, 190 °C, 5h, 67%; (b)  $P(\text{OEt})_3$ ,  $\text{NiCl}_2$ , 180 °C, 5h, 43%; (c) 1)  $(\text{CH}_3)_3\text{SiBr}$ ,  $\text{CH}_2\text{Cl}_2$ , 36h, RT, 2)  $\text{MeOH}$ , RT, 30 min, quantitative, (d)  $\text{PO}(\text{Cl})_3$ ,  $\text{PCl}_5$ , 90 °C, 17h; (e)  $\text{CH}_2\text{ClBr}$ ,  $\text{DMSO}$ , 80 °C, 4h, 13%; (f)  $\text{Py}$ , 60 °C, 24h, 24% 1-in, 19% 1-out (over two steps).

The multistep synthesis of the phosphonate dichloride (**III**) started from an aromatic nucleophilic substitution reaction between 6-bromo-2-naphthol and aniline to obtain the 6-bromo-N-phenyl-2-naphthylamine (**I**) (scheme 2.2)



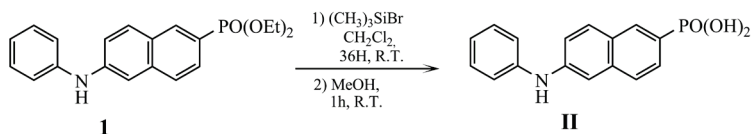
**Scheme 2.2.** Synthesis of 6-bromo-N-phenyl-2-naphthylamine **I**.

The second step was the introduction of the phosphonate moiety through an Arbuzov reaction with triethylphosphite that led to diethyl 6-(phenylamino)naphthalen-2-phosphonate (**1**) (scheme 2.3)



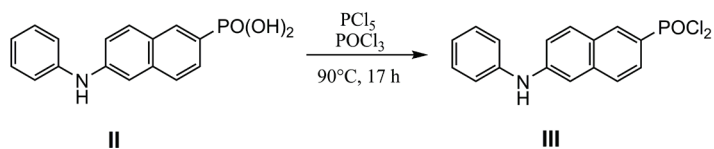
**Scheme 2.3.** Synthesis of diethyl 6-(phenylamino)naphthalene-2-phosphonate **1**.

Then the reaction of the phosphonate ester **1** with  $(\text{CH}_3)_3\text{SiBr}$  followed by addition of methanol led to 6-(phenylamino)naphthalen-2-phosphonic acid **II** in quantitative yield (Scheme 2.4).



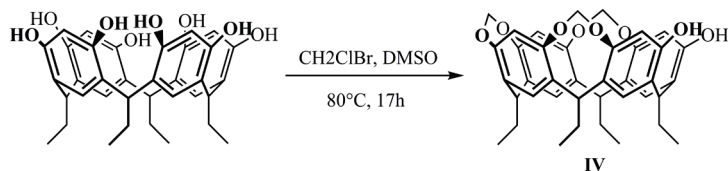
**Scheme 2.4.** Synthesis of 6-(phenylamino)naphthalen-2-phosphonic acid **II**.

The last step was the synthesis of the phosphonate dichloride **III** by treating compound **II** with  $\text{PCl}_5$  in  $\text{POCl}_3$  as solvent (scheme 2.5). Due to its reactivity the phosphonate dichloride **II** was not isolated and was used directly as bridging reagent for the resorcinarene **IV**.



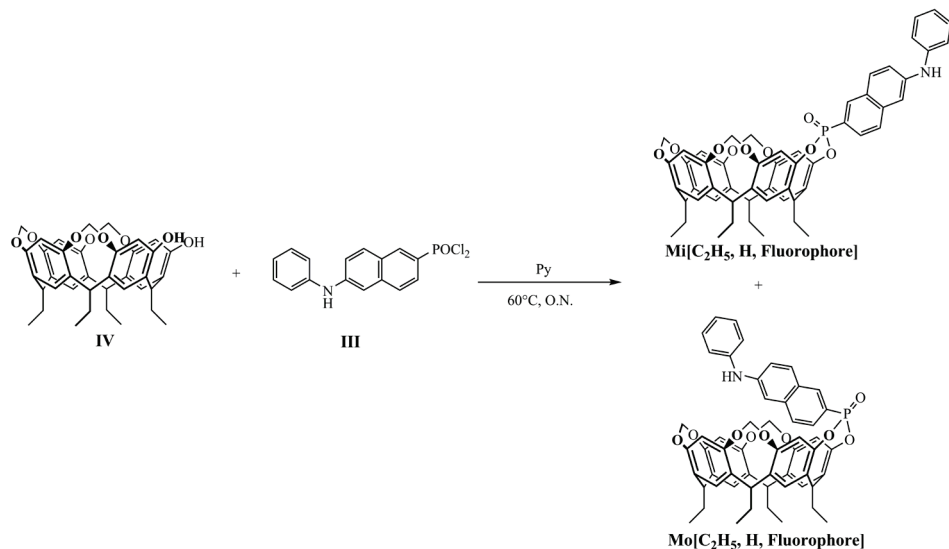
**Scheme 2.4.** Synthesis of 6-(phenylamino)naphthalen-2-ylphosphonic dichloride **III**.

Tri-methylene bridged resorcinarene **IV** was synthesised treating the starting resorcinarene<sup>14</sup> with  $\text{CH}_2\text{ClBr}$  in the presence of  $\text{K}_2\text{CO}_3$  as base (Scheme 2.5).



**Scheme 2.5.** Synthesis of tri-methylene bridged resorcinarene **IV**.

The target **Mi** cavitand was obtained by bridging resorcinarene **IV** with the fluorescent moiety using the phosphonate dichloride **III** in the presence of pyridine as base and solvent (Scheme 2.6). This reaction led to the formation of both the in (**Mi**) and out (**Mo**) isomers.



*Scheme 2.5. Synthesis of **Mi**/**Mo** cavitands.*

The out isomer **Mo**, obtained as a byproduct, was used as control system to exclude unspecific responses, and to demonstrate the necessity of the inward orientation of the P=O unit to synergistically activate both H-bonding and CH- $\pi$  interactions.

The attribution of the two isomers was achieved by <sup>1</sup>H- and <sup>31</sup>P-NMR spectroscopy. The <sup>1</sup>H NMR spectrum shows an upfield shift of the resonances belonging to the naphthalenic moiety oriented inside the cavity in **Mo**, which is the result of the shielding effect exerted by the aromatic rings of the resorcinarene skeleton. For the same reason, also the <sup>31</sup>P-NMR spectrum of **Mo** presents a significant upfield shift compared to **Mi**, as already reported by Dutasta et al.<sup>15</sup>

The fluorescent model compound **1**, was used as a model system to demonstrate the importance of the cavity surrounding the P=O unit in the recognition event.

### 2.3 Fluorescent measurements

PVC thin films containing 0.2% w/w of cavitands **Mi**, **Mo** and model compound **1** were deposited on glass substrates via spin coating. Dioctyl sebacate was added to these matrixes as plasticizer before deposition to enhance the layer permeability. In order to measure the surface fluorescence of a solid substrate subject to a continuous gas flow, we designed a cell with some special features: a window, where the glass slide was sealed, the coated face inside the cell, to expose the surface to the excitation light and to collect the emission, plus an inlet and an outlet for the flowing gas (Figure 2.4). The orientation of the cell was optimized to rule out the reflection of the excitation light and to maximize the fluorescence signal. An attenuator filter was used to diminish the number of incoming photon to decrease problems related to photochemical stability, thus allowing long measurements in continuous flow. The single wavelength emission was monitored at 460 nm, where the highest intensity excursion is observed upon complexation.

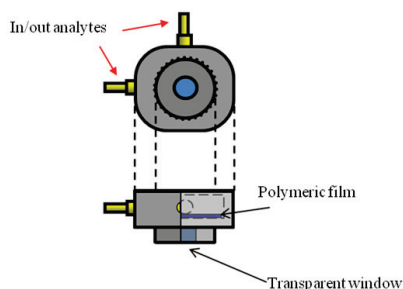
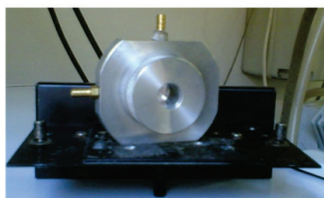


**Figure 2.4.** Hand made chamber

**Mi** film showed upon excitation at 370 nm an intense, broad and not structured band emission with a maximum at 420 nm. Upon addition of different alcohols, the maximum of this band was red-shifted by 5 nm, with a more pronounced difference in the tail of the spectrum (Figure 2.5).

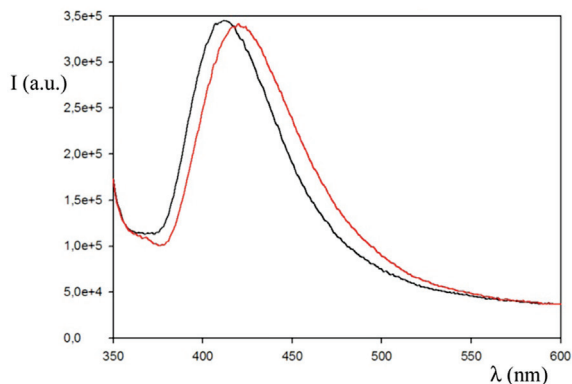


**Figure 2.5.** Emission spectra of *Mi* layer in pure  $N_2$  flux (black line) and the same layer exposed to 500 ppm of EtOH in  $N_2$  (red line).

Although relatively small, this difference was sufficient to monitor the concentration of the alcohols in the gas phase. Figure 2.6 shows the profile of the fluorescence intensity of a PVC film containing **Mi** exposed to a flux of pure  $N_2$  alternated with a flux of ethanol in  $N_2$  with a decreasing concentration down to 25 ppm. The changes in fluorescence intensity were fast and fully reversible. Under the same conditions, both the **Mo** and **1** films showed negligible changes in the emission maximum. The intensity changes were comparable for the whole  $C_1$ - $C_4$  alcohol series with the exception of 1-butanol. Figure 2.7 shows the relative fluorescence intensity changes of a PVC film containing the receptor **Mi** exposed to different alcohols at various concentrations in  $N_2$ . Figure 2.8 reports the relative fluorescence intensity changes of a PVC film containing the receptor **Mi** or **Mo** exposed to different alcohols in  $N_2$  at 500 ppm.



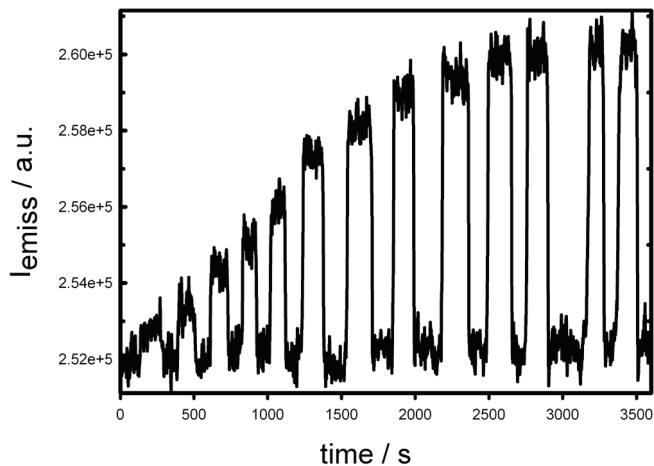


**Figure 2.6.** Fluorescence intensity ( $\lambda_{exc} = 350 \text{ nm}$ ,  $\lambda_{exc} = 460 \text{ nm}$ ) of a PVC film containing the receptor **Mi** subject to a pure  $N_2$  flux alternated with a ethanol flux in  $N_2$  with decreasing concentration (from 630 to 40 ppm, see also figure 2.6).

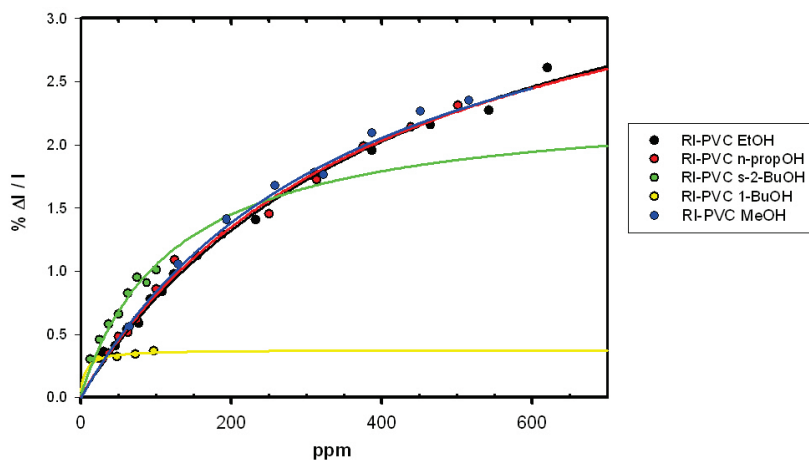


**Figure 2.7.** Relative fluorescence intensity changes ( $\lambda_{exc} = 350 \text{ nm}$ ,  $\lambda_{exc} = 460 \text{ nm}$ ) of a PVC film containing the receptor **Mi** exposed to different alcohols in  $N_2$ : blue, methanol, black, ethanol; red, n-propanol; yellow, 1-butanol; green, 2-butanol.

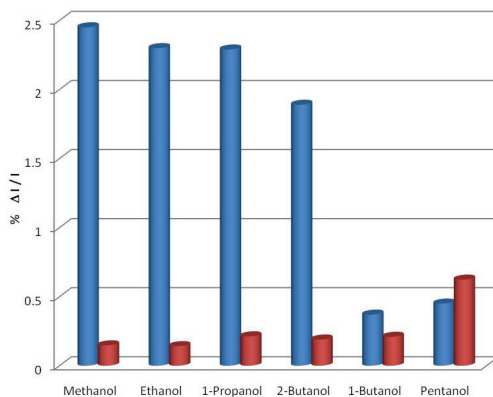


**Figure 2.8.** Relative fluorescence intensity changes ( $\lambda_{exc} = 350 \text{ nm}$ ,  $\lambda_{exc} = 460 \text{ nm}$ ) of a PVC film containing the receptor **Mi** or **Mo** exposed to different alcohols in  $N_2$ : methanol, ethanol, *n*-propanol, 2-butanol, 1-butanol, 1-pentanol (500 ppm each).

## 2.4 Conclusions.

In conclusion, this work demonstrates that it is possible to achieve high selectivity in chemical vapour sensing by harnessing the binding specificity of a cavitated receptor. The key requirement for transferring the molecular recognition properties from the solid state to the gas-solid interface is the selection of the transduction mechanism, which must be turned on exclusively by the desired complexation mode with the analyte. In our case, the H-bonding of the alcohol to the P=O induces a detectable red shift of the fluorescence emission of the 2,6-ANS fluorophore directly linked to the phosphonate acceptor. The source of selectivity can be dissected into three components. First, the ubiquitous non specific extra-cavity adsorption, being luminescence silent, does not contribute to the overall response, as it did in QCM devices. Second, in the layer the intracavity H-bonding in **Mi** is highly favoured over the extracavity one in **Mo** or **1**, due to the cavity effect. Third, the synergy between CH- $\pi$  interactions and H-bonding in **Mi** leads to a strong bias toward C<sub>1</sub>-C<sub>4</sub> alcohol detection. The molecular level resolution of this last contribution is truly remarkable, since it allows to discriminate alcohols on the basis of a single methylene unit difference. In this way, all responses due to non specific

interactions of the analytes and competitive binding by interferents have been removed.

Since most organic and polymer-based sensors detect analytes mainly on the basis of polarity, the approach described here represents a solution to the general problem of discriminating analytes by chemical class rather than by polarity in vapor sensing. This approach can be extended to many different classes of organic receptors, opening the way for the rational design of sensor materials in relation to the analytes to be detected. Although it is still necessary to improve the characteristics of the fluorescence moiety to increase sensitivity and reduce the signal to noise ratio, we think that **Mi** represent an important step forward to the design of more efficient chemical vapor sensors.

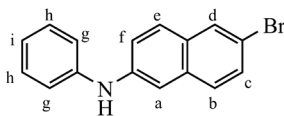
## ***2.5 Acknowledgments.***

Special thanks to Dr. Paolo Betti of the University of Parma to Damiano Genovese, Dr. Sara Bonacchi, Dr. Marco Montalti and Prof. Luca Prodi of University of Bologna for fluorescent measurements, to Dr. Rita De Zorzi and Prof. Silvano Geremia of University of Trieste for X-ray crystal structures.

## ***2.6 Experimental section.***

### **6-bromo-N-phenylnaphthalen-2-amine (I)**

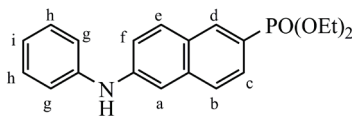
A mixture of 6-bromo-2-naphthol (8.2 g, 37.1 mmol), aniline (12.5 mL, 0.14 mol), xylene (12 mL), and p-toluensulfonic acid monohydrate (1.41 g, 7.41 mmol) was heated to reflux under nitrogen. A portion of xylene was distilled off to raise the reflux temperature to 190°C and the reaction temperature was maintained at 190°C for 5h. After cooling to 85°C, anhydrous sodium acetate (1.83 g, 23.3 mmol) and 50 mL of ethanol were added. The mixture was heated to reflux and the solution was cooled to 5°C. The cooled slurry mixture was filtered and the solid was washed and dried. The solid was suspended in warm water, filtered, and the resulting solid was washed with water to give the pure product (7.40 g, 67%).

**I**

$^1\text{H NMR}$  (300MHz, 298K,  $\text{CDCl}_3$ ):  $\delta$  (ppm) 7.87 (s, 1H,  $\text{H}_d$ ), 7.63 (d, 1H,  $\text{H}_e$ ,  $J=8.8$  Hz), 7.50 (d, 1H,  $\text{H}_b$ ,  $J=8.8$  Hz), 7.44 (dd, 1H,  $\text{H}_c$ ,  $J=8.8$  Hz,  $J=1.8$  Hz), 7.37 (d, 1H,  $\text{H}_a$ ,  $J=1.8$  Hz), 7.32 (m, 2H,  $\text{H}_h$ ), 7.22 (dd, 1H,  $\text{H}_f$ ,  $J=8.8$  Hz,  $J=2.3$  Hz), 7.17 (d, 2H,  $\text{H}_g$ ,  $J=8.6$  Hz), 7.01 (t, 1H,  $\text{H}_i$ ,  $J=7.3$  Hz); **GC-MS(EI)**:  $m/z$  calcd for  $\text{C}_{16}\text{H}_{12}\text{BrN}$  (297.0 Da)  $[\text{M}]^+$ : .297.0; found 297

### Diethyl 6-(phenylamino)naphthalen-2-phosphonate (**2**)

In a sealed tube **I** (2.5 g, 8.40 mmol) was melt at  $180^\circ\text{C}$  and a catalytic amount of  $\text{NiCl}_2$  (100 mg, 0.77 mmol) was added. Under argon atmosphere 6 mL of triethyl phosphite was added dropwise and the reaction was stirred for 5h at  $180^\circ\text{C}$ . The reaction was cooled to room temperature and poured into cool water and extracted with  $\text{CH}_2\text{Cl}_2$ . The pure product (1.3 g, 43%) was obtained by column chromatography on silica gel by using Ethyl acetate/ $\text{CH}_2\text{Cl}_2$  (7:3 v/v) as eluent and dried under *vacuum* for several hours at  $150^\circ\text{C}$ .

**1**

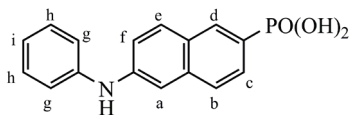
$^1\text{H NMR}$  (600MHz, 298K,  $\text{CDCl}_3$ ):  $\delta$  (ppm) 8.32 (d, 1H,  $\text{H}_d$ ,  $J=15$  Hz), 7.83 (d, 1H,  $\text{H}_e$ ,  $J=8.4$  Hz), 7.67 (m, 2H,  $\text{H}_b + \text{H}_c$ ), 7.43 (d, 1H,  $\text{H}_a$ ,  $J=1.8$  Hz), 7.38 (m, 2H,  $\text{H}_h$ ), 7.28 (m, 1H,  $\text{H}_f$ ), 7.26 (d, 2H,  $\text{H}_g$ ,  $J=8.4$  Hz), 7.08 (t, 1H,  $\text{H}_i$ ,  $J=7.8$  Hz), 4.16 (m, 4H,  $\text{OCH}_2\text{CH}_3$ ), 1.37 (m, 6H,  $\text{OCH}_2\text{CH}_3$ );  $^{31}\text{P NMR}$  (162 MHz, 298K,  $\text{CDCl}_3$ ):  $\delta$  (ppm) 18.3 (s, 1P); **GC-MS(EI)**:  $m/z$  calcd for  $\text{C}_{20}\text{H}_{22}\text{NO}_3\text{P}$  (355.1 Da)  $[\text{M}]^+$ : .355.1; found 355

### 6-(phenylamino)naphthalen-2-phosphonic acid (**II**)

To a solution of **2** (550 mg, 1.64 mmol) in  $\text{CH}_2\text{Cl}_2$ ,  $(\text{CH}_3)_3\text{SiBr}$  (1.19 mL, 9.02 mmol) was added under argon atmosphere. The solution was stirred for 36h at

room temperature, then the solvent was removed and the solid was dissolved in methanol and stirred for 30 minutes at room temperature.

The solution was dried to give the pure product as white solid (570 mg, quantitative yield).



II

$^1\text{H NMR}$  (300MHz, 298K,  $\text{CD}_3\text{OD}$ ):  $\delta$  (ppm) 8.32 (d, 1H,  $\text{H}_d$ ,  $J=15\text{Hz}$ ), 7.83 (d, 1H,  $\text{H}_e$ ,  $J=8.4\text{ Hz}$ ), 7.67 (m, 2H,  $\text{H}_b + \text{H}_c$ ), 7.33-7.25 (m, 6H,  $\text{H}_a + \text{H}_h + \text{H}_f + \text{H}_g$ ), 6.98 (t, 1H,  $\text{H}_i$ ,  $J=7.8\text{ Hz}$ );  $^{31}\text{P NMR}$  (162 MHz, 298K  $\text{CDCl}_3$ ):  $\delta$  (ppm) 18.8 (s, 1P); **ESI-MS**:  $m/z$  calcd for  $\text{C}_{16}\text{H}_{14}\text{NO}_3\text{P}$  (299.1Da)  $[\text{M}+\text{H}]^+$ :300.1 found 300.

### 6-(phenylamino)naphthalen-2-ylphosphonic dichloride (III)

To a solution of **II** (223 mg, 0.67 mmol) in 4 mL of phosphoryl trichloride,  $\text{PCl}_5$  (138 mg, 0.66 mmol) was added, under nitrogen atmosphere. The dark solution was stirred at  $90^\circ\text{C}$  for 17h than the solvent was removed under vacuum and the dark solid was used immediately in the next step without further purification and characterization.

### Trimethylene-bridged resorcinarene ( $\text{R} = \text{C}_2\text{H}_5$ ) (IV)

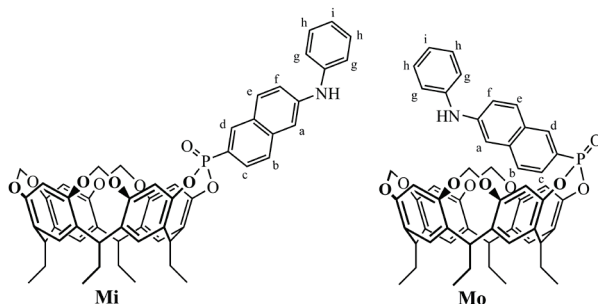
To a solution of resorcinarene ( $\text{R} = \text{C}_2\text{H}_5$ ) (2.5 g, 4.16 mmol) in 45 mL of dry DMSO,  $\text{K}_2\text{CO}_3$  (5.75 g, 41.6 mmol) and  $\text{CH}_2\text{ClBr}$  (0.881 mL, 12.48 mmol) were added, under nitrogen. The purple mixture was stirred in a sealed tube at  $80^\circ\text{C}$  for 4 hours. The reaction was quenched by addition 10 %  $\text{HCl}_{(\text{aq})}$  solution and the resulting mixture filtered and washed with water. The crude product was purified by column chromatography on silica gel by using hexane/ethyl acetate (7:3 v/v) as eluant to give cavitand as a white solid (205 mg, 13%).

$^1\text{H NMR}$  (300 MHz, 298K,  $\text{CDCl}_3$ ):  $\delta$  (ppm) 7.14 (s, 2H,  $\text{ArH}_{\text{down}}$ ), 7.08 (s, 2H,  $\text{ArH}_{\text{down}}$ ), 6.48 (s, 2H,  $\text{ArH}_{\text{up}}$ ), 6.36 (s, 2H,  $\text{ArH}_{\text{up}}$ ), 5.73 (d, 2H,  $\text{H}_{\text{out}}$ ,  $J=7.2\text{ Hz}$ ), 5.70 (d, 1H,  $\text{H}_{\text{out}}$ ,  $J=7.2\text{ Hz}$ ), 4.64 (m, 3H,  $\text{Ar-CH-Ar}$ ), 4.46 (d, 2H,  $\text{CH}_{\text{in}}$ ,  $J=7.2\text{ Hz}$ ), 4.35 (d, 1H,  $\text{CH}_{\text{in}}$ ,  $J=7.2\text{ Hz}$ ), 4.20 (t, 1H,  $\text{Ar-CH-Ar}$ ,  $J=7.2\text{ Hz}$ ),

2.55 (m, 8H, CHCH<sub>2</sub>CH<sub>3</sub>), 1.24 (m, 3H, CH<sub>3</sub>), 0.90 (m, 9H, CH<sub>3</sub>); ESI-MS: *m/z* calcd for C<sub>39</sub>H<sub>40</sub>O<sub>8</sub> (636.3Da) [M+H]<sup>+</sup>: 637.3 found 637.2.

### Synthesis of cavitands **Mi** and **Mo**

To a solution of **III** (283 mg, 0.77 mmol) in 15 mL of dry pyridine in a sealed tube, Ethyl-footed trimethylene-bridged resorcinarene (**IV**) (244 mg, 0.38 mmol) was added, under argon, and the solution was stirred at 60°C for 24h. The solvent was removed under *vacuum* and the crude product was dissolved in CH<sub>2</sub>Cl<sub>2</sub> and washed with water. The organic layer was dried and the pure product was obtained by preparative TLC on silica gel by using ethyl acetate/CH<sub>2</sub>Cl<sub>2</sub> (3:7 v/v) as eluant to give **1-in** (83 mg, 24%) and **1-out** (65 mg, 19%).

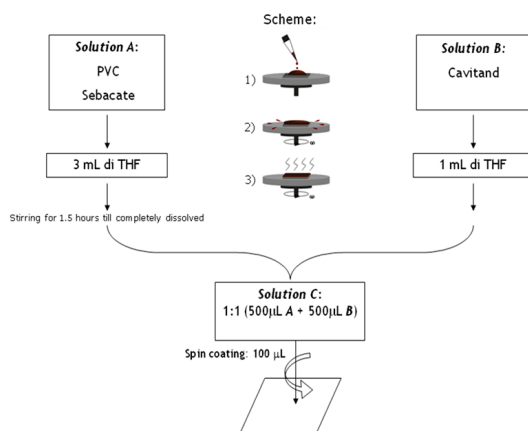


**Mi**: <sup>1</sup>H NMR (600 MHz, 298K, Acetone-d<sub>6</sub>): δ (ppm) 8.38 (d, 1H, **H<sub>d</sub>**, J<sub>H-P</sub>=15.6 Hz), 7.87 (d, 1H, **H<sub>e</sub>**, J=8.4 Hz), 7.78 (m, 1H, **H<sub>c</sub>**), 7.73 (m, 1H, **H<sub>b</sub>**), 7.55 (s, 2H, Ar**H<sub>down</sub>**), 7.49 (s, 2H, Ar**H<sub>down</sub>**), 7.45 (s, 1H, **H<sub>a</sub>**), 7.31 (d, 1H, **H<sub>f</sub>**, J=9.0 Hz), 7.23 (m, 4H, **H<sub>g</sub>**+**H<sub>h</sub>**), 6.90 (t, 1H, **H<sub>i</sub>**, J=7.8 Hz), 6.60 (s, 1H, Ar**H<sub>up</sub>**), 6.59 (s, 1H, Ar**H<sub>up</sub>**), 6.41 (s, 2H, Ar**H<sub>up</sub>**), 5.65 (d, 2H, **H<sub>out</sub>**, J=7.8 Hz), 5.52 (d, 1H, **H<sub>out</sub>**, J=7.2 Hz), 4.57 (d, 2H, **H<sub>in</sub>**, J=7.2 Hz), 4.53 (m, 3H, Ar-**CH**-Ar), 4.46 (m, 1H, Ar-**CH**-Ar), 4.15 (d, 2H, **H<sub>in</sub>**, J=7.2 Hz), 2.36 (m, 2H, **CH<sub>2</sub>**-CH<sub>3</sub>), 2.28 (m, 6H, **CH<sub>2</sub>**-CH<sub>3</sub>), 0.87 (m, 12H, CH<sub>3</sub>); <sup>31</sup>P NMR (162 MHz, 298K, Acetone-d<sub>6</sub>): δ (ppm) 14.4 (s, 1P); ESI-MS *m/z* (%): 900 [M+H<sup>+</sup>,100], 923 [(M+Na<sup>+</sup>,25)]. ESI-MS: *m/z* calcd for C<sub>55</sub>H<sub>50</sub>NO<sub>9</sub>P (899.3Da): [M+H]<sup>+</sup>:900.3 found 900; [M+Na]<sup>+</sup>:923.3 found 923

**Mo**: <sup>1</sup>H NMR (600 MHz, 298K, Acetone-d<sub>6</sub>): δ (ppm) 7.79 (s, 2H, Ar**H<sub>down</sub>**), 7.72 (s, 2H, Ar**H<sub>down</sub>**), 7.40 (m, 2H, **H<sub>h</sub>**), 7.28 (d, 2H, **H<sub>g</sub>**, J=7.8 Hz), 7.18 (s, 1H, **H<sub>a</sub>**), 7.11(dd, 1H, **H<sub>f</sub>**, J=8.4Hz, J=1.8Hz), 7.08 (t, 1H, **H<sub>i</sub>**, J=7.2 Hz), 6.73

(d, 1H,  $\mathbf{H}_d$ ,  $J_{H-P}=14.4$  Hz), 6.64 (m, 1H,  $\mathbf{H}_b$ ), 6.51 (m, 3H,  $\text{Ar}\mathbf{H}_{up} + \mathbf{H}_c$ ), 6.27 (m, 1H,  $\mathbf{H}_c$ ), 6.12 (s, 1H,  $\text{Ar}\mathbf{H}_{up}$ ), 5.77 (d, 1H,  $\mathbf{H}_{out}$ ,  $J=7.2$  Hz), 5.40 (d, 2H,  $\mathbf{H}_{out}$ ,  $J=7.2$  Hz), 4.76 (t, 1H,  $\text{Ar-CH-Ar}$ ,  $J=8.4$  Hz), 4.54 (m, 4H,  $\text{Ar-CH-Ar} + \mathbf{H}_{in}$ ), 4.26 (t, 1H,  $\text{Ar-CH-Ar}$ ,  $J=7.0$  Hz), 2.36 (m, 2H,  $\mathbf{CH}_2\text{-CH}_3$ ), 2.27 (m, 6H,  $\mathbf{CH}_2\text{-CH}_3$ ), 0.92-0.81 (m, 12H,  $\mathbf{CH}_3$ );  $^{31}\text{P}$  NMR (162 MHz, 298K, Acetone- $d_6$ ):  $\delta$  (ppm) 8.5 (s, 1P); **ESI-MS**  $m/z$  (%): 900 [ $\text{M} + \text{H}^+$ , 100], 923 [ $\text{M} + \text{Na}^+$ , 25]. **ESI-MS**:  $m/z$  calcd for  $\text{C}_{55}\text{H}_{50}\text{NO}_9\text{P}$  (899.3Da): [ $\text{M} + \text{H}$ ] $^+$ : 900.3 found 900; [ $\text{M} + \text{Na}$ ] $^+$ : 923.3 found 923.

### Thin films deposition via spin coating



**Scheme 2.6.** Scheme of thin films deposition via spin coating

**Solution A:** In a volumetric flask 120 mg of Low Molecular Weight PVC (Aldrich) and 240  $\mu\text{L}$  of dioctyl sebacate (Aldrich) were dissolved in 3 mL of distilled THF, the mixture was stirred and sonicated for 1.5 h until complete solution of PVC.

**Solution B:** In a volumetric flask 0.66 mg of fluorescent cavitand **Mi** or **Mo** was dissolved in 1 mL of distilled THF.

**Solution C:** The solution was made by mixing 500  $\mu\text{L}$  of Solution A with 500  $\mu\text{L}$  of Solution B.

We used a spin coater (Specialty Coating Systems, Inc., Model P6700) to coat a 18x18 mm glass slide (Menzel-Glaser) with a few drops (30  $\mu$ L ca.) of this solution, at an increasing (within two minutes) spin rate from 400 to 4000 rpm.

### **Fluorescent measurements**

We delivered a constant amount of gas to the cell, in order to avoid spurious responses arising from physical changes in the system other than the recognition event. We diluted the analyte by tuning the relative flows of an inert gas ( $N_2$ ) and of the analyte, in a way that the overall gas flow was set constant at 400 sccm. We thus used two flow controllers (MKS Instruments) to regulate the flow of  $N_2$  and analyte coming from the tanks; the two flows converged in a joint, then reached the cell and the sensing substrate. A scheme of this instrumental setting is displayed in Figure 2.9.



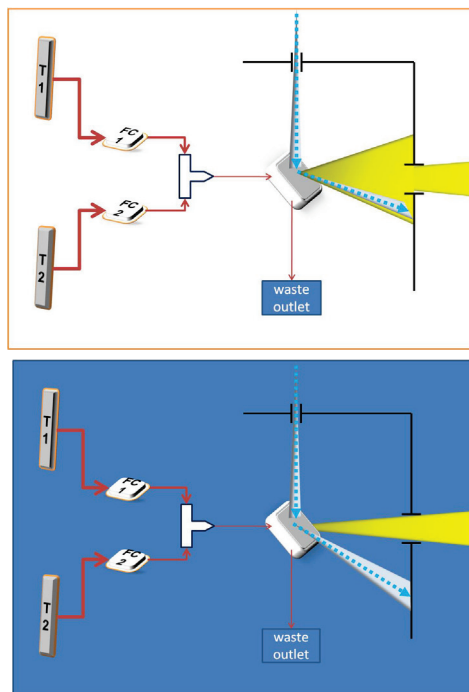


**Figure 2.9.** Scheme of the fluorimeter coupled with the gas flow circuit. T1 and T2 are the two tanks, filled with  $N_2$  and analyte, FC1 and FC2 are the flow controllers, the red arrows indicate the gas flow direction. The blue dotted arrow is the excitation light, reflected from the cell far from the emission slit. The yellow cone stands for the emitted light, which is collected through the slit to the detector.

All the crystal structures described in this Chapter have been resolved by Rita De Zorzi at the Department of Chemistry of the University of Trieste. Details about the crystal structure determination can be found in Chapter 6 of De Zorzi's PhD thesis.

## 2.7 References.

- <sup>1</sup> Special issue on Modern Topics in Chemical Sensing, *Chem. Rev.* **2008**, issue 2, J. Janata Ed.
- <sup>2</sup> *Sensors, A Comprehensive Survey*; W. Göpel, J. Hesse, J. N. Zemel, Eds.; VCH Weinheim, Germany **1991**, Vol. 2.
- <sup>3</sup> L. Prodi, *New. J. Chem.* **2005**, 29, 20.
- <sup>4</sup> H. Hierlemann, R. Gutierrez-Osuna, *Chem. Rev.*, **2008**, 108, 563 and references cited therein.
- <sup>5</sup> a) F.C.J.M. Van Veggel in *Comprehensive Supramolecular Chemistry* Vol. 10, (Eds.: J. L. Atwood, J. E. D. Davies, D. D. MacNicol, F. Vögtle, D. N. Reinhoudt), PERGAMON, Oxford, **1996**, pp. 171-185; b) J.J. Lavigne, E.V. Anslyn, *Angew. Chem. Int. Ed.*, **2001**, 40, 3118, *Angew. Chem.* **2001**, 113, 3212; c) L. Pirondini, E. Dalcanale, *Chem. Soc. Rev.* **2007**, 36, 695; d) E.V. Anslyn, *J. Org. Chem.* **2007**, 72, 687.
- <sup>6</sup> a) W. Grate and G.C. Frye, in *Sensors Update*, eds. H. Baltes, W. Göpel and J. Hesse, Wiley-VCH, Weinheim, **1996**, Vol. 2, 37-83; b) M. Toneyzer, M. Melegari, G. Maggioni, R. Milan, G. Della Mea, E. Dalcanale, *Chem. Mater.* **2008**, 20, 6535.
- <sup>7</sup> R. Pinalli, M. Suman, E. Dalcanale, *Eur. J. Org. Chem.* **2004**, 451.
- <sup>8</sup> R. Pinalli, F. F. Nachtigall, F. Ugozzoli, E. Dalcanale, *Angew. Chem.* **1999**, 111, 2530; *Angew. Chem. Int. Ed.* **1999**, 38, 2377.
- <sup>9</sup> M. Suman, M. Freddi, C. Massera, F. Ugozzoli, E. Dalcanale, *J. Am. Chem. Soc.* **2003**, 125, 12068.
- <sup>10</sup> M. Melegari, M. Suman, L. Pirondini, D. Moiani, C. Massera, F. Ugozzoli, E. Kalenius, P. Vainiotalo, J.-C. Mulatier, J.-P. Dutasta, E. Dalcanale, *Chem. Eur. J.* **2008**, 14, 5772.
- <sup>11</sup> (a) A.P. de Silva, H.Q.N. Gunaratne, T. Gunnlaugsson, A.J.M. Huxley, C.P. McCoy, J.T. Rademacher, T. E. Rice, *Chem. Rev.* **1997**, 97, 1515; (b) L. Prodi, F. Bolletta, M. Montalti, N. Zaccheroni, *Coord. Chem. Rev.* **2000**, 205, 59.
- <sup>12</sup> E. Biavardi, G. Battistini, M. Montalti, R. M. Yebeutchou, L. Prodi, E. Dalcanale, *Chem. Commun.* **2008**, 1638.
- <sup>13</sup> A Tiiii cavitand bearing the fluorophore on each P=O unit would have lead to self-quenching in the solid state, while a Tiiii cavitand with a single P=O with the fluorophore and three normal ones would have lead to an undesired dilution of the H-bonding perturbation on four sites, three of them luminescence silent.
- <sup>14</sup> (a) P. Timmerman, H. Boerrigter, W. Verboom, J. G. Van Hummel, S. Harkema, D. N. Reinhoudt, *J. Inclusion Phenom.* **1994**, 19, 167, (b) E. Menozzi, M. Busi, C. Massera, F. Ugozzoli, D. Zuccaccia, A. Macchioni, E. Dalcanale, *J. Org. Chem.* **2006**, 71, 2617.
- <sup>15</sup> P. Delangle, J.-C. Mulatier, B. Tinant, J.-P. Dutasta *Eur. J. Org. Chem.* **2001**, 3695.

# Selective methanol detection: synthesis of a new sterically hindered fluorescent cavitand

# 3

## *3.1 Introduction*

One of the key issue in the development of new, efficient chemical sensors is the quest for selectivity, defined as the ability of the sensors to respond primarily to only one species in the presence of other analytes. In this context, as for biological systems, the concepts of shape recognition and binding site complementarity are central for effective molecular recognition in artificial host-guest systems.

The previous chapter has shown that the use of fluorimetry, as transduction mode, increases the specificity of phosphonate cavitand based supramolecular sensors toward short chain alcohols ( $C_1$ - $C_4$ ). The next step is the development of an even more specific sensor able to detect only methanol. This requires not only the use of fluorimetry to exploit the increase of specificity shown in chapter 2, but also a rational design of the cavitand receptor, conceiving a smaller cavity able to host only few complementary guests.

Previous studies have demonstrated that, replacing one or two P=O with P=S groups in tetrakisphosphonate cavitands enhances the selectivity for short chain alcohols in mass sensors.<sup>1</sup> In particular the presence of two bulky P=S bridges, unable to H-bond to the analyte, makes the resulting cavitands by far, more

specific in recognizing MeOH and EtOH with the respect to the T<sub>iiii</sub> compound. For the longer chain alcohols the simultaneous presence of H-bonding and CH- $\pi$  interactions requires a conformational arrangement which is disfavored in the presence of two P=S groups.

Therefore we have designed a new fluorescent thiophosphonate cavita<sub>nd</sub> (Figure 3.1) replacing the three methyl group of the M<sub>i</sub> cavita<sub>nd</sub>, studied in the previous chapter, with three bulky P=S groups in order to obtain a receptor specific for methanol.

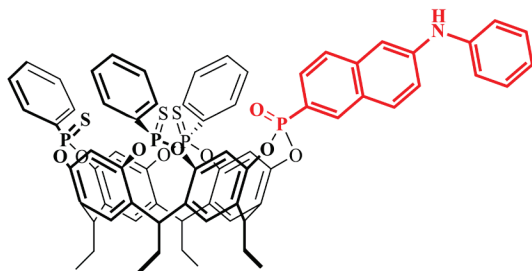
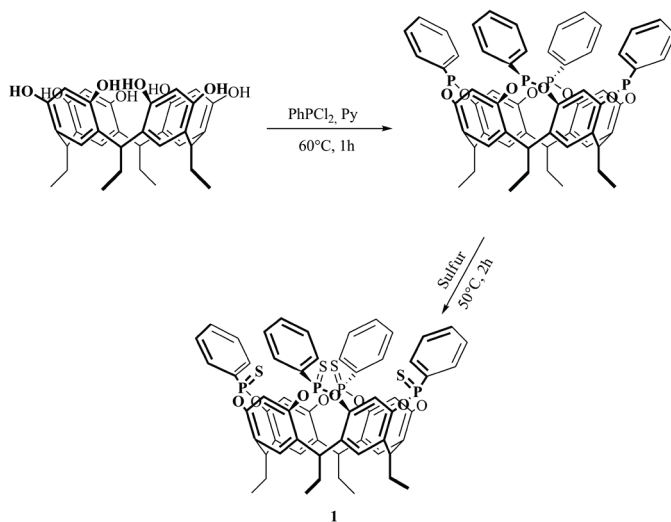


**Figure 3.1.** Target fluorescent cavita<sub>nd</sub>.

The introduction of three bulky P=S bridging groups instead of other three P=O groups, without fluorophore attached, not only reduces the size of the cavity but also, confines the H-bonding on the remaining P=O, since the P=S is by far less efficient on H-bonding, avoiding a reduction of the fluorophore perturbation and consequently of the sensitivity of the sensor.

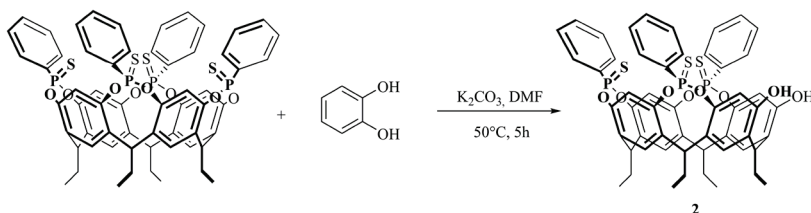
### 3.2 *Synthesis of the new target fluorescent cavita<sub>nd</sub>*

The better way to obtain the target cavita<sub>nd</sub> is a three steps process starting with the synthesis of the tetrathiophosphonate TS<sub>iiii</sub>[C<sub>2</sub>H<sub>5</sub>, H, Ph] cavita<sub>nd</sub> **1**. This reaction was carried out following a procedure reported in literature<sup>2</sup> that led selectively to the iiii stereoisomer with the four P=S group oriented inwards. Resorcin[4]arene was treated with PhPCl<sub>2</sub> in the presence of pyridine to give exclusively the tetraphosphonito cavita<sub>nd</sub>. The subsequent *in situ* oxidation with sulfur, which proceeded with retention of configuration at phosphorous centre, led to **1** in good yield (Scheme 3.1).



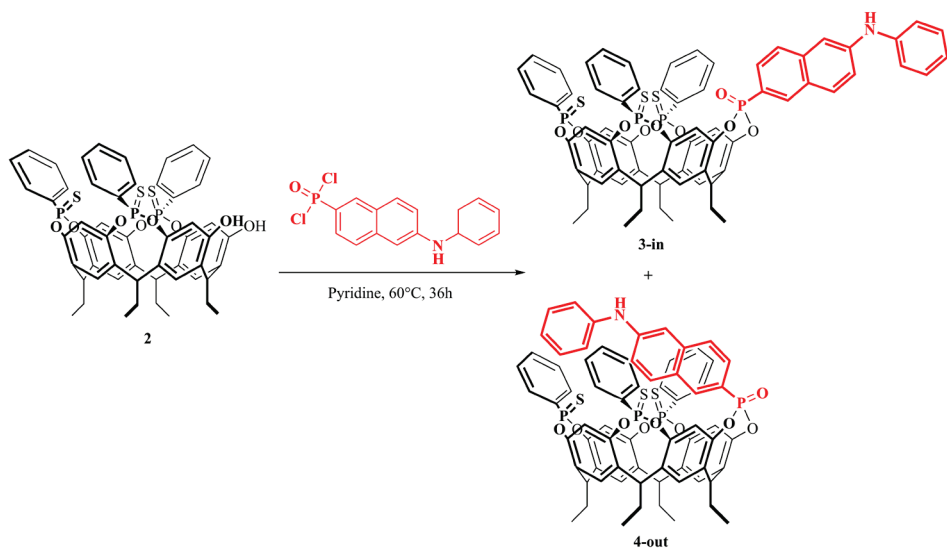
**Scheme 3.1.** Synthesis of the  $TS_{iii}[C_2H_5, H, Ph]$ .

The trithiophosphonate (3PSiii) resorcinarene **2** was obtained by selective excision of one of the four P=S bridges of the  $TS_{iii}[C_2H_5, H, Ph]$  **1** following a procedure reported in literature.<sup>3</sup> This protocol requires the use of a stoichiometric amount of catechol in the presence of  $K_2CO_3$  (Scheme 3.2).



**Scheme 3.2.** Synthesis of the trithiophosphonate resorcinarene.

The last step was the introduction of the fluorescent phosphonate moieties. This reaction was made in pyridine under mild condition using the same fluorescent phosphonate dichloride described in the previous chapter. This reaction led to the formation of both the in (**3-in**) and out (**4-out**) isomers (Scheme 3.3).



**Scheme 3.3.** Synthesis of the fluorescent in and out cavitands.

The identification of the two isomers was achieved by  $^1\text{H}$ - and  $^{31}\text{P}$ -NMR spectroscopy. The  $^1\text{H}$ -NMR spectra have shown an upfield of the peaks belonging to the naphthalenic moiety oriented inside the cavity of **1-out**, which is the result of the shielding effect exerted by the aromatic rings of the resorcinarene moiety. For the same reason, also the  $^{31}\text{P}$ -NMR spectra have shown a significant upfield shift of the peak of **1-out** compared to **1-in** (Figure 3.2), as already seen by Dutasta and Coworkers.<sup>4</sup>

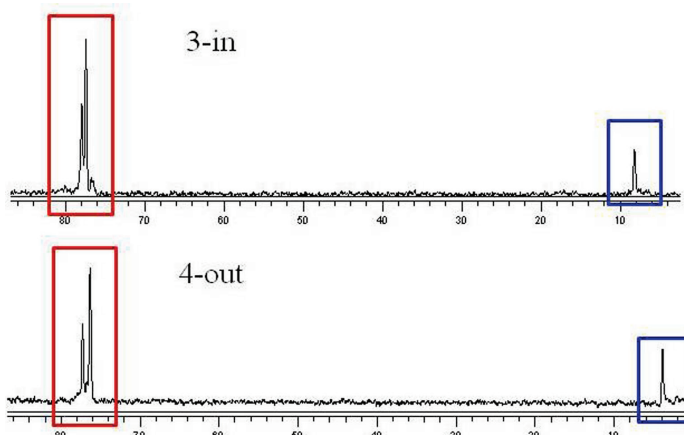


**Figure 3.2.**  $^{31}\text{P}$ -NMR in  $\text{CDCl}_3$ . Isomers **3-in** (up) and **4-out** (down).

### 3.3 Fluorescent measurements in solution

The cavitand receptors **3-in** and **4-out** were tested in solution in order to verify the absorption and emission behaviour toward alcohols. In particular we recorded the absorption and emission spectra of a solution of **3-in** in  $\text{CHCl}_3$  after the addition of increasing amount of methanol (Figure 3.3), ethanol (Figure 3.4) and n-butanol (Figure 3.5).

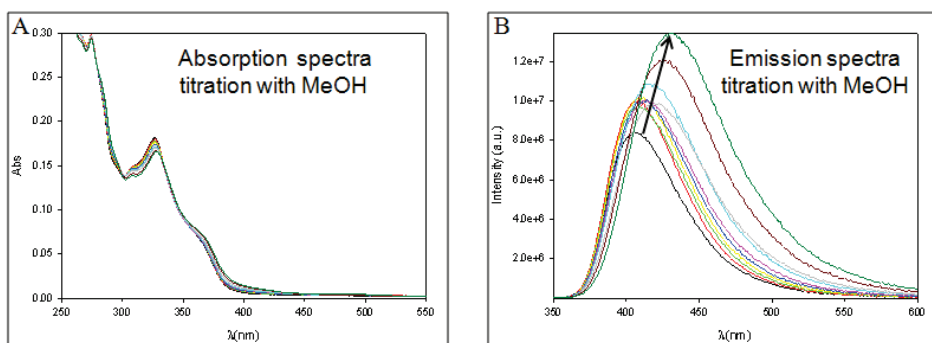


**Figure 3.3.** Absorption (A) and emission (B) spectra of **3-in** in solution of chloroform after addition of increasing amount of MeOH.

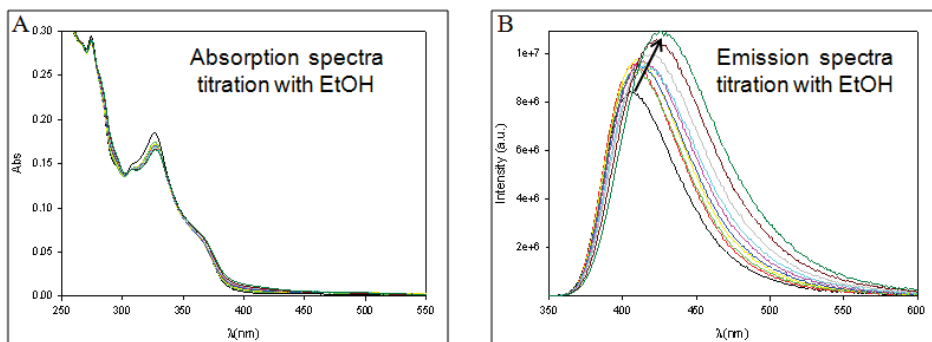


**Figure 3.4.** Absorption (A) and emission (B) spectra of **3-in** in solution of chloroform after addition of increasing amount of EtOH.

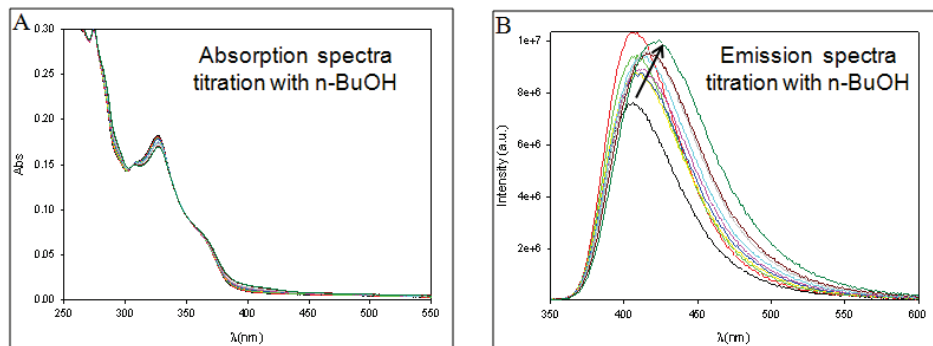


**Figure 3.5.** Absorption (A) and emission (B) spectra of **3-in** in solution of chloroform after addition of increasing amount of *n*-BuOH.

All the absorption spectra reported above, have not shown any significant changes after the addition of the alcohols, whereas the emission spectra have shown the expected red shift and enhancement in intensity.

In solution the response of the **3-in** toward methanol was slightly higher (Figure 3.6) than toward ethanol and *n*-butanol, but not enough to say that the receptor is selective only for methanol. The lack of selectivity in solution might be due to the solvation effect that, at high concentration of the guest, overcomes the specific host-guest interactions.

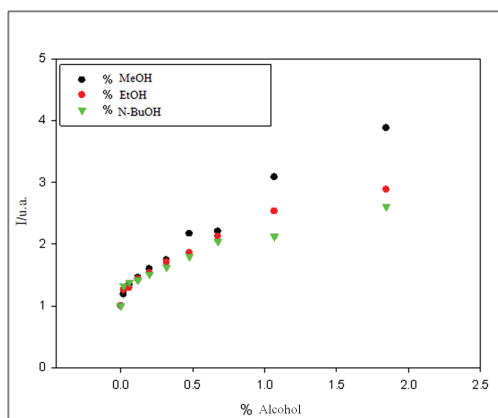


**Figure 3.6.** Comparison of the trend of the intensity emission light at a fixed wavelength of **3-in** in  $\text{CHCl}_3$  versus the amount of methanol, ethanol and *n*-butanol.



We have also compared the emission behaviour of **3-in** and **4-out** toward ethanol (Figure 3.7). In both the cases, in the emission spectra, after the addition of ethanol we observed an increase of intensity and a bathochromic shift of the maximum. In solution the response of the out isomers to the guest, might be attributed to the solvation effect.

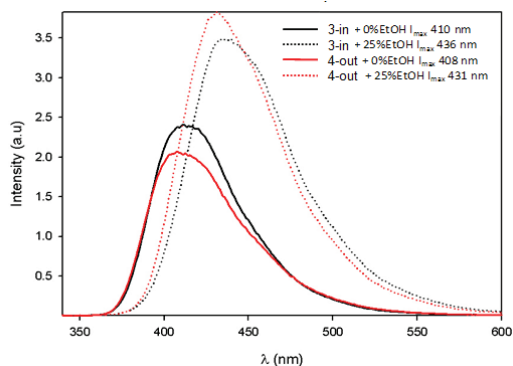


**Figure 3.7.** Emission spectra of **3-in** and **4-out** in  $\text{CHCl}_3$  before and after the addition of ethanol.

From these first results we can say that, in solution, both the specific H-bonding interaction between the P=O and the alcohols and the solvation effect causing a red shift of the emission spectra. To better understand the real capabilities of our receptor to bind selectively methanol, avoiding the solvation effect, we needed to perform experiments at the gas-solid interface.

### 3.4 Sensor measurements

To use the cavitants for fluorescent sensing experiments at the gas-solid interface, they must be deposited via spin coating on a transparent glass surface. In order to obtain a good thin film, the cavitants, in solution of THF, were diluted in a Polyvinylchloride (PVC) matrix. PVC was chosen because it allows to prepare transparent thin films. To reduce the  $T_g$  of the PVC, and make a thin film permeable to the analyte, we also needed to add the colourless plasticizer dioctyl sebacate.

For the sensing measurements we used the hand-made prototype of a sealed chamber described in the previous chapter.

To use this system as a sensors, in a dynamic setting, we needed to record a signal versus time, so we decided to measure only the variation of emission intensity at a fixed wavelength with the “time drive” function of the Luminescence Spectrometer.

To make precise measurements, using all the analyte at the same concentration, we used a mass flow controller.

We did some preliminary measurement at the gas-solid interface using methanol, ethanol and n-butanol (Figure 3.8), but unfortunately even after several attempts we could not obtain any good result. As shown in Figure 3.8 all the measurements we did with the three different guest were irreproducible and give strange low responses not related to the analytes concentration.

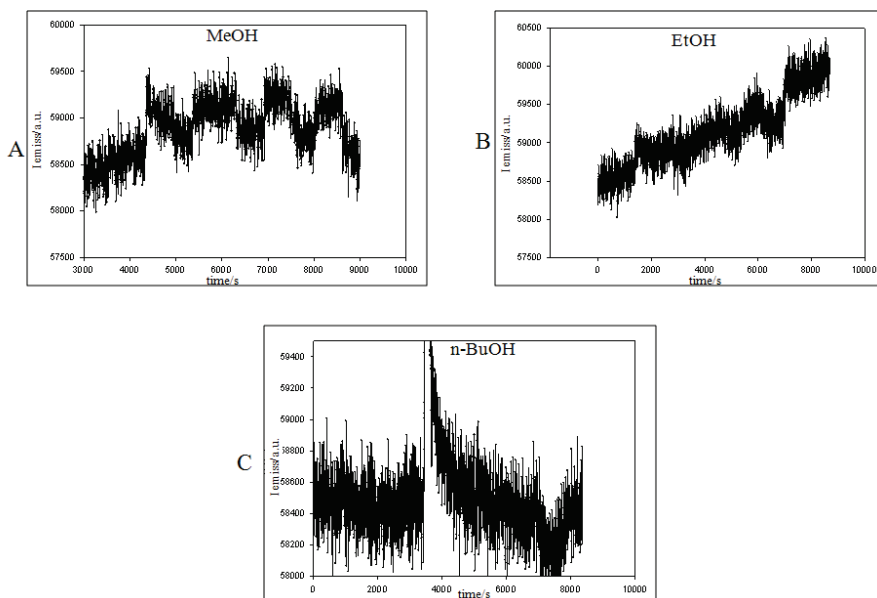


**Figure 3.8.** Sensor measurements.

Moreover, when we introduced only N<sub>2</sub> into the chamber we observed a decrease of the emission intensity, which we did not observe in the case of the fluorescent M<sub>1</sub> cavitand (chapter 2). This last effect might be due to the packing of the cavitand in the thin film. Some of the amino group can form H-bonding

interaction with the phosphonate moieties, and the N<sub>2</sub> could cause a swelling of the film and consequently the break of these interactions and the blue shift of the emission spectra.

### 3.5 Conclusions

The sensing experiments at the gas-solid interface shown that the cavitand **3-in** is not able to complex any alcohols, probably because of its too small cavity. After the sensing experiments, the red shift of the emission spectra of **3-in**, that we observed in solution, can be attributed to a purely solvation effect.

Further studies can be made by using a mixed-bridged dithiophosphonate cavitand, that, as already demonstrated, is capable of binding short chain alcohols with high selectivity towards methanol and ethanol.<sup>1</sup>

### 3.6 Acknowledgments

Special thanks to Paolo Betti of University of Parma and Luca Prodi, Marco Montalti, Damino Genovese e Sara Bonacchi of University of Bologna.

### 3.7 Experimental section

#### Cavitand TS<sub>iii</sub>[C<sub>2</sub>H<sub>5</sub>, H, Ph] (**1**)

To a solution of resorcinarene (R= C<sub>2</sub>H<sub>5</sub>) (1.50 g, 2.50 mmol) in dry pyridine (50 mL), dichlorophenylphosphine (1.32 mL, 10.20 mmol) was added dropwise, under argon atmosphere. The solution was stirred at 60 °C for 1 h. Sulfur (0.51 g, 2.00 mmol) was added and the mixture was heated at 50°C for 2 h. The solvent was removed under *vacuum* and the solid was washed and sonicated with water, then filtered and dried. The crude product was purified by column chromatography (SiO<sub>2</sub>, gradient from 4:6 to 3:7, hexane/CH<sub>2</sub>Cl<sub>2</sub> v/v) affording **1** as white solid (1.85 g, 64%). <sup>1</sup>H NMR (300 MHz, CDCl<sub>3</sub>): δ= 8.17 (m, 8H, P(S)ArH<sub>o</sub>), 7.56 (m, 4H, P(S)ArH<sub>p</sub>), 7.51 (m, 8H, P(S)ArH<sub>m</sub>), 7.30 (s, 4H, ArH<sub>down</sub>), 6.67 (s, 4H, ArH<sub>up</sub>), 4.64 (t, 4H, ArCH, J=7.1 Hz), 2.39 (m, 8H,

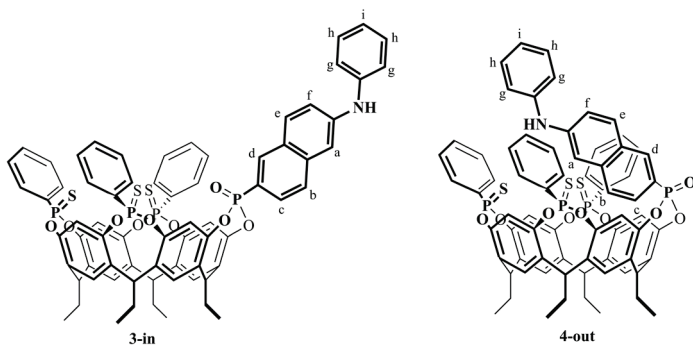
$\text{CH}_2\text{CH}_3$ ), 1.06 (t, 12H,  $\text{CH}_2\text{CH}_3$ ,  $J=6.8$  Hz);  $^{31}\text{P}$  NMR (162 MHz,  $\text{CDCl}_3$ ):  $\delta = 77.77$  (s, 4P, P=S). **ESI-MS**  $m/z$  (%): 1175.3  $[\text{M}+\text{Na}]^+$ .

### Trithiophosphonate resorcinarene (**2**)

Cavitand **1** (1.00 g, 0.86 mmol) was dissolved in dry DMF (30 mL) at  $50^\circ\text{C}$ . Cathecol (0.10 g, 0.91 mmol) and  $\text{K}_2\text{CO}_3$  (1.20 g, 8.67 mmol) were added and the mixture was stirred at  $80^\circ\text{C}$  for 5 h. The solvent was removed under *vacuum* and the solid was washed and sonicated with water, then filtered and dried. The crude product was purified by column chromatography ( $\text{SiO}_2$ , 99:1,  $\text{CH}_2\text{Cl}_2/\text{EtOH}$  v/v) affording **2** as white solid (0.46 g, 52%).  $^1\text{H}$  NMR (300 MHz,  $\text{CDCl}_3$ ):  $\delta = 8.17$  (m, 6H, P(S)ArH<sub>o</sub>), 7.57-7.53 (m, 9H, P(S)ArH<sub>p</sub>+P(S)ArH<sub>m</sub>), 7.32 (s, 2H, ArH<sub>down</sub>), 7.20 (s, 2H, ArH<sub>down</sub>), 6.68 (s, 2H, ArH<sub>up</sub>), 6.49 (s, 2H, ArH<sub>up</sub>), 4.64 (m, 4H, ArCH), 2.39-2.26 (m, 8H,  $\text{CH}_2\text{CH}_3$ ), 1.07-1.00 (m, 12H,  $\text{CH}_2\text{CH}_3$ );  $^{31}\text{P}$  NMR (162 MHz,  $\text{CDCl}_3$ ):  $\delta = 77.42$  (s, 1P, P=S), 76.27 (s, 2P, P=S); **ESI-MS**  $m/z$  (%): 1015.6  $[\text{M}+\text{H}]^+$ , 1037.3  $[\text{M}+\text{Na}]^+$ , 1054.7  $[\text{M}+\text{K}]^+$ .

### Cavitand (**3-in** and **4-out**)

To a solution of 6-(phenylamino)naphthalene-2-ylphosphonic dichloride (0.19 g, 0.56 mmol) in dry pyridine (15 mL) in a sealed tube, resorcinarene **2** (0.20 g, 0.19 mmol) was added under argon, and the solution was stirred at  $60^\circ\text{C}$  for 24h. The solvent was removed under *vacuum* and the crude was dissolved in  $\text{CH}_2\text{Cl}_2$  and washed with water. The organic layer was dried and the crude product was purified by preparative TLC ( $\text{SiO}_2$ , 5:5, ethylacetate/hexane, v/v) to give **3-in** (30 mg, 12%) and **4-out** (26 mg, 10%).



**3-in:**  $^1\text{H NMR}$  (600 MHz, Acetone- $d_6$ ):  $\delta = 8.38$  (d, 1H,  $H_d$ ,  $J_{\text{H-P}} = 16$  Hz), 8.09 (m, 6H, P(S)Ar $H_o$ ), 7.85-7.82 (m, 2H,  $H_e + H_c$ ), 7.75 (s, 2H, Ar $H_{\text{down}}$ ), 7.72-7.69 (m, 3H, Ar $H_{\text{down}} + H_b$ ), 7.50 (m, 9H, P(S)Ar $H_m + \text{P(S)Ar}H_p$ ), 7.43 (d, 1H,  $H_a$ ,  $J = 2.4$  Hz), 7.29 (dd, 1H,  $H_f$ ,  $J = 9.0$  Hz,  $J = 2.4$  Hz), 7.23-7.19 (m, 4H,  $H_h + H_g$ ), 6.87 (t, 1H,  $H_i$ ,  $J = 7.8$  Hz), 6.63 (s, 2H, Ar $H_{\text{up}}$ ), 6.51 (s, 2H, Ar $H_{\text{up}}$ ), 4.70 (t, 1H, ArCH,  $J = 7.8$  Hz), 4.60 (m, 3H, ArCH), 2.35 (m, 2H,  $\text{CH}_2\text{CH}_3$ ), 2.28 (m, 6H,  $\text{CH}_2\text{CH}_3$ ), 0.93- 0.80 (m, 12H,  $\text{CH}_3$ );  $^{31}\text{P NMR}$  (162 MHz,  $\text{CDCl}_3$ ):  $\delta = 78.90$  (s, 1P, P=S), 77.21 (s, 2P, P=S), 8.21 (s, 1P, P=O); **Exact mass:** m/z calculated for  $\text{C}_{70}\text{H}_{60}\text{NO}_9\text{P}_4\text{S}_3$   $[\text{M}+\text{H}]^+$ : 1278.23807, found: 1278,2426.

**4-out:**  $^1\text{H NMR}$  (600 MHz, Acetone- $d_6$ ):  $\delta = 8.16$  (m, 2H, P(S)Ar $H_o$ ), 8.07 (d, 1H,  $H_d$ ,  $J_{\text{H-P}} = 16.0$  Hz), 7.90 (m, 4H, P(S)Ar $H_o$ ), 7.87 (s, 2H, Ar $H_{\text{down}}$ ), 7.82 (s, 2H, Ar $H_{\text{down}}$ ), 7.65 (d, 1H,  $H_f$ ,  $J = 9.0$  Hz), 7.58 (m, 3H, P(S)Ar $H_m + \text{P(S)Ar}H_p$ ), 7.51 (m, 2H,  $H_g$ ), 7.41-7.38 (m, 8H, P(S)Ar $H_m + \text{P(S)Ar}H_p + H_h$ ), 7.20-7.10 (m, 3H,  $H_a + H_e + H_c$ ), 6.91 (m, 1H,  $H_b$ ), 6.80 (t, 1H,  $H_i$ ,  $J = 8.5$  Hz), 6.58 (s, 2H, Ar $H_{\text{up}}$ ), 6.07 (s, 2H, Ar $H_{\text{up}}$ ), 4.91 (t, 1H, ArCH,  $J = 7.8$  Hz), 4.66 (t, 1H, ArCH,  $J = 7.8$  Hz), 4.60 (bt, 2H, ArCH), 2.46-2.43 (m, 8H,  $\text{CH}_2\text{CH}_3$ ), 0.97-0.90 (m, 12H,  $\text{CH}_3$ );  $^{31}\text{P NMR}$  (162 MHz,  $\text{CDCl}_3$ ):  $\delta = 77.20$  (s, 1P, P=S), 76.32 (s, 2P, P=S), 3.85 (s, 1P, P=O); **Exact mass:** m/z calculated for  $\text{C}_{70}\text{H}_{60}\text{NO}_9\text{P}_4\text{S}_3$   $[\text{M}+\text{H}]^+$ : 1278.23807, found: 1278,2426.

### Uv-visible titration of 3-in with methanol

- solvent  $\text{CHCl}_3$  (99.8%, Riedel-de Haen, CHROMASOLV<sup>®</sup>, amylene stabilized);
- solution of **3-in** ( $3.21 \cdot 10^{-5}$  M);
- guest: methanol;
- absorption spectra: 250-550 nm,

### Uv-visible titration of 3-in with ethanol

- solvent  $\text{CHCl}_3$  (99.8%, Riedel-de Haen, CHROMASOLV<sup>®</sup>, amylene stabilized);
- solution of **3-in** ( $3.21 \cdot 10^{-5}$  M);

- guest: ethanol absolute;
- absorption spectra: 250-550 nm,

#### **Uv-visible titration of 3-in with n-butanol**

- solvent  $\text{CHCl}_3$  (99.8%, Riedel-de Häen, CHROMASOLV<sup>®</sup>, amylene stabilized);
- solution of **3-in** ( $3.21 \cdot 10^{-5} \text{ M}$ );
- guest: n-butanol;
- absorption spectra: 250-550 nm,

#### **Fluorescence titration of 3-in with methanol**

- solvent  $\text{CHCl}_3$  (99.8%, Riedel-de Häen, CHROMASOLV<sup>®</sup>, amylene stabilized);
- solution of **3-in** ( $3.21 \cdot 10^{-5} \text{ M}$ );
- guest: methanol;
- emission spectra: 350-600 nm;
- excitation wavelength: 330 nm;

#### **Fluorescence titration of 3-in with ethanol**

- solvent  $\text{CHCl}_3$  (99.8%, Riedel-de Häen, CHROMASOLV<sup>®</sup>, amylene stabilized);
- solution of **3-in** ( $3.21 \cdot 10^{-5} \text{ M}$ );
- guest: ethanol absolute;
- emission spectra: 350-600 nm;
- excitation wavelength: 330 nm;

#### **Fluorescence titration of 3-in with n-butanol**

- solvent  $\text{CHCl}_3$  (99.8%, Riedel-de Häen, CHROMASOLV<sup>®</sup>, amylene stabilized);
- solution of **3-in** ( $3.21 \cdot 10^{-5} \text{ M}$ );
- guest: n-butanol;
- emission spectra: 350-600 nm;
- excitation wavelength: 330 nm;

### **Fluorescence titration of 4-out with ethanol**

- solvent  $\text{CHCl}_3$  (99.8%, Riedel-de Hen, CHROMASOLV<sup>®</sup>, amylene stabilized);
- solution of **4-out** ( $9.6 \cdot 10^{-4}$  M);
- guest: ethanol;
- emission spectra: 350-600 nm;
- excitation wavelength: 305 nm;

### **Fluorescent measurements at the gas solid interface:**

General procedure:

Carrier gas: Nitrogen;

Analyte: from certificate graduate cylinder by SAPIO S.r.l. These cylinders were prepared with gravimetric procedure (ISO6142):

- methanol:  $516.00 \pm 0.02$  ppm, 150 bar;
- ethanol:  $504.00 \pm 0.02$  ppm, 26 bar;
- n-propanol:  $501.40 \pm 0.02$  ppm, 10 bar;
- n-butanol:  $100.40 \pm 0.02$  ppm, 10 bar;
- n-pentanol:  $98.30 \pm 0.02$  ppm, 10 bar;

Total flux: 400 sccm;

To obtain the exact concentration of analytes require for the measurements, the analyte were diluted in nitrogen, using two mass flow controllers.

Excitation wavelength = 330 nm

Emission spectra: 350-600 nm,

Time drive parameters:

- Time increment: 4 sec
- Integration time: 4 sec
- excitations: 330 nm,
- emission: 460 nm;
- excitations slit 2 nm;
- emission slit: 5 nm,
- excitation filter: Neutral Density Filters (Nominal Transmittance 008)

**Thin film deposition:**

Solution A:

in a volumetric flask 120 mg of Low Molecular Weight PVC and 260  $\mu\text{l}$  of Bis(2-ethylhexyl) sebacate were dissolved in 3 mL of distilled THF, The mixture was stirred and sonicated for 1.5 h, until complete solution of PVC.

Solution B:

in a volumetric flask 0.50 mg ( $4 \cdot 10^{-4}$  mmol) of fluorescent receptor was dissolved in 1 mL of distilled THF.

Solution C:

the solution was made by mixing 500  $\mu\text{l}$  of solution A with 500  $\mu\text{l}$  of solution B. The spin coating was made on glass substrate (2 cm $\times$ 2cm) using one to five drops of solution C.



### ***3.8 References***

- <sup>1</sup> M. Melegari, Ph.D. Thesis, University of Parma, **2008**.
- <sup>2</sup> B. Bibal, B. Tinant, J.-P. Declercq, J.-P. Dutasta, *Chem. Commun.*, **2002**, 432.
- <sup>3</sup> B. Cantadori, P. Betti, F. Boccini, C. Massera, E. Dalcanale, *Supramol. Chem.* **2008**, 20, 29.
- <sup>4</sup> P. Delangle, J.-C. Mulatier, B. Tinant, J.-P. Dutasta, *Eur. J. Org. Chem.* **2001**, 3695.



# Inherently chiral phosphonate cavitands as enantioselective receptors for chiral alcohols and L-amino acids.

# 4

## *4.1 Introduction*

Chiral recognition is a key issue in both living and artificial systems. It is essential for biological function and has a central role in asymmetric synthesis and chiral separation.<sup>1</sup>

In biological systems enantiomeric discrimination is performed by interaction of chiral molecules with enantiomerically pure receptors.<sup>2</sup> The progress of supramolecular chemistry has given a great impulse to the development of chiral host molecules and their great effectiveness in enantiomeric separations has been demonstrated by chromatographic methods,<sup>3</sup> capillary electrophoresis<sup>4</sup> and other approaches.<sup>5</sup>

Zhang, Bradshaw and Izatt<sup>6</sup> have proposed the following rules for effective enantiomeric recognition with chiral macrocyclic receptors:

- 1- an essential requirement is that the chiral macrocycles form reasonably stable complexes with the guest enantiomers so that the repulsive interactions can effectively lessen the stability of the complex of one enantiomer;

- 2- large chiral barrier(s) result in a high degree of enantiomeric recognition;
- 3- low conformational flexibility of diastereomeric complexes plays an important role in good enantiomeric recognition. Two factors, rigid macrocycles and multipoint interactions, ensure a fixed conformation of the complexes;
- 4- the structural complementarity between chiral macrocycles and enantiomers ensures that the chiral barriers of macrocycles make full use of steric repulsion for enantiomeric recognition;
- 5- macrocyclic receptors possessing  $C_2$ ,  $C_3$ , and  $D_2$  symmetry usually show higher enantioselectivity than those of  $C_1$  and  $D_3$  symmetry.

In the last years calixarenes and resorcin[4]arenes have proved to be good candidates for the design of such chiral supramolecular receptors.<sup>7,8</sup>

In the case of resorcin[4]arenes based cavitands, there are two different ways to obtain chiral systems. In the first one chirality is induced by the introduction of stereogenic centre at the upper or lower rim, with the aromatic cavity only being used as a rigid scaffold (Figure 4.1).



**Figure 4.1.** Model of a chiral cavitand containing a stereogenic centre.

The second way is the design of inherently chiral molecules. As defined by Szumna<sup>9</sup> in a recent review, “*inherent chirality arises from the introduction of a curvature in an ideal planar structure that is devoid of perpendicular symmetry planes in its bidimensional representation*”

The desymmetrization of the cavity can be achieved by introducing at least three different bridging group, obtaining compounds of type ABCD or AABC (Figure 4.2). An examples of this cavitand has recently been reported by Dutasta and coworkers.<sup>8</sup>

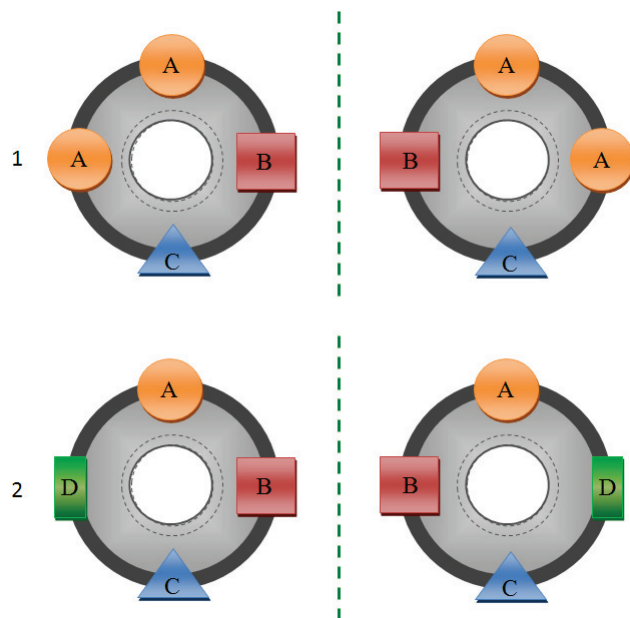


**Figure 4.2.** Model of inherently chiral cavitands type AABC (1) and ABCD (2).

The second strategy that lead to inherently chiral cavitand is the introduction of three identical bridging group and a fourth asymmetric one (Figure 4.3).<sup>10</sup>

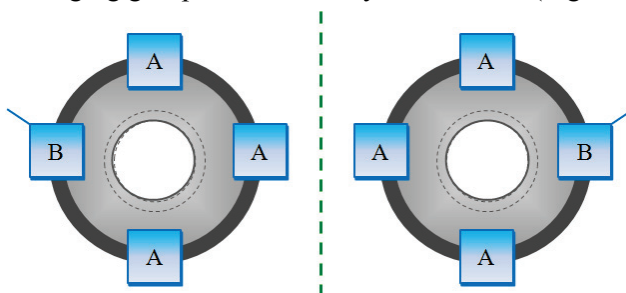


**Figure 4.3.** Model of inherently chiral cavitands type AAAB.

Thanks to the stronger chiral characters of the inner cavity, chiral cavitands type AABC and ABCD are the best candidates to be used as enantioselective receptors.

Phosphorous derivative of resorcin[4]arenes have shown outstanding recognition properties toward short chain alcohols, methylammonium or

methylpyridinium cations due to the synergistic formations of H-bonding, CH- $\pi$ , and cation-dipole interactions.

In this chapter we wanted to exploit the binding properties of phosphonate cavitands to obtain a chiral receptor for enantioselective recognition of chiral alcohols and N-methyl amino acids.

In particular we have designed the mixed-bridged thiophosphonate cavitand type AABC shown in figure 4.4, containing two inward P=O groups in adjacent position, one inward P=S group and a methylene bridge.

This cavitand, combining the good complexation properties of phosphonate cavitands and an inherently chiral cavity, is a promising receptors for enantiomeric separation of the target analytes.

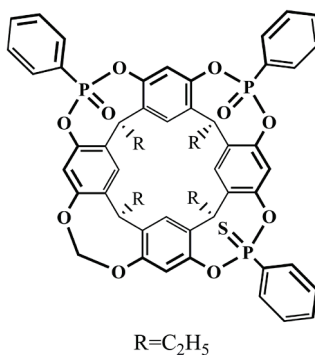
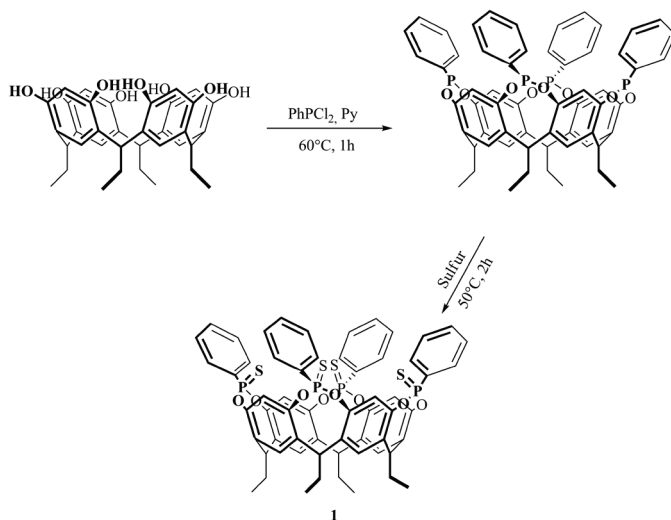


**Figure 4.4.** Target inherently chiral cavitand.

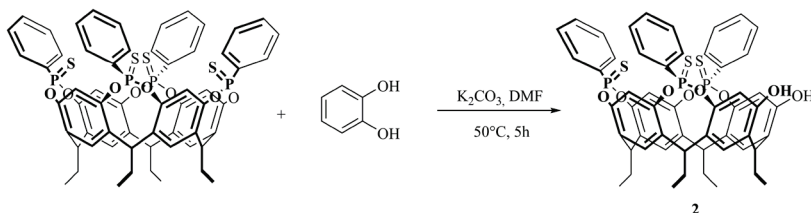
## 4.2 Synthesis of the receptor

The target cavitand was synthesised in six steps starting from the synthesis of the tetrathiophosphonate cavitand **1**. This reaction was carried out as described in chapter three. Resorcin[4]arene was treated with PhPCl<sub>2</sub> in the presence of pyridine to give exclusively the tetraphosphonito cavitand. The subsequent *in situ* oxidation with sulfur, which proceeded with retention of configuration at phosphorous centre, led to **1** in good yield (Scheme 4.1).



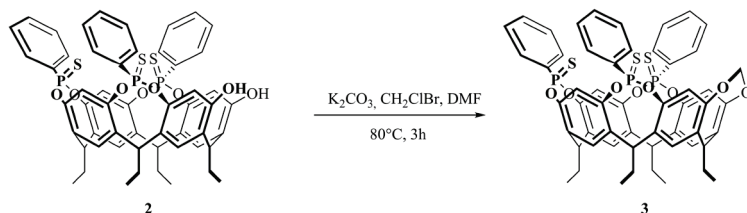
**Scheme 4.1.** Synthesis of the  $TS_{iii}[C_2H_5, H, Ph]$ .

The second step was the selective excision of one of the four P=S bridges of the  $TS_{iii}[C_2H_5, H, Ph]$  **1** to obtain  $3PS_{iii}$  resorcinarene **2** as already described in chapter three by using a stoichiometric amount of catechol in the presence of  $K_2CO_3$  (Scheme 4.2).



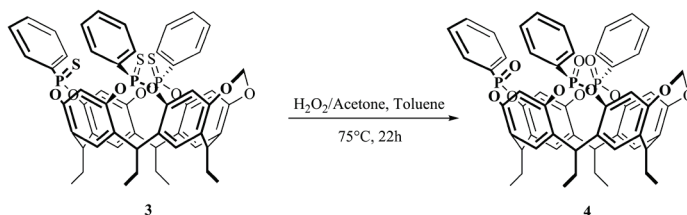
**Scheme 4.2.** Synthesis of the trithiophosphonate resorcinarene.

The  $3PS_{iii}Me$  cavitands **3** was obtained quantitatively by a bridging reaction of resorcinarene **2** with  $CH_2ClBr$  in the presence of  $K_2CO_3$  (Scheme 4.3).



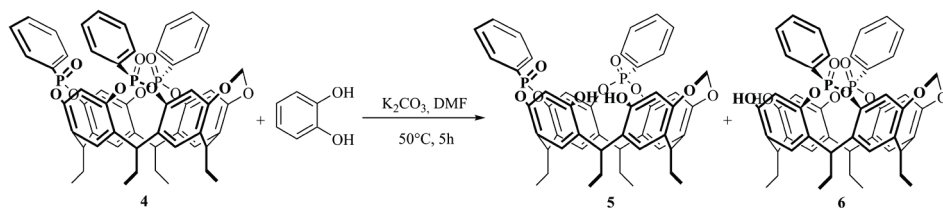
**Scheme 4.3.** Synthesis of the  $3PS_{iii}Me$  cavitand.

The next step was the conversion of the three P=S group into P=O group, by reaction with  $H_2O_2$  (Scheme 4.4), that led to  $3PO_{iii}Me$  cavitands **4** in quantitative yield.



**Scheme 4.4.** Synthesis of the  $3PO_{iii}Me$  cavitand.

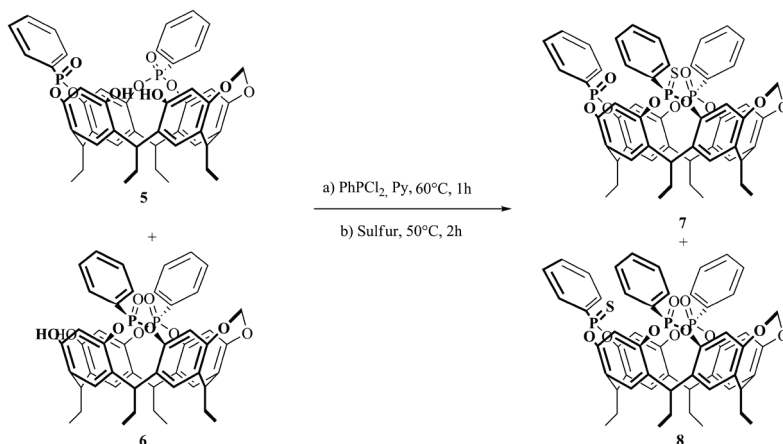
This reaction was followed by the excision of one of the P=O bridges of the  $3PO_{iii}Me$  cavitand **4** using, as described above, a stoichiometric amount of catechol in the presence of  $K_2CO_3$  (Scheme 4.5) to obtain the two isomers  $(AB)2PO_{ii}Me$  **5** and  $(AC)2PO_{ii}Me$  **6**.



**Scheme 4.5.** Synthesis of the  $(AB)2PO_{ii}Me$  **5** and  $(AC)2PO_{ii}Me$  **6** resorcinarenes.

The last step was the introduction of the inward PS bridging group through a reaction between a mixture of the resorcinarenes  $(AB)2PO_{ii}Me$  **5** and  $(AC)2PO_{ii}Me$  **6** and  $PhPCl_2$  in the presence of pyridine to give the cavitands  $(AB)2PO_{ii}1PS_iMe$  **7** and  $(AC)2PO_{ii}1PS_iMe$  **8** (Scheme 4.6).





**Scheme 4.6.** Synthesis of the (AB)2PO<sub>ii</sub>1PS<sub>i</sub>Me **7** and (AC)2PO<sub>ii</sub>1PS<sub>i</sub>Me **8** cavitands.

Cavitands (AB)2PO<sub>ii</sub>1PS<sub>i</sub>Me **7** and (AC)2PO<sub>ii</sub>1PS<sub>i</sub>Me **8** are diastereoisomers, but only the (AB)2PO<sub>ii</sub>1PS<sub>i</sub>Me **7** is an inherently chiral cavitand type AABC. Indeed, the presence of three different bridging groups and of the two P=O groups in adjacent position causes a desymmetrization of the cavity. In contrast, the (AC)2PO<sub>ii</sub>1PS<sub>i</sub>Me **8**, with the two P=O groups facing each other, has a plane of symmetry and so it is not chiral.

The two diastereoisomers AB and AC have been separated by customary chromatographic column since they have a different R<sub>f</sub>. The identification of the two isomers has been done by <sup>1</sup>H NMR. The signals corresponding to the proton in apical position are diagnostic. Indeed in the case of the symmetric AC isomer we observed only two signal corresponding to this protons (Figure 4.5), whereas in the case of the AB isomer we observed four different signal (Figure 4.6) because of the absence of any element of symmetry. In this case the two different P=O signals of the AB isomer do not differentiate at the <sup>31</sup>P NMR.

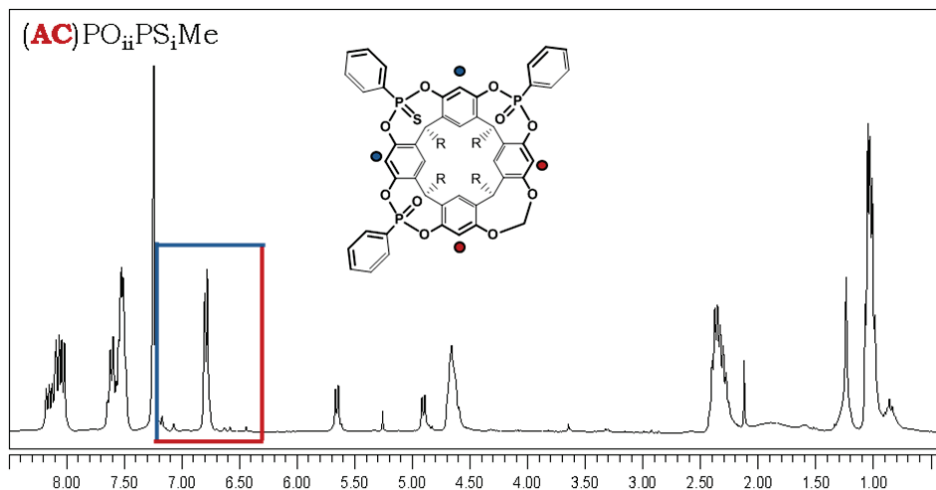


**Figure 4.5.**  $^1H$  NMR spectrum of the (AC) $2PO_{ii}PS_iMe$  8 cavitant.

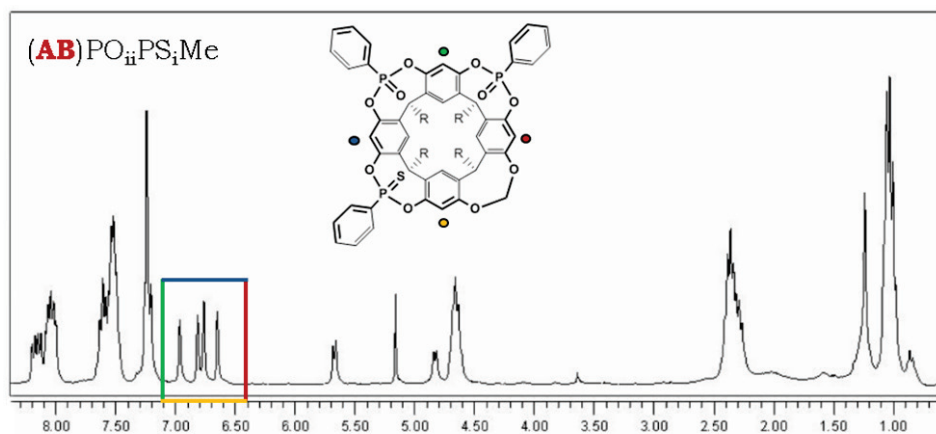


**Figure 4.6.**  $^1H$  NMR spectrum of the (AB) $2PO_{ii}1PS_iMe$  7 cavitant.

The two enantiomers of the AB cavitant (Figure 4.7) have been designated as cR or cS, where c stands for curvature, following the notation proposed by the group of Mandolini and Schiaffino.<sup>11</sup> In our case, the bridges have been labeled as 1, 2, 3 according to the CIP sequence rules.<sup>12</sup> An ideal observer standing on the concave side of the surface will see the three highest priority atoms 1, 2, and 3 describing a clockwise cR or a counterclockwise array cS.

So far the two enantiomers of the AB cavitand have not been separated. We are still trying to separate them either via diastereoselective crystallization with chiral guests or via chiral HPLC.

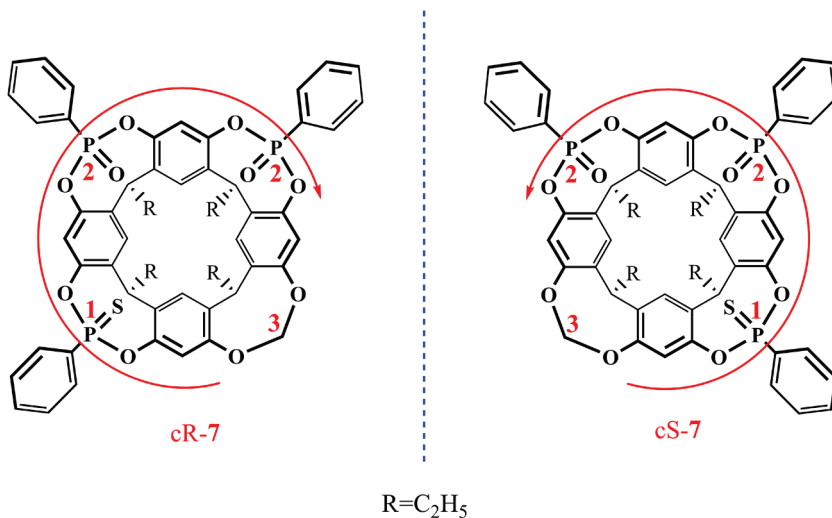


**Figure 4.7.** Enantiomers of racemic  $(AB)_2PO_{ii}1PS_iMe$  7 cavitand.

### 4.3 Evaluation of $(AB)_2PO_{ii}1PS_iMe$ enantioselective recognition properties in the solid state

In order to evaluate the complexation properties of  $(AB)_2PO_{ii}1PS_iMe$  7 toward chiral alcohols we decided to study them in the solid state. In particular a preliminary study using racemic 2-butanol (Figure 4.8) as guest was performed, obtaining very interesting and promising results.

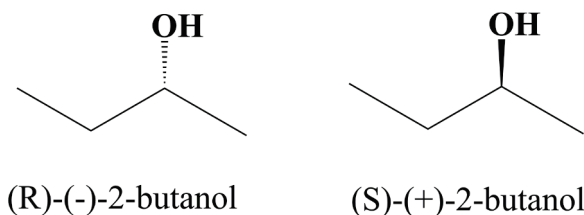


**Figure 4.8.** Structure of (R)-(-)-2-butanol and (S)-(+)-2-butanol.

The crystal structure reported in figure 4.9, shows an enantioselective complexation of the chiral guest, demonstrating the complete enantioselectivity of the chiral cavitand **7**. In the solid state indeed, it is important to notice that the cR-(AB)<sub>2</sub>PO<sub>ii</sub>1PS<sub>i</sub>Me enantiomer complexes exclusively the (R)-(-)-2-butanol, whereas the cS-(AB)<sub>2</sub>PO<sub>ii</sub>1PS<sub>i</sub>Me enantiomer binds only the (S)-(+)-2-butanol.

The cavitand-alcohol interaction mode is based on the synergy between the H-bonding to a P=O group and the CH- $\pi$  interactions of the methyl residue with the cavity for both complexes. Both enantiomers present the same interaction mode with the preferred receptor. Therefore, this enantioselectivity is principally based on the steric repulsion between the host and the guest having in this case opposite configuration (cR-S; cS-R).

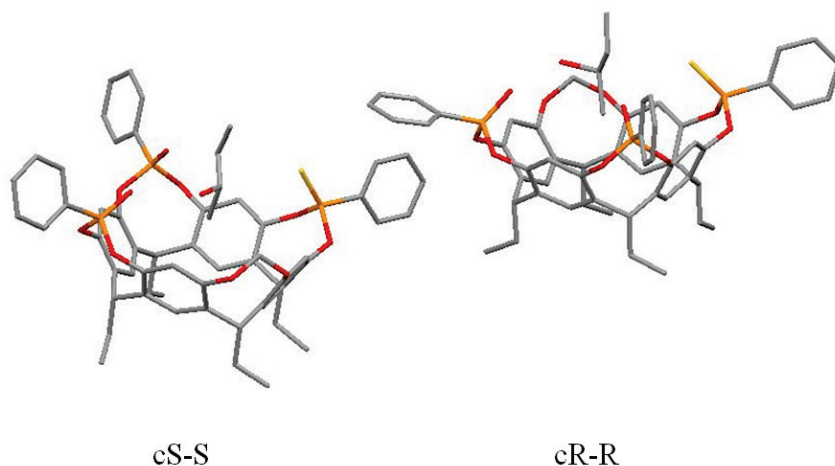


**Figure 4.9.** Side view of the crystal structure of racemic (AB)<sub>2</sub>PO<sub>ii</sub>1PS<sub>i</sub>Me•(±)iBuOH complexes.

Indeed, the conformational rigidity of the two enantiomeric cavitands reduces the structural complementarity between the R/S cavitands and the S/R guests (Figure 4.10), resulting in complete enantioselectivity in the crystal structure.

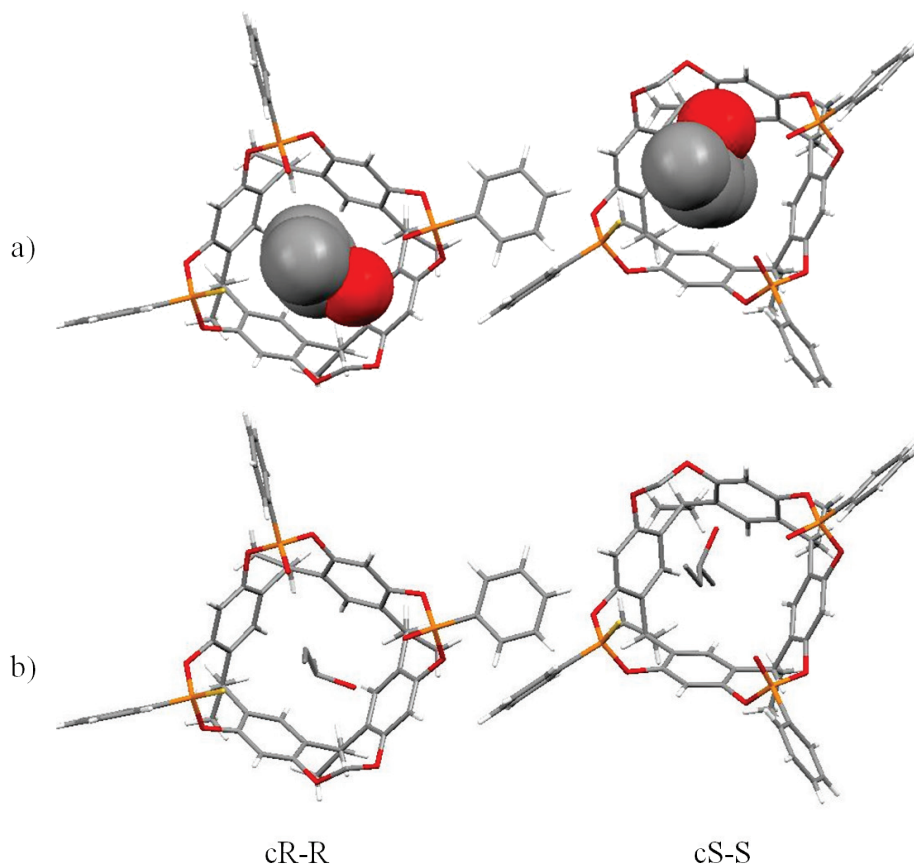


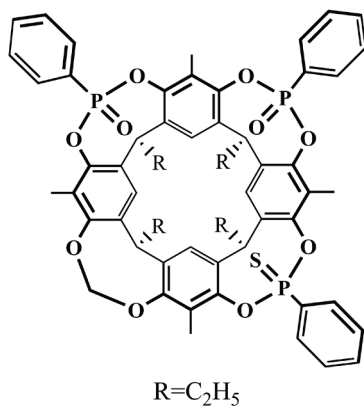
**Figure 4.10.** Top view of the crystal structure of racemic  $(AB)_2PO_{ii}1PSiMe \cdot (\pm)iBuOH$  complexes: a) guests represented with spacefill style to highlight their steric hindrance; b) guests represented with stick style .

After these first good results, a diastereoselective crystallization with a pure enantiomers of the chiral alcohol as solvent was attempted to separate the two enantiomers. The racemic mixture of  $AB_2PO_{ii}1PSiMe$  cavitand was dissolved separately in (R)-(-)-2-butanol and (S)-(+)-2-butanol. In both cases no crystals were formed, but only amorphous powder precipitated. This negative result might be rationalized in terms of packing in the crystal structure. It is well-known that racemic mixtures of enantiomeric complexes crystallized better than pure ones due to their complementary packing in the solid state.

After the failure of diastereoselective crystallization some attempts of enantioseparation by chiral HPLC were performed. Work is in progress in this direction.

#### 4.4 Synthesis of a new target receptor

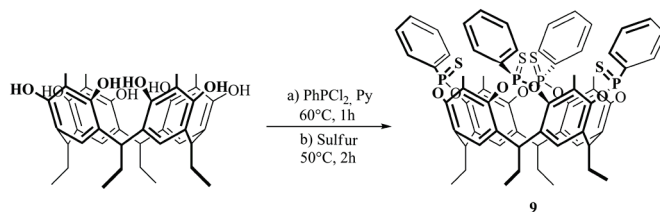
In order to obtain a stronger receptor in terms of complexation we decided to synthesise an  $(AB)_2PO_{ii}1PS_iMe$  with methyl groups in apical position instead of protons (Figure 4.11). This substitution makes the cavity deeper and enhances its  $\pi$ -basic character, promoting CH- $\pi$  interactions between the alcohol alkyl chain and the resorcinarene skeleton.



15

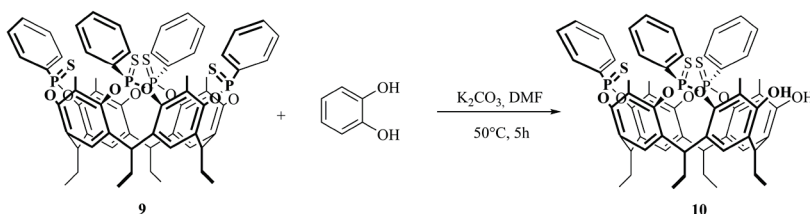
**Figure 4.11.**  $(AB)_2PO_{ii}1PS_iMe[C_2H_5, CH_3, Ph]$  cavitaand.

The  $(AB)_2PO_{ii}1PS_iMe[C_2H_5, CH_3, Ph]$  has been synthesised in the same way described above for the  $(AB)_2PO_{ii}1PS_iMe[C_2H_5, H, Ph]$ . The first step was the synthesis of the  $TS_{iiii}[C_2H_5, CH_3, Ph]$  **9**. Resorcin[4]arene was treated with  $PhPCl_2$  in the presence of pyridine to give exclusively the tetraphosponito cavitaand. The subsequent *in situ* oxidation with sulfur, proceeded with retention of configuration at phosphorous centre, giving **9** in good yield (Scheme 4.7).



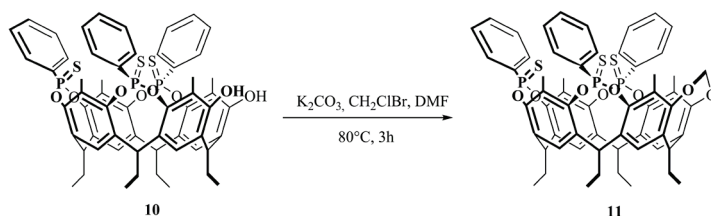
**Scheme 4.7.** Synthesis of the  $\text{TS}_{\text{iii}}[\text{C}_2\text{H}_5, \text{CH}_3, \text{Ph}]$ .

The next step was the selective excision of one of the four P=S bridges of the  $\text{TS}_{\text{iii}}[\text{C}_2\text{H}_5, \text{CH}_3, \text{Ph}]$  **9**, using a stoichiometric amount of cathecol in the presence of  $\text{K}_2\text{CO}_3$ , that led to  $3\text{PS}_{\text{iii}}$  resorcinarene **10** (Scheme 4.8).



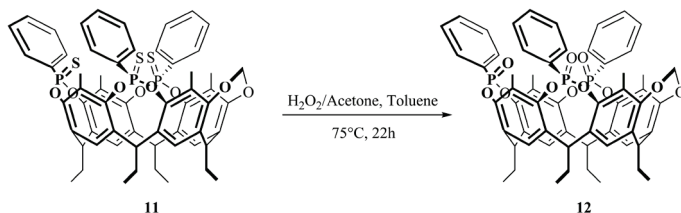
**Scheme 4.8.** Synthesis of the trithiophosphonate resorcinarene.

The following bridging reaction of resorcinarene **10** with  $\text{CH}_2\text{ClBr}$  in the presence of  $\text{K}_2\text{CO}_3$  led to  $3\text{PS}_{\text{iii}}\text{Me}$  cavitands **11** in quantitative yield (Scheme 4.9).



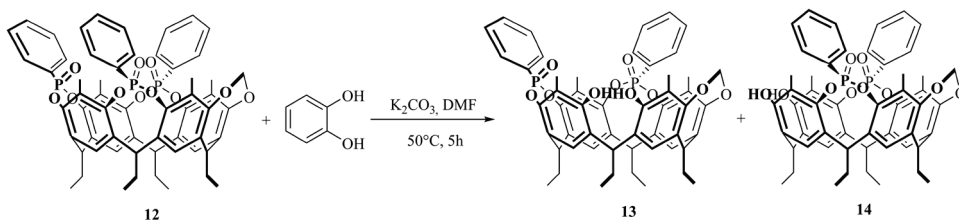
**Scheme 4.9.** Synthesis of the  $3\text{PS}_{\text{iii}}\text{Me}$  cavitand.

The fourth step was the conversion of the three P=S group into P=O group, by reaction with  $\text{H}_2\text{O}_2$  (Scheme 4.10), that give  $3\text{PO}_{\text{iii}}\text{Me}$  cavitands **12** quantitatively.



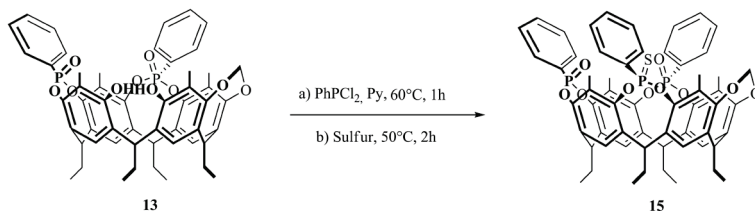
**Scheme 4.10.** Synthesis of the  $3\text{PO}_{\text{iii}}\text{Me}$  cavitand.

This reaction was followed by the excision of one of the  $\text{P}=\text{O}$  bridges of the  $3\text{PO}_{\text{iii}}\text{Me}$  cavitand **12** using, as described above, a stoichiometric amount of catechol in the presence of  $\text{K}_2\text{CO}_3$  (Scheme 4.11) to obtain the two isomers  $(\text{AB})_2\text{PO}_{\text{ii}}\text{Me}$  **13** and  $(\text{AC})_2\text{PO}_{\text{ii}}\text{Me}$  **14**.



**Scheme 4.11.** Synthesis of the  $(\text{AB})_2\text{PO}_{\text{ii}}\text{Me}$  **13** and  $(\text{AC})_2\text{PO}_{\text{ii}}\text{Me}$  **14** resorcinarenes.

In this case the two diastereoisomers AB and AC have been separated at this step by customary chromatographic column thanks to their different  $R_f$ . The last step was the introduction of the inward PS bridging group through a reaction between the resorcinarene  $(\text{AB})_2\text{PO}_{\text{ii}}\text{Me}$  **13** and  $\text{PhPCl}_2$  in the presence of pyridine followed by oxidation with sulfur to give the cavitand  $(\text{AB})_2\text{PO}_{\text{ii}}\text{IPS}_{\text{i}}\text{Me}$  **15** (Scheme 4.12).





**Scheme 4.12.** Synthesis of the  $(AB)2PO_{ii}1PS_iMe$  **15** and  $(AC)2PO_{ii}1PS_iMe$  **16** cavitands.

Also in this case all attempts to separate the cavitand enantiomers via distereoselective crystallization failed.

A crystal structure of the free cavitand with trifluoroethanol sits inside the cavity was obtained from trifluoroethanol (Figure 4.12).

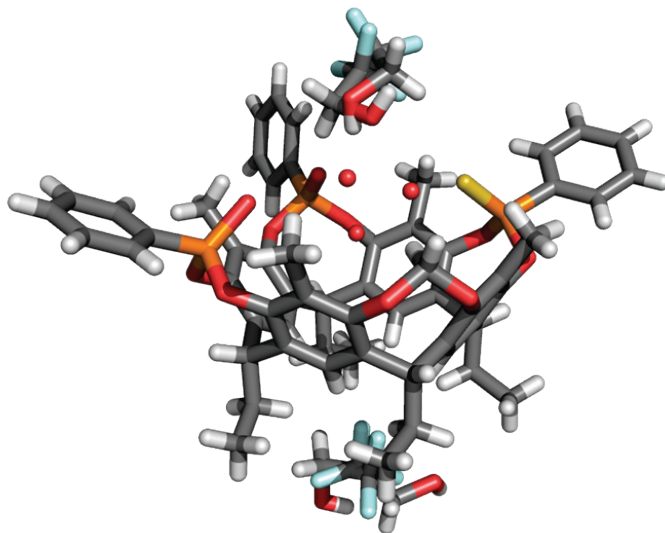


**Figure 4.12.** Portion of the crystal structure of  $(AB)2PO_{ii}1PS_iMe[C_2H_5, CH_3, Ph]$ .

The crystal packing (Figure 4.13) shows that each crystallographic cell contains the two enantiomers, which interact with each other by CH- $\pi$  interactions between the aromatic ring and the methylene bridging group.

Even in this case, in the solid state the packing of the two enantiomers in the crystallographic cell is preferred.

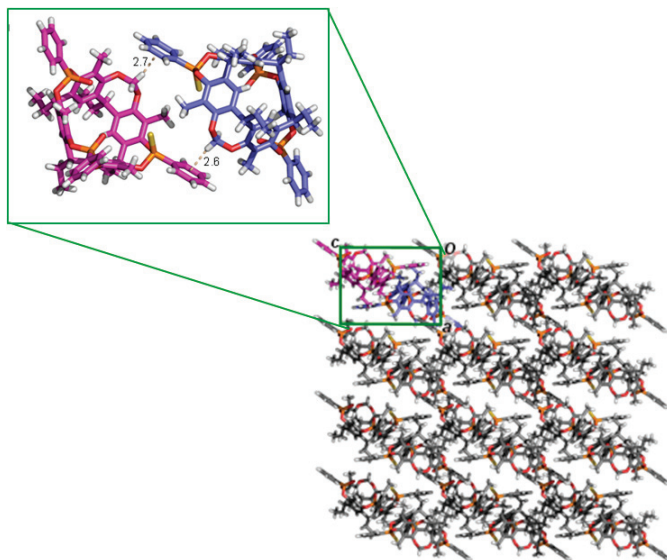


**Figure 4.13.** Crystal packing of racemic  $(AB)2PO_{ii}1PS_iMe[C_2H_5, CH_3, Ph]$  cavitand.

#### 4.5 Evaluation of $(AB)2PO_{ii}1PS_iMe$ enantioselective recognition properties in solution toward *N*-methyl amino acids

To study the recognition properties of cavitand  $(AB)2PO_{ii}1PS_iMe$  **15** in solution toward enantiopure chiral guests,  $^1H$  and  $^{31}P$  NMR titrations with *N*-methyl-*L*-leucine hydrochloride (Figure 4.14) in chloroform were performed. We chose this guest because tetraphosphonate cavitands have shown outstanding complexation properties toward *N*-methyl ammonium salts with association constant exceeding  $10^9 M^{-1}$  in chlorinated solvents.<sup>13</sup>

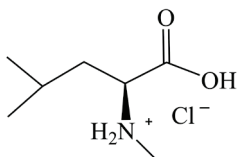


**Figure 4.14.** Chemical structure of *N*-methyl-*L*-leucine hydrochloride.

Increasing amounts of *N*-methyl-*L*-leucine hydrochloride as solid were added to a solution of racemic **15**. *N*-methyl-*L*-leucine hydrochloride is insoluble in

chloroform, but in the presence of the cavitand, which play the role of a solid-liquid extractant, its complete solubilisation was observed.  $^1\text{H}$  and  $^{31}\text{P}$  NMR spectra were recorded at 253K because at room temperature the diastereomeric complexes could not be observed due to the fast host-guest exchange rate on the NMR timescale. At 253K the host-guest exchange becomes slow and the signal corresponding to the two diastereoisomeric complexes could be observed.  $^{31}\text{P}$  NMR spectra reported in figure 4.15 shows that after the addition of 0.4 eq. of N-methyl-L-leucine hydrochloride the signal corresponding to the P=O groups of the free cavitand (6.85 and 8.20 ppm) were still present but also a new set of four signals corresponding to the P=O of the two diastereoisomeric complexes (9.84, 10.16, 11.95, 12.10) was observed.

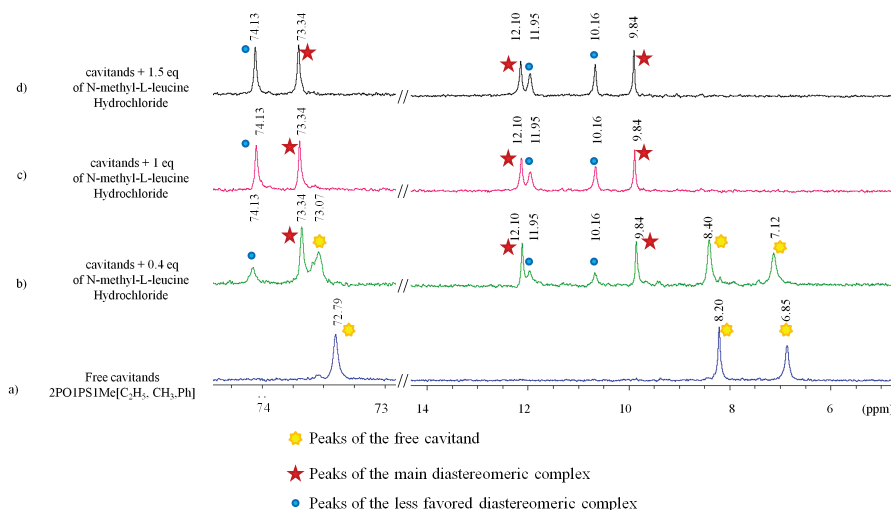


**Figure 4.15.**  $^{31}\text{P}$  NMR spectra ( $\text{CDCl}_3$ ) of (a) **15**; (b) **15** after the addition of 0.4 eq of guest; (c) **15** after the addition of 1 eq of guest; (d) **15** after the addition of 1.5 eq of guest.

Comparing the integrals of the  $^{31}\text{P}$  NMR peaks of the two diastereomeric complexes in the presence of a 1:0.4 host-guest ratio a 2.5:1 diastereomeric ratio was observed. This means that, as expected, one of the two enantiomers better accommodates the guest, demonstrating the enantioselectivity of the receptors. The addition of 1 equivalent of the guest caused the saturation of the host and consequently led to the disappearance of the peaks of the free cavitand and to an

increase of the intensity of the ones corresponding to the two diastereomeric complexes. In the presence of a stoichiometric amount of the guest, the high association constant caused the full complexation of the guest, overcoming the enantioselectivity of the receptor.

Also the peak of the P=S groups (72.79 ppm in the free cavitands), after the addition of the guest was split into two signals (73.34, 74.13 ppm) due to the presence of two diastereomeric complexes.

In the case of the  $^1\text{H}$  NMR spectra (Figure 4.16), after the addition of the guest, two signals at negative ppm corresponding to the N-CH<sub>3</sub> proton of the guest was observed. The two signals are due to the presence of two diastereomeric complexes whereas the highfield chemical shift of these protons is the result of the shielding effect exerted by the aromatic rings of the resorcinarene moiety and confirmed the N-CH<sub>3</sub> complexation inside the cavity.

The resonance of the methyl group of the preferred complex is shifted upfield more than the other one upon complexation, a clear indication of its higher affinity.

The correct attribution of the chirality of the cavitand which binds selectively N-methyl-L-leucine needs the resolution of the racemic cavitand mixture into its enantiomers.

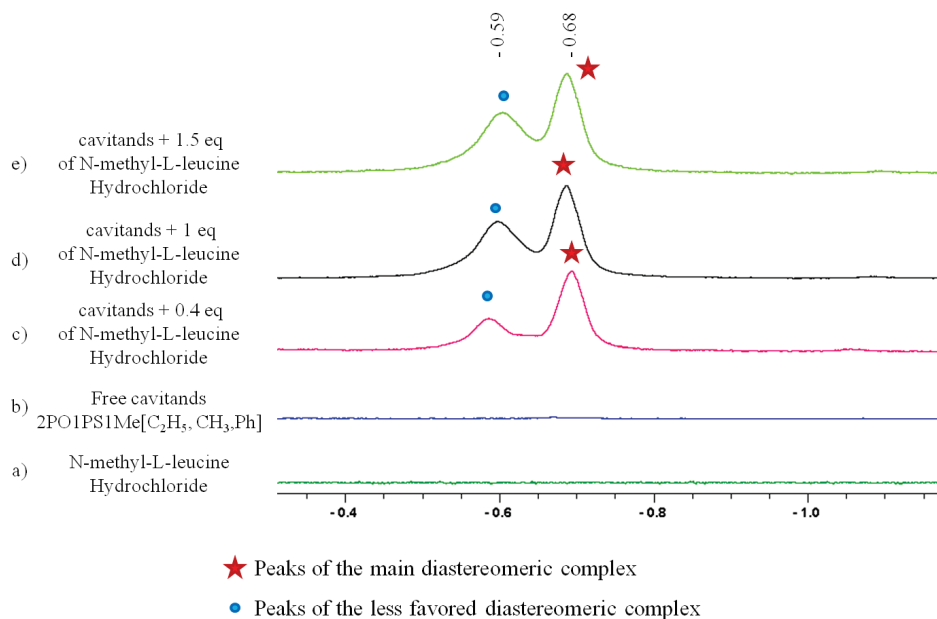


**Figure 4.16.**  $^1\text{H}$  NMR spectra ( $\text{CDCl}_3$ ) of (a) N-methyl-L-leucine hydrochloride; (b) **15**; (c) **15** after the addition of 0.4 eq of guest; (d) **15** after the addition of 1 eq of guest; (e) **15** after the addition of 1.5 eq of guest.

## 4.6 Conclusions

Cavitands (AB)<sub>2</sub>PO<sub>ii</sub>1PS<sub>i</sub>Me[C<sub>2</sub>H<sub>5</sub>, H, Ph] **7** and (AB)<sub>2</sub>PO<sub>ii</sub>1PS<sub>i</sub>Me[C<sub>2</sub>H<sub>5</sub>, CH<sub>3</sub>, Ph] **15** have shown promising enantioselective recognition properties towards chiral alcohols and N-methyl amino acids either at the solid state or in solution.

In particular, the cS and cR-enantiomers of cavitand **7** in the solid state showed a complete preference toward respectively the (S)-2-butanol and (R)-2-butanol. The selective complexation of N-methyl-L-leucine by one of the two enantiomers of cavitand **15** in solution demonstrates that one of them better accommodates the guest. In both the cases the steric repulsion between the receptor and the enantiomer in the wrong configuration resulting in high enantioselectivity of the system. In solution the high association constant of <sup>+</sup>N-CH<sub>3</sub> salts, overcome the chiral selectivity when the host-guest ratio is 1:1. Ongoing effort are made to separate the enantiomers in order to better

investigate their recognition properties and to test them as chiral receptor for sensing measurement at the gas-solid interface with QCM transducers and for discrimination of L and D N-methyl amino acids in solution.

#### 4.7 Acknowledgments

Special thanks to Carlo Nicosia of University of Parma and Prof. Silvano Geremia of University of Trieste.

#### 4.8 Experimental section

##### Cavitand TS<sub>iiii</sub>[C<sub>2</sub>H<sub>5</sub>, H, Ph] (1)

To a solution of resorcinarene (R= C<sub>2</sub>H<sub>5</sub>) (1.50 g, 2.50 mmol) in dry pyridine (50 mL), dichlorophenylphosphine (1.32 mL, 10.20 mmol) was added dropwise, under argon atmosphere. The solution was stirred at 60 °C for 1 h. Sulfur (0.51 g, 2.00 mmol) was added and the mixture was heated at 50°C for 2 h. The solvent was removed under *vacuum* and the solid was washed and sonicated with water, then filtered and dried. The crude product was purified by column chromatography (SiO<sub>2</sub>, gradient from 4:6 to 3:7, hexane/CH<sub>2</sub>Cl<sub>2</sub> v/v) affording **1** as white solid (1.85 g, 64%). <sup>1</sup>H NMR (300 MHz, CDCl<sub>3</sub>): δ= 8.17 (m, 8H, P(S)ArH<sub>o</sub>), 7.56 (m, 4H, P(S)ArH<sub>p</sub>), 7.51 (m, 8H, P(S)ArH<sub>m</sub>), 7.30 (s, 4H, ArH<sub>down</sub>), 6.67 (s, 4H, ArH<sub>up</sub>), 4.64 (t, 4H, ArCH, J=7.1 Hz), 2.39 (m, 8H, CH<sub>2</sub>CH<sub>3</sub>), 1.06 (t, 12H, CH<sub>2</sub>CH<sub>3</sub>, J=6.8 Hz); <sup>31</sup>P NMR (162 MHz, CDCl<sub>3</sub>): δ = 77.77 (s, 4P, P=S). ESI-MS m/z (%): 1175.3 [M+Na]<sup>+</sup>.

##### Trithiophosphonate[C<sub>2</sub>H<sub>5</sub>, H, Ph] resorcinarene (2)

Cavitand **1** (1.00 g, 0.86 mmol) was dissolved in dry DMF (30 mL) at 50°C. Cathecol (0.10 g, 0.91 mmol) and K<sub>2</sub>CO<sub>3</sub> (1.20 g, 8.67 mmol) were added and the mixture was stirred at 80°C for 5 h. The solvent was removed under *vacuum* and the solid was washed and sonicated with water, then filtered and dried. The crude product was purified by column chromatography (SiO<sub>2</sub>, 99:1, CH<sub>2</sub>Cl<sub>2</sub>/EtOH v/v) affording **2** as white solid (0.46 g, 52%). <sup>1</sup>H NMR (300 MHz, CDCl<sub>3</sub>): δ= 8.17 (m, 6H, P(S)ArH<sub>o</sub>), 7.57-7.53 (m, 9H, P(S)ArH<sub>p</sub>+P(S)ArH<sub>m</sub>), 7.32 (s, 2H, ArH<sub>down</sub>), 7.20 (s, 2H, ArH<sub>down</sub>), 6.68 (s, 2H, ArH<sub>up</sub>),

6.49 (s, 2H, ArH<sub>up</sub>), 4.64 (m, 4H, ArCH), 2.39-2.26 (m, 8H, CH<sub>2</sub>CH<sub>3</sub>), 1.07-1.00 (m, 12H, CH<sub>2</sub>CH<sub>3</sub>); <sup>31</sup>P NMR (162 MHz, CDCl<sub>3</sub>): δ = 77.42 (s, 1P, P=S), 76.27 (s, 2P, P=S); **ESI-MS** m/z (%): 1015.6 [M+H]<sup>+</sup>, 1037.3 [M+Na]<sup>+</sup>, 1054.7 [M+K]<sup>+</sup>.

### **3PS<sub>iii</sub>Me[C<sub>2</sub>H<sub>5</sub>, H, Ph] cavitand (3)**

To a solution of **2** (0.20 g, 0.19 mmol) in DMF (15 mL), K<sub>2</sub>CO<sub>3</sub> (0.16 g, 1.18 mmol) and CH<sub>2</sub>BrCl (128 μL, 0.62 mmol) were added under nitrogen.

The mixture was stirred at 90°C for 3 hours. The solvent was removed under vacuum and the solid was dissolved in CH<sub>2</sub>Cl<sub>2</sub> and washed with water affording the pure product **3** as a white solid in quantitative yield (198 mg). <sup>1</sup>H NMR (CDCl<sub>3</sub>, 300 MHz): δ = 8.17 (m, 6H, P(S)ArH<sub>o</sub>); 7.60 (m, 3H, P(S)ArH<sub>p</sub>); 7.54 (m, 6H, P(S)ArH<sub>m</sub>); 7.26 (s, 4H, ArH<sub>down</sub>); 6.66 (s, 2H, ArH<sub>up</sub>); 6.59 (s, 2H, ArH<sub>up</sub>); 5.75 (d, 1H, CH<sub>2(out)</sub>, J=7.4 Hz); 4.64 (m, 4H, ArCH); 4.51 (d, 1H, CH<sub>2(in)</sub>, J=7.4 Hz); 2.35 (m, 8H, CH<sub>2</sub>CH<sub>3</sub>); 1.06 (m, 12H, CH<sub>2</sub>CH<sub>3</sub>); <sup>31</sup>P NMR: (CDCl<sub>3</sub>, 400 MHz): δ = 7.38 (s, 1P, P=S); 6.50 (s, 2P, P=S); **ESI-MS** (m/z): 1044.3 [M+NH<sub>4</sub>]<sup>+</sup>, 1049.3 [M+Na]<sup>+</sup>, 1065.3 [M+K]<sup>+</sup>.

### **3PO<sub>iii</sub>Me[C<sub>2</sub>H<sub>5</sub>, H, Ph] cavitand (4)**

To a solution of cavitand **3** (0.11 g, 0.11 mmol) in toluene (10 mL) a solution of H<sub>2</sub>O<sub>2</sub> 35% (0.65 mL, 6.66 mmol) in acetone (2.6 mL) was added dropwise. The mixture was stirred at 75°C for 24h. The reaction was quenched by addition of H<sub>2</sub>O. The aqueous phase was extracted with CH<sub>2</sub>Cl<sub>2</sub>. The two organic phases were put together and evaporated. The crude product was purified by column chromatography (SiO<sub>2</sub>, 97:3, CH<sub>2</sub>Cl<sub>2</sub>/EtOH v/v) affording **4** as white solid (109 mg, 96%). <sup>1</sup>H NMR (CDCl<sub>3</sub>, 300 MHz): δ = 8.03 (m, 6H, P(O)ArH<sub>o</sub>); 7.66 (m, 3H, P(O)ArH<sub>p</sub>); 7.57 (m, 6H, P(O)ArH<sub>m</sub>); 7.29 (s, 2H, ArH<sub>down</sub>); 7.26 (s, 2H, ArH<sub>down</sub>); 6.99 (s, 2H, ArH<sub>up</sub>); 6.83 (s, 2H, ArH<sub>up</sub>); 5.69 (d, 1H, CH<sub>2(out)</sub>, J=7.4 Hz); 5.03 (d, 1H, CH<sub>2(in)</sub>, J=7.4 Hz); 4.71 (m, 4H, ArCH); 2.35 (m, 8H, CH<sub>2</sub>CH<sub>3</sub>); 1.07 (m, 12H, CH<sub>2</sub>CH<sub>3</sub>); <sup>31</sup>P NMR: (CDCl<sub>3</sub>, 400 MHz): δ = 7.40 (s, 1P, P=O); 6.73 (s, 2P, P=O); **ESI-MS** (m/z): 1001.4 [M+Na]<sup>+</sup>, 1017.4 [M+K]<sup>+</sup>.

**(AB)2PO<sub>ii</sub>Me[C<sub>2</sub>H<sub>5</sub>, H, Ph] (5) and (AC)2PO<sub>ii</sub>Me[C<sub>2</sub>H<sub>5</sub>, H, Ph] (6)**

To a solution of cavitand **4** (0.10 g, 0.10 mmol) in DMF (10 mL), catechol (0.01 g, 0.10 mmol) and K<sub>2</sub>CO<sub>3</sub> (0.14 g, 1.02 mmol) were added and the mixture was stirred at 80°C for 5 h. The solvent was removed under *vacuum* and the solid was washed and sonicated with water, then filtered and dried. The crude product was purified by column chromatography (SiO<sub>2</sub>, 92:8, CH<sub>2</sub>Cl<sub>2</sub>/EtOH v/v) to obtain a mixture of the two isomers **5** and **6** (46 mg, 52%). The mixture of the two isomers were used in the next step without any further purification. **ESI-MS** (m/z): 857.3 [M+H]<sup>+</sup>, 880.3 [M+Na]<sup>+</sup>, 895.3 [M+K]<sup>+</sup>.

**(AB)2PO<sub>ii</sub>1PS<sub>i</sub>Me[C<sub>2</sub>H<sub>5</sub>, H, Ph] (7) and (AC)2PO<sub>ii</sub>1PS<sub>i</sub>Me[C<sub>2</sub>H<sub>5</sub>, H, Ph] (8)**

To a solution of cavitands **5** and **6** (0.09 g, 0.11 mmol) in dry pyridine (5 mL), dichlorophenylphosphine (15 μL, 0.11 mmol) was added dropwise, under argon atmosphere. The solution was stirred at 70 °C for 1 h. Sulfur (0.007 g, 0.03 mmol) was added and the mixture was heated at 50°C for 2 h. The solvent was removed under *vacuum* and the solid was washed and sonicated with water, then filtered and dried. The crude product was purified by column chromatography (SiO<sub>2</sub>, 95:5, CH<sub>2</sub>Cl<sub>2</sub>:MeOH v/v) affording cavitands **7** (25 mg, 23%) and **8** (32 mg, 29%).

**7:** <sup>1</sup>H NMR (CDCl<sub>3</sub>, 300 MHz): δ = 8.16 (m, 2H, P(S)ArH<sub>o</sub>); 8.00 (m, 4H, P(O)ArH<sub>o</sub>); 7.63-7.49 (m, 9H, P(X)ArH<sub>p</sub>, P(X)ArH<sub>m</sub>, X=O,S); 7.22 (m, 4H, ArH<sub>down</sub>); 6.96 (s, 1H, ArH<sub>up</sub>); 6.81 (s, 1H, ArH<sub>up</sub>); 6.76 (s, 1H, ArH<sub>up</sub>); 6.65 (s, 1H, ArH<sub>up</sub>); 5.67 (d, 1H, CH<sub>2(out)</sub>, J=7.4 Hz); 5.16 (d, 1H, CH<sub>2(in)</sub>, J=7.4 Hz); 4.71 (m, 4H, ArCH); 2.35 (m, 8H, CH<sub>2</sub>CH<sub>3</sub>); 1.07 (m, 12H, CH<sub>2</sub>CH<sub>3</sub>); <sup>31</sup>P NMR: (CDCl<sub>3</sub>, 400 MHz): δ = 75.64 (s, 1P, P=S); 6.97 (s, 2P, P=O); **ESI-MS** (m/z): 995.4 [M+H]<sup>+</sup>, 1017.4 [M+Na]<sup>+</sup>, 1074.4 [M+K]<sup>+</sup>.

**8:** <sup>1</sup>H NMR (CDCl<sub>3</sub>, 300 MHz): δ = 8.15 (m, 2H, P(S)ArH<sub>o</sub>); 8.05 (m, 4H, P(O)ArH<sub>o</sub>); 7.64-7.48 (m, 9H, P(X)ArH<sub>p</sub> + P(X)ArH<sub>m</sub>, X=O,S); 7.24 (m, 4H, ArH<sub>down</sub>); 6.80 (s, 2H, ArH<sub>up</sub>); 6.78 (s, 2H, ArH<sub>up</sub>); 5.67 (d, 1H, CH<sub>2(out)</sub>, J=7.4 Hz); 4.90 (d, 1H, CH<sub>2(in)</sub>, J=7.4 Hz); 4.65 (m, 4H, ArCH); 2.35 (m, 8H, CH<sub>2</sub>CH<sub>3</sub>); 1.02 (m, 12H, CH<sub>2</sub>CH<sub>3</sub>); <sup>31</sup>P NMR (CDCl<sub>3</sub>, 400 MHz): δ = 76.79



(s, 1P, P=S); 6.99 (s, 2P, P=O). **ESI-MS (m/z)**: 995.4 [M+H]<sup>+</sup>, 1017.4 [M+Na]<sup>+</sup>, 1074.4 [M+K]<sup>+</sup>.

### **Cavitand TS<sub>iii</sub>[C<sub>2</sub>H<sub>5</sub>, CH<sub>3</sub>, Ph] (9)**

To a solution of resorcinarene (R= C<sub>2</sub>H<sub>5</sub>) (3.00 g, 4.57 mmol) in dry pyridine (65 mL), dichlorophenylphosphine (2.53 mL, 18.6 mmol) was added dropwise, under argon atmosphere. The solution was stirred at 60 °C for 1 h. Sulfur (0.70 g, 2.70 mmol) was added and the mixture was heated at 50°C for 2 h. The solvent was removed under *vacuum* and the solid was washed and sonicated with water, then filtered and dried. The crude product was purified by column chromatography (SiO<sub>2</sub>, gradient from 5:5 to 4:6, hexane/CH<sub>2</sub>Cl<sub>2</sub> v/v) affording **9** as white solid (1.93 g, 60%). **<sup>1</sup>H NMR** (300 MHz, CDCl<sub>3</sub>): δ= 8.24 (m, 8H, P(S)ArH<sub>o</sub>), 7.61 (m, 12H, P(S)ArH<sub>p</sub>, P(S)ArH<sub>m</sub>), 7.26 (s, 4H, ArH<sub>down</sub>), 4.63 (t, 4H, ArCH, J=6.8 Hz), 2.39 (m, 8H, CH<sub>2</sub>CH<sub>3</sub>), 1.36 (s, 12H, CH<sub>3</sub>), 1.05 (t, 12H, CH<sub>2</sub>CH<sub>3</sub>, J=7.1 Hz); **<sup>31</sup>P NMR** (162 MHz, CDCl<sub>3</sub>): δ = 72.43 (s, 4P, P=S). **ESI-MS m/z (%)**: 1209.8 [M+H]<sup>+</sup>, 1226.8 [M+NH<sub>4</sub>]<sup>+</sup>, 1231.8 [M+Na]<sup>+</sup>, 1247.7 [M+K]<sup>+</sup>.

### **Trithiophosphonate[C<sub>2</sub>H<sub>5</sub>, CH<sub>3</sub>, Ph] resorcinarene (10)**

Cavitand **9** (2.00 g, 1.65 mmol) was dissolved in dry DMF (55 mL) at 50°C. Cathecol (0.19 g, 1.74 mmol) and K<sub>2</sub>CO<sub>3</sub> (2.28 g, 16.5 mmol) were added and the mixture was stirred at 80°C for 5 h. The solvent was removed under *vacuum* and the solid was washed and sonicated with water, then filtered and dried. The crude product was purified by column chromatography (SiO<sub>2</sub>, gradient from 100% CH<sub>2</sub>Cl<sub>2</sub> to 98:2, CH<sub>2</sub>Cl<sub>2</sub>/EtOH v/v) affording **10** as white solid (0.59 g, 30%). **<sup>1</sup>H NMR** (300 MHz, CDCl<sub>3</sub>): δ= 8.25 (m, 6H, P(S)ArH<sub>o</sub>), 7.61 (m, 9H, P(S)ArH<sub>p</sub>+ P(S)ArH<sub>m</sub>), 7.28 (s, 2H, ArH<sub>down</sub>), 7.18 (s, 2H, ArH<sub>down</sub>), 4.59 (m, 3H, ArCH), 4.59 (t, 1H, ArCH, J=6.9 Hz), 2.40-2.19 (m, 8H, CH<sub>2</sub>CH<sub>3</sub>), 2.17 (s, 6H, CH<sub>3</sub>), 2.12 (s, 6H, CH<sub>3</sub>), 1.05-0.94 (m, 12H, CH<sub>2</sub>CH<sub>3</sub>); **<sup>31</sup>P NMR** (162 MHz, CDCl<sub>3</sub>): δ = 72.36 (s, 1P, P=S), 71.82 (s, 2P, P=S); **ESI-MS m/z (%)**: 1070.9 [M+H]<sup>+</sup>, 1108.9 [M+K]<sup>+</sup>.

**3PS<sub>iii</sub>Me[C<sub>2</sub>H<sub>5</sub>, CH<sub>3</sub>, Ph] cavitand (11)**

To a solution of **10** (1.10 g, 1.04 mmol) in DMF (50 mL), K<sub>2</sub>CO<sub>3</sub> (0.86 g, 6.48 mmol) and CH<sub>2</sub>BrCl (2.02 mL, 3.10 mmol) were added under nitrogen. The mixture was stirred at 90°C for 3 hours. The solvent was removed under vacuum and the solid was dissolved in CH<sub>2</sub>Cl<sub>2</sub> and washed with water affording the pure product **11** as white solid in quantitative yield (1.10 g). <sup>1</sup>H NMR (CDCl<sub>3</sub>, 300 MHz): δ = 8.23 (m, 6H, P(S)ArH<sub>o</sub>); 7.61 (m, 9H, P(S)ArH<sub>p</sub>, P(S)ArH<sub>m</sub>); 7.21 (s, 4H, ArH<sub>down</sub>); 5.89 (d, 1H, CH<sub>2(out)</sub>, J=6.4 Hz); 4.77 (t, 1H, ArCH, J=7.7 Hz); 4.59 (t, 3H, ArCH, J=7.7 Hz); 4.41 (d, 1H, CH<sub>2(in)</sub>, J=6.4 Hz); 2.36 (m, 8H, CH<sub>2</sub>CH<sub>3</sub>); 2.16 (s, 6H, CH<sub>3</sub>), 2.11 (s, 6H, CH<sub>3</sub>), 1.08-0.96 (m, 12H, CH<sub>2</sub>CH<sub>3</sub>); <sup>31</sup>P NMR: (CDCl<sub>3</sub>, 400 MHz): δ = 7.39 (s, 1P, P=S); 6.51 (s, 2P, P=S); ESI-MS (m/z): 1083.4 [M+H]<sup>+</sup>, 1105.4 [M+Na]<sup>+</sup>, 1121.4 [M+K]<sup>+</sup>.

**3PO<sub>iii</sub>Me [C<sub>2</sub>H<sub>5</sub>, CH<sub>3</sub>, Ph] cavitand (12)**

To a solution of cavitand **11** (1.10 g, 1.02 mmol) in toluene (120 mL) a solution of H<sub>2</sub>O<sub>2</sub> 35% (5.12 mL, 50.80 mmol) in acetone (25 mL) was added dropwise. The mixture was stirred at 75°C for 24h. The reaction was quenched by addition of H<sub>2</sub>O. The aqueous phase was extracted with CH<sub>2</sub>Cl<sub>2</sub>. The two organic phases were put together and evaporated. The crude product was purified by column chromatography (SiO<sub>2</sub>, 98:2, CH<sub>2</sub>Cl<sub>2</sub>/EtOH v/v) affording **12** as white solid (1.02 g, 95%). <sup>1</sup>H NMR (CDCl<sub>3</sub>, 300 MHz): δ = 8.14 (m, 6H, P(O)ArH<sub>o</sub>); 7.67 (m, 3H, P(O)ArH<sub>p</sub>); 7.59 (m, 6H, P(O)ArH<sub>m</sub>); 7.14 (s, 2H, ArH<sub>down</sub>); 7.10 (s, 2H, ArH<sub>down</sub>); 5.87 (d, 1H, CH<sub>2(out)</sub>, J=7.1 Hz); 4.94 (d, 1H, CH<sub>2(in)</sub>, J=7.1 Hz); 4.79 (t, 1H, ArCH, J=7.5 Hz); 4.69 (t, 3H, ArCH, J=7.4 Hz); 2.37 (m, 8H, CH<sub>2</sub>CH<sub>3</sub>); 2.16 (s, 3H, CH<sub>3</sub>), 2.11 (s, 6H, CH<sub>3</sub>), 2.10 (s, 3H, CH<sub>3</sub>), 1.07 (m, 12H, CH<sub>2</sub>CH<sub>3</sub>); <sup>31</sup>P NMR: (CDCl<sub>3</sub>, 400 MHz): δ = 5.20 (s, 2P, P=O); 5.18 (s, 1P, P=O); ESI-MS (m/z): 1035.4 [M+H]<sup>+</sup>, 1057.2 [M+Na]<sup>+</sup>.

**(AB)2PO<sub>ii</sub>Me[C<sub>2</sub>H<sub>5</sub>, CH<sub>3</sub>, Ph] (13) and (AC)2PO<sub>ii</sub>Me[C<sub>2</sub>H<sub>5</sub>, CH<sub>3</sub>, Ph] (14)**

To a solution of cavitand **12** (0.83 g, 0.81 mmol) in DMF (85 mL), catechol (0.09 g, 0.81 mmol) and K<sub>2</sub>CO<sub>3</sub> (1.11 g, 8.10 mmol) were added and the mixture was stirred at 80°C for 5 h. The solvent was removed under *vacuum*

and the solid was washed and sonicated with water, then filtered and dried. The crude product was purified by column chromatography (SiO<sub>2</sub>, 7:3, ethyl acetate/hexane v/v) affording resorcinarenes **13** (110 mg, 15%) and **14** (177 mg, 24%).

**13:** <sup>1</sup>H NMR (CDCl<sub>3</sub>, 300 MHz): δ = 8.15 (m, 4H, P(O)ArH<sub>o</sub>); 7.67 (m, 2H, P(O)ArH<sub>p</sub>); 7.58 (m, 4H, P(O)ArH<sub>m</sub>); 7.16 (s, 1H, ArH<sub>down</sub>); 7.11 (s, 1H, ArH<sub>down</sub>); 7.05 (s, 1H, ArH<sub>down</sub>); 7.03 (s, 1H, ArH<sub>down</sub>); 5.90 (d, 1H, CH<sub>2(out)</sub>, J=6.9 Hz); 4.63 (m, 4H, CH<sub>2(in)</sub> and ArCH); 4.88 (t, 1H, ArCH, J=7.5 Hz); 2.31 (m, 8H, CH<sub>2</sub>CH<sub>3</sub>); 2.22 (s, 3H, CH<sub>3</sub>), 2.15 (s, 3H, CH<sub>3</sub>), 2.13 (s, 3H, CH<sub>3</sub>), 2.09 (s, 3H, CH<sub>3</sub>), 1.05 (m, 12H, CH<sub>2</sub>CH<sub>3</sub>); <sup>31</sup>P NMR: (CDCl<sub>3</sub>, 400 MHz): δ = 6.54 (s, 1P, P=O); 5.36 (s, 1P, P=O); **ESI-MS** (m/z): 935.1 [M+Na]<sup>+</sup>.

**14:** <sup>1</sup>H NMR (CDCl<sub>3</sub>, 300 MHz): δ = 8.95 (m, 4H, P(O)ArH<sub>o</sub>); 7.55 (m, 2H, P(O)ArH<sub>p</sub>); 7.47 (m, 4H, P(O)ArH<sub>m</sub>); 7.07 (s, 2H, ArH<sub>down</sub>); 6.95 (s, 2H, ArH<sub>down</sub>); 5.77 (d, 1H, CH<sub>2(out)</sub>, J=6.9 Hz); 4.68 (t, 1H, ArCH, J=7.9 Hz); 4.58 (t, 2H, ArCH, J=7.3 Hz); 4.40 (d, 1H, CH<sub>2(in)</sub>, J=6.9 Hz); 4.24 (t, 1H, ArCH, J=7.5 Hz); 2.26 (m, 8H, CH<sub>2</sub>CH<sub>3</sub>); 2.14 (s, 6H, CH<sub>3</sub>), 2.10 (s, 6H, CH<sub>3</sub>), 1.01 (m, 12H, CH<sub>2</sub>CH<sub>3</sub>); <sup>31</sup>P NMR: (CDCl<sub>3</sub>, 400 MHz): δ = 6.44 (s, 2P, P=O); **ESI-MS** (m/z): 935.3 [M+Na]<sup>+</sup>.

### (AB)<sub>2</sub>PO<sub>ii</sub>1PS<sub>i</sub>Me[C<sub>2</sub>H<sub>5</sub>, CH<sub>3</sub>, Ph] (**15**)

To a solution of cavitands **13** (0.10 g, 0.10 mmol) in dry pyridine (6 mL), dichlorophenylphosphine (13.5 μL, 0.10 mmol) was added dropwise, under argon atmosphere. The solution was stirred at 70 °C for 1 h. Sulfur (0.006 g, 0.03 mmol) was added and the mixture was heated at 50°C for 2 h. The solvent was removed under *vacuum* and the solid was washed and sonicated with water, then filtered and dried. The crude product was purified by column chromatography (SiO<sub>2</sub>, 1:1, ethyl acetate/hexane, v/v) affording cavitand **15** as white solid (17.8 mg, 17%).

**15:** <sup>1</sup>H NMR (CDCl<sub>3</sub>, 300 MHz): δ = 8.25 (m, 2H, P(S)ArH<sub>o</sub>); 8.12 (m, 4H, P(O)ArH<sub>o</sub>); 7.65 (m, 9H, P(X)ArH<sub>p</sub>, P(X)ArH<sub>m</sub>, X=O,S); 7.17 (s, 1H,

ArH<sub>down</sub>); 7.14 (s, 2H, ArH<sub>down</sub>); 7.11 (s, 1H, ArH<sub>down</sub>); 5.84 (d, 1H, CH<sub>2(out)</sub>, J=7.1 Hz); 5.78 (d, 1H, CH<sub>2(in)</sub>, J=7.1 Hz); 4.75 (m, 4H, ArCH); 2.37 (m, 8H, CH<sub>2</sub>CH<sub>3</sub>); 2.28 (s, 3H, CH<sub>3</sub>), 2.22 (s, 3H, CH<sub>3</sub>), 2.20 (s, 3H, CH<sub>3</sub>), 2.16 (s, 3H, CH<sub>3</sub>), 1.07 (m, 12H, CH<sub>2</sub>CH<sub>3</sub>); **<sup>31</sup>P NMR:** (CDCl<sub>3</sub>, 400 MHz): δ = 72.79 (s, 1P, P=S); 8.20 (s, 1P, P=O) 6.85 (s, 1P, P=O); **ESI-MS (m/z):** 1068.16 [M+NH<sub>4</sub>]<sup>+</sup>, 1073.2 [M+Na]<sup>+</sup>, 1089.2 [M+K]<sup>+</sup>.

### NMR titrations

Cavitand **15** (10 mg, 0.01 mmol) was dissolved in CDCl<sub>3</sub> (0.5 ml). This solution was titrated with solid N-methyl-L-leucine hydrochloride. <sup>1</sup>H and <sup>31</sup>P NMR spectra were recorded after each addition on a Bruker AVANCE 400 instrument. The temperature was held constant at 253K.

## 4.9 References

- <sup>1</sup> C. Moberg, *Angew. Chem. Int. Ed. Engl.* **2006**, *45*, 4721.
- <sup>2</sup> J. D. Rawn, *Biochemistry*, Patterson, Burlington, **1989**.
- <sup>3</sup> a) T. J. Ward, *Anal. Chem.* **2002**, *74*, 2863; b) V. Schurig, *J. Chromatogr., A*, **2002**, *965*, 315 b) V. Schurig, *J. Chromatogr., A*, **1994**, *666*, 111.
- <sup>4</sup> a) T.K. Natishan, *J. Liq. Chromatogr. Relat. Technol.* **2005**, *28*, 1115; b) J.L. Veuthey, *Anal. Bioanal. Chem.* **2005**, *381*, 93.
- <sup>5</sup> a) P. Castelnovo, C. Albanesi, *J. Chromatogr., A*, **1995**, *715*, 143; b) D.W. Armstrong, Y.-W. Zhou, *J. Liq. Chromatogr.* **1994**, *17*, 1695.
- <sup>6</sup> X.X. Zhang, J.S. Bradshaw, R. M. Izatt, *Chem. Rev.* **1997**, *97*, 3313.
- <sup>7</sup> a) C.S.M. Visotsky, V. Bohmer, *Adv. Sup. Chem.* **2000**, *7*, 139; b) V. Simulescu, G. Ilia, *J. Inclusion Phenom. Macrocycl. Chem.* **2010**, *66*, 3.
- <sup>8</sup> J. Vachon, S. Harthong, B. Dubessy, J.-P. Dutasta, N. Vanthuyne, C. Roussel, J.-V. Naubron, *Tetrahedron: Asymmetry*, **2010**, *21*, 1534.
- <sup>9</sup> A. Szumna, *Chem. Soc. Rev.* **2010**, *39*, 4274.
- <sup>10</sup> a) P. Soncini, S. Bonsignore, E. Dalcanale, F. Ugozzoli, *J. Org. Chem.* **1992**, *57*, 4608; b) A. Renslo, F.C. Tucci, D.M. Rudkevich, J. Jr Rebek, *J. Am. Chem. Soc.* **2000**, *122*, 4573.
- <sup>11</sup> A. Dalla Cort, L. Mandolini, C. Pasquini, L. Schiaffino, *New J. Chem.* **2004**, *28*, 1198.
- <sup>12</sup> IUPAC 1968 Tentative Rules, Section E, Fundamental Stereochemistry, in *J. Org. Chem.* **1970**, *35*, 2849.
- <sup>13</sup> R.M. Yebeutchou, F. Tancini, N. Demitri, S. Geremia, R. Mendichi, E. Dalcanale, *Angew. Chem. Int. Ed. Engl.* **2008**, *47*, 4504.



# Quinoxaline-bridged cavitands as molecular receptors for nitroaromatic explosives

# 5

## *5.1 Introduction*

An explosive is defined as a material (chemical or nuclear) that can be triggered to undergo very rapid, and self-propagating decomposition resulting in the formation of more stable material, liberation of heat or the development of sudden pressure effect.<sup>1</sup>

The energetic materials used by military as propellants and explosives are mostly organic compounds containing nitro (NO<sub>2</sub>) groups.

The detections of these explosive compounds is a highly significant task in forensic, antiterrorist activities and global de-mining projects. Moreover, the health risks associated with release of nitroaromatic explosives into the environment from military sites and former ammunition plants have led to major effort in developing explosive detection systems. Indeed, an important characteristics of nitroaromatic compounds is their ability to rapidly penetrate the skin. 2,4,6-Trinitrotoluene (TNT) explosive can readily enter groundwater supplies and has been classified as toxic at concentration above 2 ng ml<sup>-1</sup> by the Environmental Protection Agency<sup>2</sup> as it presents harmful effects to all life forms.<sup>3</sup>

In this context, the development of new, efficient, simple and inexpensive analytical method for the extraction, pre-concentration and detection of nitroaromatic compounds at traces level from liquid, solid and gaseous sample is of great importance.

The supramolecular approach to analytical chemistry<sup>4</sup> is particularly appealing due to the possibility of designing selective receptors as a function of the analytes to be detected. The rational design of highly selective receptors requires a molecular level understanding of the receptor-analyte interactions. Another essential feature is the reversibility of the responses, which requires recourse to weak interactions, since the formation of covalent or ionic bonds would result in an irreversible saturation of the receptors. By contrast to the widespread use of supramolecular chemistry in sensing<sup>5</sup> and in analytical separative methodologies,<sup>6</sup> this approach has not been deeply exploited in extraction techniques.<sup>7</sup>

In this chapter new mixed-bridged triquinoxaline and carboxyl acid cavitands (3QxCOOHCav) (Figure 5.1) are proposed as receptor for the realization of new selective materials to be used as trapping devices for nitroaromatic compounds.

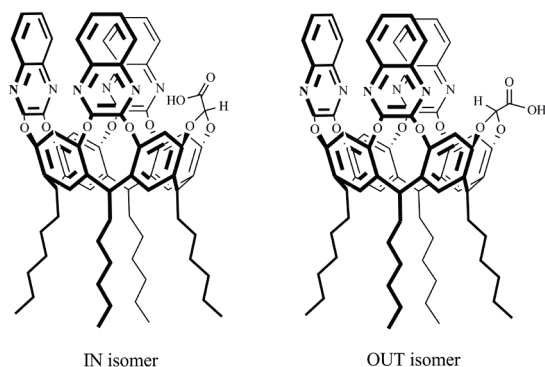


**Figure 5.1.** In and Out isomers of 3QxCOOH cavitands.



## 5.2 Quinoxaline-bridged cavitands

The design of 3QxCOOHCav has been based on our first experience in selective detection of aromatic compounds with tetraquinoxaline-bridged cavitands (QxCav). The molecular recognition properties of QxCav toward aromatic hydrocarbons are well known both in the gas phase<sup>8</sup> and in the solid state.<sup>9</sup> In both environments aromatic CH- $\pi$  interactions<sup>10</sup> are responsible for the observed complexation, both with the quinoxaline cavity walls<sup>11</sup> and with the resorcinarene scaffold.<sup>12</sup> These multiple weak interactions, made possible by the complete confinement of the guest within the cavity, render QxCav cavitands the receptor of choice for selecting aromatic over aliphatic hydrocarbons.

The transfer of these complexation properties at the gas-solid interface has been already proven with QxCav in gas sensing<sup>13</sup> using both mass<sup>14</sup> and surface plasmon resonance transducers.<sup>15</sup> Extraction of micro pollutants from water using QxCav in pure form has also been demonstrated.<sup>16</sup> In the latter case, selectivity in the inclusion has been attributed to the hydrophobicity of the guest, which prefers cavity inclusion to water solvation. SPME gel-coating based on QxCav as receptor has also been developed and proposed as a valid alternative to commercial fibers for selective determination of benzene and chlorobenzene at ultra-trace levels in environmental air and water samples.<sup>7</sup>

In the case of the 3QxCOOHCav reported in this chapter, in addition to CH- $\pi$  interactions between the aromatic skeleton of nitroaromatic compounds and the cavity bottom and walls, the presence of the COOH introduces a synergistic H-bonding interaction with the NO<sub>2</sub> group of the analytes. In order to demonstrate the importance of this additional H-bonding interaction we have also studied the complexation properties of mixed-bridged triquinoxaline and methylene cavitands (3QxMeCav) (Figure 5.2) toward nitroaromatic compounds.

Moreover, a QxCav (Figure 5.2) has also been prepared in order to compare the role of its fully aromatic cavity to the incomplete one of the 3Qx in the confinement of the guest within the cavity.

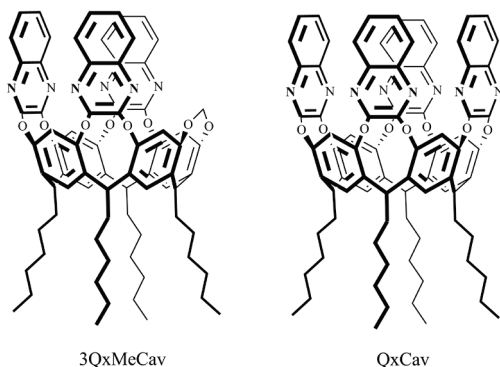
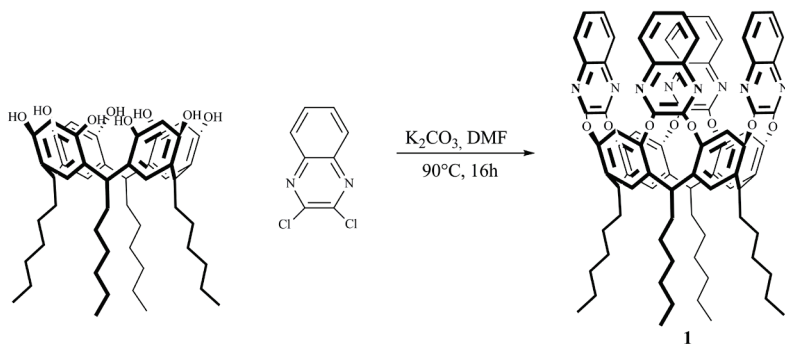


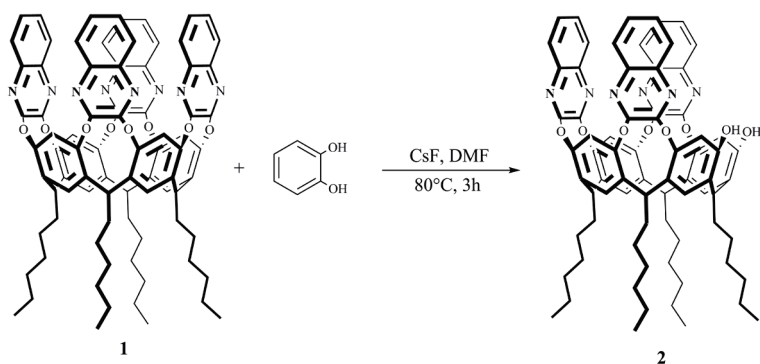
**Figure 5.2.** 3QxMeCav (left) and QxCav (right).

The preparation of the target molecule 3QxCOOHCav (in and out isomers) involve a multistep process starting from the synthesis of QxCav. This reaction was carried out following the established procedures for the preparation of homo-bridged cavitands (scheme 5.1).<sup>17</sup> Resorcin[4]arene was treated with 2,3-dichloroquinoxaline in the presence of  $K_2CO_3$  to give tetraquinoxaline-bridged cavitand **1** in good yield.



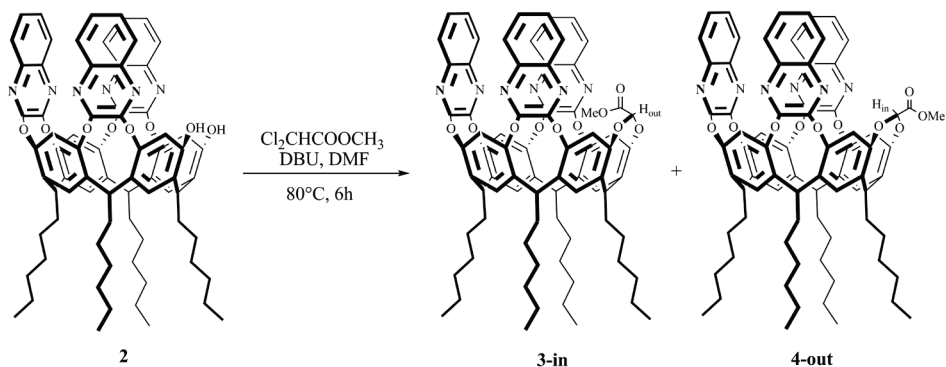
**Scheme 5.1.** Synthesis of Tetraquinoxaline cavitand (QxCav).

In the second step the triquinoxaline resorcinarene **2** was made following the procedure reported in literature for the selective excision of quinoxaline units from tetraquinoxaline cavitand.<sup>18</sup> This protocol require the use of a stoichiometric amount of cathecol in the presence of CsF as base (Scheme 5.2).



*Scheme 5.2. Excision of a Quinoxaline unit.*

The third step was the introduction of the desired carboxylic acid in the form of ester using methyl dichloroacetate as bridging reagent to give cavitands **3-in** and **4-out** (Scheme 5.3).



*Scheme 5.3. Synthesis of 3QxCOOCH<sub>3</sub> Cavitands.*

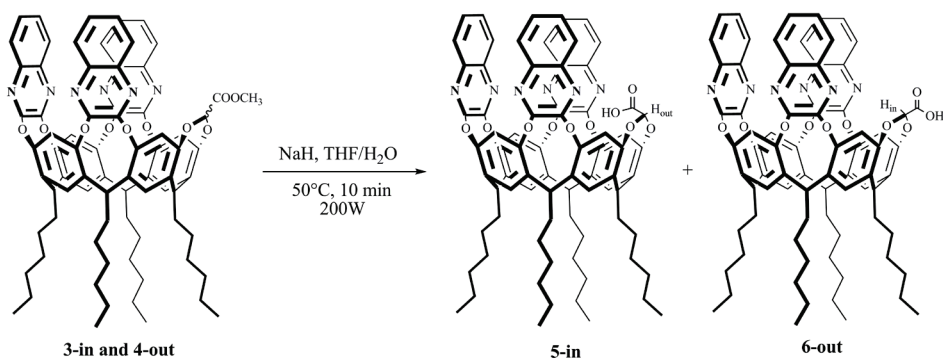
The configuration of the two isomers has been assigned via <sup>1</sup>H NMR on the basis of the different chemical shifts of the proton on the carbomethoxy group and the corresponding hydrogen on the same bridge, according to their orientation inward or outward with respect to the cavity (Table 5.1).

Protons inside the cavity resonate at higher field with respect to their outside counterparts, a feature diagnostic of inward orientation.

Cavitands	Chemical Shift (ppm) H on the bridge	Chemical Shift (ppm) CH3 on carbomethoxy group
<b>3-in</b>	5.99 (H <sub>out</sub> )	3.06 (CH <sub>3</sub> in)
<b>4-out</b>	4.34 (H <sub>in</sub> )	3.83 (CH <sub>3</sub> out)

**Table 5.1.** <sup>1</sup>H NMR diagnostic chemical shifts for the assignment of in/out isomers.

The last step was the microwave-assisted hydrolysis of both **3-in** and **4-out** cavitands with NaH in THF/water. This reaction led to the corresponding target carboxylic acid derivatives 3QxCOOHCav-In (**5-in**) and 3QxCOOHCav-Out (**6-out**) (Scheme 5.4).



**Scheme 5.4.** Synthesis of 3QxCOOH Cavitands.

As for 3QxCOOCH<sub>3</sub> cavitands, the configuration of the two isomers has been assigned via <sup>1</sup>H NMR (Table 5.2).

Cavitands	Chemical Shift (ppm) H on the bridge
<b>5-in</b>	5.60 (H <sub>out</sub> )
<b>6-out</b>	4.21 (H <sub>in</sub> )

**Table 5.2.** <sup>1</sup>H NMR diagnostic chemical shifts for the assignment of in/out isomers.

According with previous conformational behaviour studies of mixed-bridged cavitands with one of the four quinoxaline wings displaced by a different

bridge,<sup>17</sup> the <sup>1</sup>H NMR spectra of 3QxCOOHCav-Out (**6-out**) and 3QxCOOCH<sub>3</sub> (**3-in** and **4-out**) have confirmed that these cavitands, at room temperature, were fixed in the vase conformation.

In contrast to this, the <sup>1</sup>H NMR spectrum of 3QxCOOHCav-In (**5-in**) in CDCl<sub>3</sub> indicated a dynamic behaviour at room temperature with broadened signals and the H<sub>out</sub> resonance broadly smeared in the 5-6 ppm range. As it was shown before,<sup>19</sup> cavitand with four quinoxaline bridges experiences a dynamic equilibrium between the vase and the kite conformations; the vase form is preferred at T>290 K, whereas the kite conformer is predominant below 230 K.<sup>17</sup> In order to better investigate the behaviour of our 3QxCOOHCav-In we performed some <sup>1</sup>H NMR experiments in CDCl<sub>3</sub> at different temperatures (Figure 5.3).

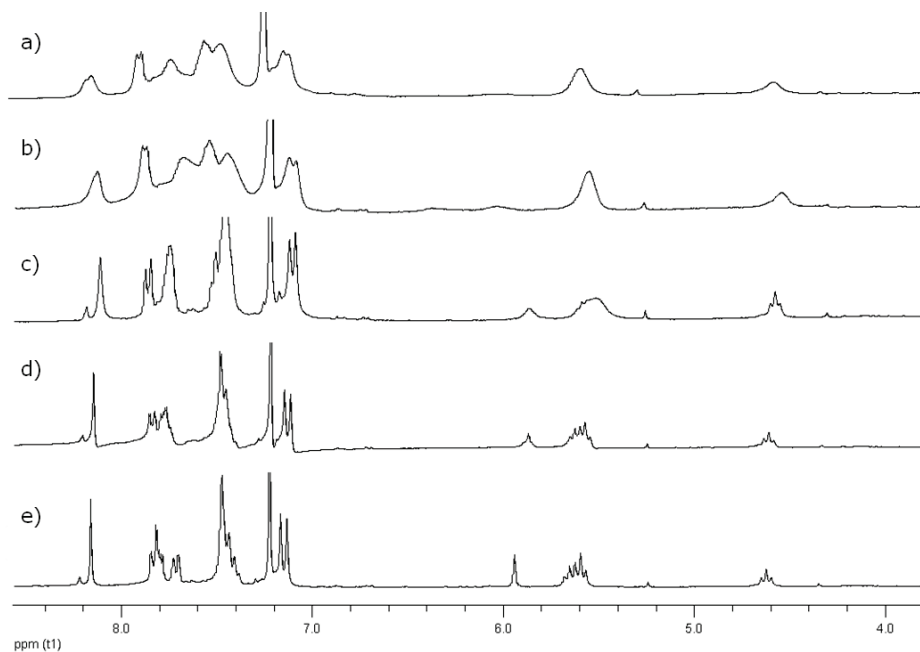
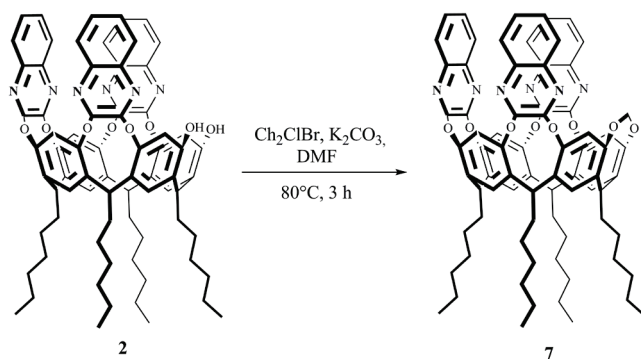


**Figure 5.3.** <sup>1</sup>H NMR spectra of **5-in** at different temperatures:  
a) T=218 K (dynamic behavior); b) T=223 K; c) T=255 K;  
d) T=298 K; e) T=323 K (cavitand in the vase conformation).

This study demonstrated that the vase conformation is favoured at higher temperature, whereas in contrast to the behaviour of the QxCav, at lower temperature this cavitand could not be frozen in the kite conformation. A possible explanation of this peculiar behaviour relies on the formation of dimers in solution driven by H-bonding between COOH moieties.

The first two steps of the synthesis of 3QxMeCav **7** are the same described for 3QxCOOHCav. The last one involved a bridging reaction of 3Qx resorcinarene **2** with  $\text{CH}_2\text{ClBr}$  in the presence of  $\text{K}_2\text{CO}_3$  that led to cavitand **7** in quantitative yield (Scheme 5.5).



*Scheme 5.5. Synthesis of 3QxMe Cavitand.*

### **5.3 Extraction capabilities of 3QxCOOH Cavitands towards nitroaromatic compounds**

As already written in the introduction, the aim of this work was the preparation of new selective materials to be used as trapping devices for nitroaromatic compounds. In particular preliminary studies to investigate the complexation properties and consequently the extraction capabilities of 3QxCOOHCav (**5-in** and **6-out**) towards nitroaromatic compounds were performed. These studies were conducted by using the Dynamic Headspace (DHS) technique. DHS techniques<sup>20</sup> (Figure 5.4) are based on the continuous transfer of volatile compounds present in a condensed phase into a gas phase (headspace). The volatiles are purged from the headspace with a flow of inert gas and can either be analysed directly<sup>21</sup> or more commonly be trapped<sup>22</sup> either cryogenically or on

a solid adsorbent. The trapped compounds can subsequently be desorbed rapidly to allow very low compound concentrations to be detected.

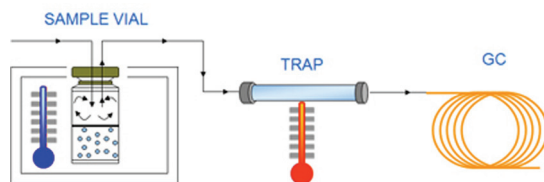


**Figure 5.4.** Operating principle of Dynamic Headspace.

We chose DHS for these preliminary studies because, unlike other techniques, cavitands can be directly introduced in the trap and used as solid adsorbent material without any further functionalization.

In collaboration with Dr. Federica Bianchi of GIAF department, we tested the sampling performance of 3QxCOOHcav (**5-in** and **6-out**), 3QxMeCav (**7**) and QxCav (**1**) towards a mixture of toluene, nitrobenzene, and 2-nitrotoluene in solution of methanol (1mg/L of each analyte). The complexation capabilities were also exploited toward a mixture of aliphatic hydrocarbons: octane, and decane in solution of n-pentane (1mg/L of each analyte). The former mixture has been analysed to demonstrate that the presence of the H-bonding donor group COOH, increases the selectivity of 3QxCOOH towards nitroaromatic compounds with respect to toluene and aromatic hydrocarbon in general. The latter has been analysed to evaluate the affinity of these quinoxaline cavitands towards aliphatic hydrocarbons.

All the measurements here reported were carried out at two different desorption temperatures: 50°C and 250°C. These temperatures have been chosen because at 50°C only the species physisorbed in the matrix were released, whereas at 250°C also the species selectively complexed by the cavity were desorbed.

The sampling experiments towards aliphatic hydrocarbons were not reported because of their too low chromatographic responses due to the very low affinity of these cavitands for these class of compounds.

The comparison of chromatographic responses of cavitands (**5-in**, **6-out**, **1** and **7**) towards toluene (figure 5.5) confirms that, in this case, the presence of the carboxylic acid did not influence host-guest interactions: the response of **5-in**,

**6-out**, and **7** at 250°C were similar. The higher response of the QxCav **1** shown that the complete paneling of the cavity with quinoxaline bridges favors the confinement of the guest.

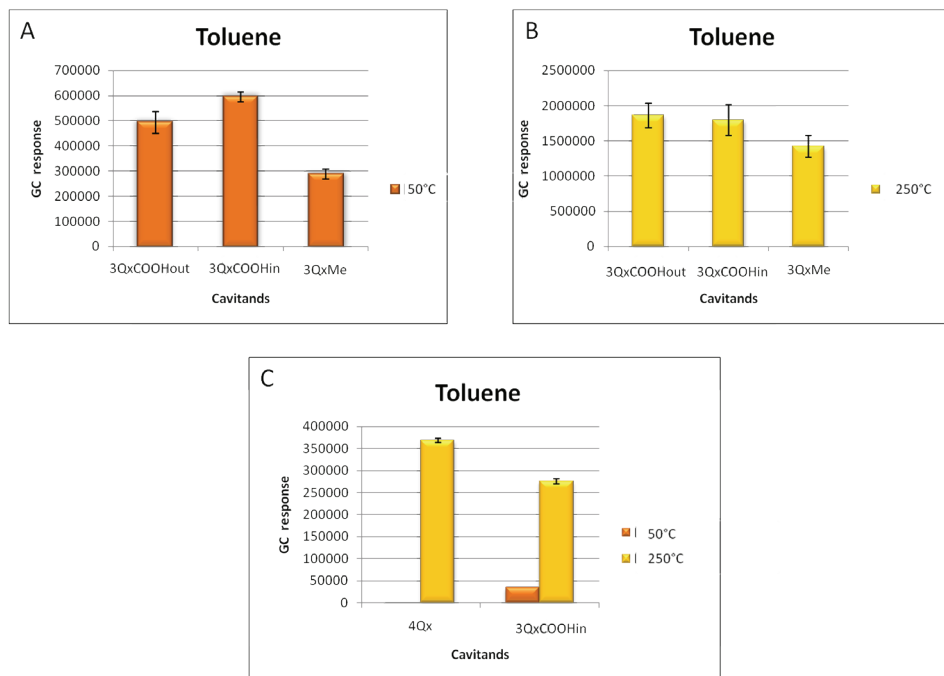


**Figure 5.5.** Performances of (A) 3QxCOOHCav-out, 3QxCOOHCav-in, 3QxMeCav toward toluene at 50°C; (B) 3QxCOOHCav-out, 3QXCOOHCav-in, 3QxMeCav toward toluene at 250°C; (C) QxCav and 3QxCOOHCav-in toward toluene at 50°C and 250°C.

The higher responses of 3QxCOOHCav **5-in** and **6-out**, towards nitrobenzene (Figure 5.6) and 2-nitrotoluene (figure 5.7) with respect to the one of 3QxMeCav **7** and QxCav **1** shown that the presence of an H-bonding donor in the form of a COOH group highly enhances the host-guest interactions with nitroaromatic compounds, independently from the inward or outward configuration. It has also to be noticed that in this case the closed cavity of QxCav did not increase the host-guest interactions. This is likely due to the increasing steric hindrance of the guest.



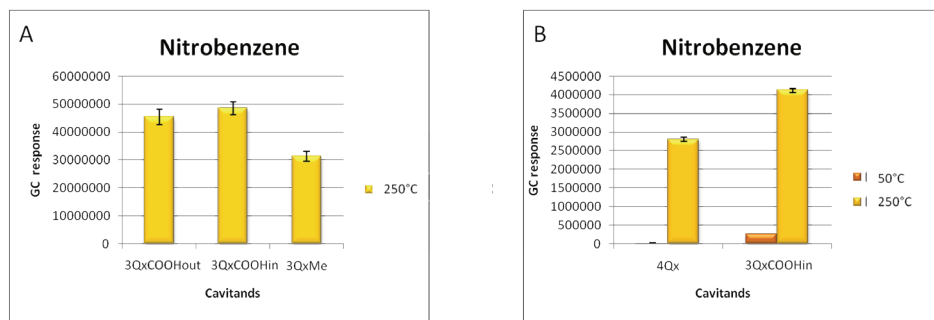


**Figure 5.6.** Performances of (A) 3QxCOOH<sub>Cav-out</sub>, 3QxCOOH<sub>Cav-in</sub>, 3QxMe<sub>Cav</sub> toward nitrobenzene at 250°C; (B) Qx<sub>Cav</sub> and 3QxCOOH<sub>Cav-in</sub> toward nitrobenzene at 50°C and 250°C.

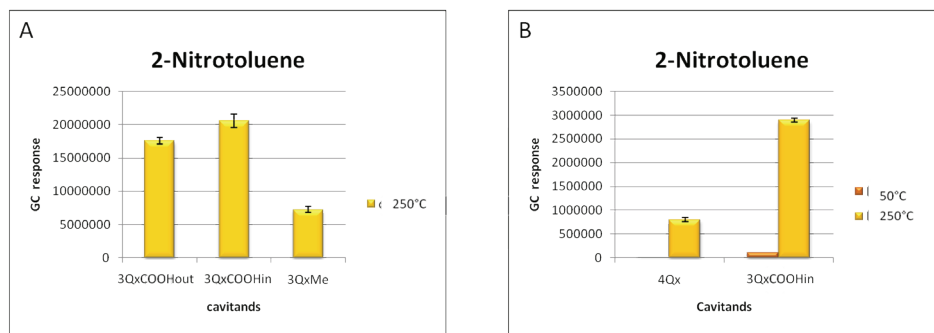


**Figure 5.7.** Performances of (A) 3QxCOOH<sub>Cav-out</sub>, 3QxCOOH<sub>Cav-in</sub>, 3QxMe<sub>Cav</sub> toward 2-nitrotoluene at 250°C; (B) Qx<sub>Cav</sub> and 3QxCOOH<sub>Cav-in</sub> toward 2-nitrotoluene at 50°C and 250°C.

Taking into account that thermal resistance of the adsorbent material is a very important parameter in the development of trapping devices, the thermal stability of both **5-in** and **6-out** cavitands was studied by thermo gravimetric analysis (TGA). Unfortunately both the cavitands have shown a low thermal stability with a weight loss of about 11.8% for **6-out** and 7.5% for **5-in** from room temperature to 350°C. This low stability can be attributed to the decarboxylation of the systems (the weight loss corresponds to CO<sub>2</sub> loss: 9.6% calculated). The weight loss of the out isomer is higher than that of the in one.

This might be due to the protective effect of the cavity in the case of the inward carboxylic acid. The thermal stabilities of both the cavitands has resulted too low to continue with these studies.

## 5.4 Conclusions

These preliminary studies has demonstrated that both 3QxCOOH cavitands in and out isomers are good supramolecular receptor for nitroaromatic compound. Unfortunately the low thermal stability shown by TGA has prevented the use of these cavitands as molecular receptors for the development of efficient trapping devices and has required the design of a new and more stable system. In particular in the future we have decided to change the design of the receptor by positioning the COOH group on the top of a QxCav (Figure 5.8). This new design will position the COOH group close to the nitro substituents of the guest and make the receptor more stable thermally. Indeed, aromatic carboxylic acid are thermally more stable than the aliphatic ones.

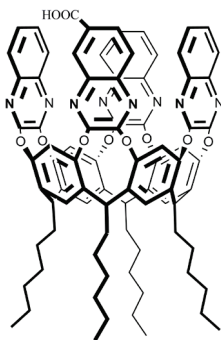


**Figure 5.8.** New target receptor

## 5.5 Acknowledgements

Special thanks to Dr. Federica Bianchi of the University of Parma for DHS studies, to Fabio Guiduzzi of Elantas Camattini for TGA and to Alessandro Bedini of the University of Parma.

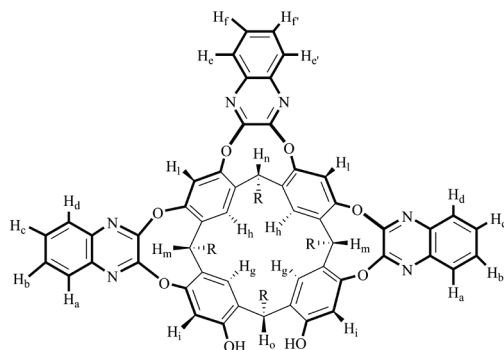
## 5.6 Experimental section

### QxCav (R= C<sub>6</sub>H<sub>13</sub>) (1)

To a solution of resorcinarene (R= C<sub>6</sub>H<sub>13</sub>) (1.60 g, 1.95 mmol) in dry DMF (36 mL), 2,3-dichloroquinoxaline (1.71 g, 8.58 mmol) and K<sub>2</sub>CO<sub>3</sub> (3.20g, 23.00 mol) were added. The mixture was heated and stirred for 16 h at 80°C. The reaction was quenched by addition of acidic water (with HCl) and the precipitate was filtered, washed with water, and dried. The crude product was crystallized from ethyl acetate : chloroform (9:1 v/v) to afford the pure product as white solid (1.30 g, 51%). <sup>1</sup>H NMR (CDCl<sub>3</sub>, 300 MHz): δ= 8.15 (s, 4H, ArH<sub>up</sub>), 7.79 (m, 8H, ArH AA' part of an AA'BB' system), 7.46 (m, 8H, ArH BB' part of an AA'BB' system), 7.21 (s, 4H, ArH<sub>down</sub>), 5.57 (t, 4H, ArCH, J=7.9 Hz), 2.26 (m, 8H, ArCHCH<sub>2</sub>), 1.48-1.31 (m, 32H, -CH<sub>2</sub>-), 0.93 (t, 12H, -CH<sub>3</sub>, J=6.8); ESI-MS: m/z 1330 [M+H]<sup>+</sup>.

### Triquinoxaline-bridged Resorcinarene (2)

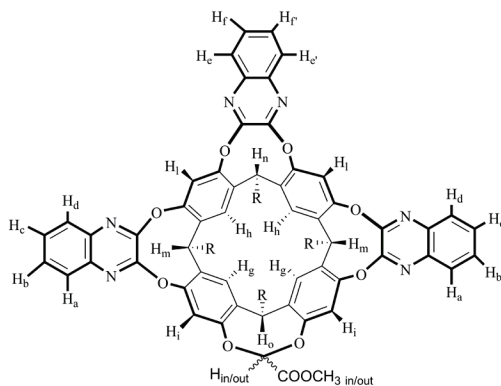
A solution of tetraquinoxaline cavitand **1** (1.85 g, 1.39 mmol) and CsF (4.23 g, 30.00 mmol) in dry DMF (250 mL) was heated to 90°C and catechol (0.16 g, 1.45 mmol) was added. The mixture was heated and stirred for 3 h at 90°C. The reaction was quenched by pouring into 300 mL of ice-cold brine, and the precipitate was filtered, washed with water, and dried. The crude product was purified by column chromatography (SiO<sub>2</sub>, gradient from 100% CH<sub>2</sub>Cl<sub>2</sub> to 90/10, CH<sub>2</sub>Cl<sub>2</sub> : EtOAc, v/v) affording triquinoxaline resorcinarene **2** as a pale yellow solid (886 mg, 53%).



**$^1\text{H NMR}$**  ( $\text{CDCl}_3$ , 300MHz)  $\delta$ = 8.25 (s, 2H,  $\text{ArH}_{l, up}$ ), 7.94 (m, 2H,  $H_d$  part D of an ABCD system), 7.82 (m, 2H,  $H_e$  e  $H_{e'}$  part AA' of an AA'BB' system), 7.68 (m, 2H,  $H_a$  part A of an ABCD system), 7.58 (m, 2H,  $H_c$  part C of an ABCD system), 7.54-7.46 (m, 4H,  $H_f$  e  $H_{f'}$  part BB' of an AA'BB' system +  $H_b$  part B of an ABCD system), 7.28 (s, 2H,  $\text{ArH}_{i, up}$ ), 7.14 (s, 2H,  $\text{ArH}_{h, down}$ ), 7.09 (s, 2H,  $\text{ArH}_{g, down}$ ), 5.60 (t, 1H,  $\text{ArCH}_n$ ,  $J=8.2$  Hz), 5.53 (t, 2H,  $\text{ArCH}_m$ ,  $J=8.1$  Hz), 4.26 (t, 1H,  $\text{ArCH}_o$ ,  $J=8.2$  Hz), 2.17 (m, 8H,  $\text{ArCHCH}_2-$ ), 1.57-1.23 (m, 32H,  $-\text{CH}_2-$ ), 0.90 (m, 12H,  $-\text{CH}_3$ ); **ESI-MS:**  $m/z$  1203  $[\text{M}+\text{H}]^+$ ,  $m/z$  1225  $[\text{M}+\text{Na}]^+$ ,  $m/z$  1241  $[\text{M}+\text{K}]^+$ .

### Triquinoxaline $\text{COOCH}_3$ -bridged Cavitands (**3-in** and **4-out**)

To a stirred solution of triquinoxaline resorcinarene **2** (0.26 g, 0.22 mmol) and methyl dichloroacetate (0.09 mL, 0.08 mmol) in dry DMF (12 mL), DBU (0.09 mL, 0.65 mmol) was added dropwise. The mixture was heated at  $80^\circ\text{C}$  for 6 h and then quenched in acidic water. The precipitate obtained was filtered and washed to neutrality. The crude product was purified by column chromatography ( $\text{SiO}_2$ , 9/1,  $\text{CH}_2\text{Cl}_2/\text{cyclohexane}$ , v/v) affording **3-in** (44 mg, 16 %) and **4-out** (80 mg, 29 %) as a white solid.



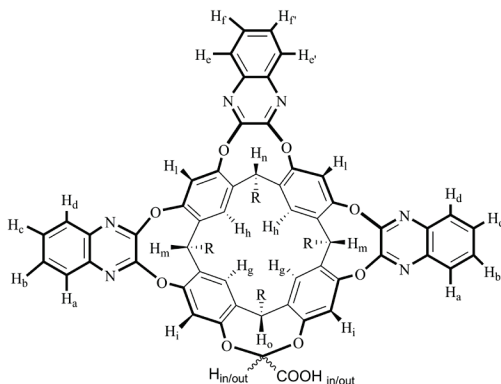
**3-in:**  $^1\text{H NMR}$  ( $\text{CDCl}_3$ , 300 MHz)  $\delta$  = 8.15 (s, 2H  $\text{ArH}_{l, up}$ ), 7.88 (m, 2H,  $H_d$  part D of an ABCD system), 7.71 (m, 2H,  $H_e$  and  $H_{e'}$  part AA' of an AA'BB' system), 7.57 (m, 2H,  $H_a$  part A of an ABCD system), 7.48 (m, 2H,  $H_c$  part C of an ABCD system), 7.39 (m, 4H,  $H_f$  and  $H_{f'}$  part BB' of an AA'BB' +  $H_b$  part

B of an ABCD system), 7.27 (s, 2H,  $ArH_{i, up}$ ), 7.13 (s, 2H,  $ArH_{h, down}$ ), 7.10 (s, 2H,  $ArH_{g, down}$ ), 5.99 (s, 1H,  $H_{out}$ ), 5.65 (t, 1H  $ArCH_n$ ,  $J=8.2$  Hz), 5.59 (t, 2H,  $ArCH_m$ ,  $J=7.8$  Hz), 4.60 (t, 1H,  $ArCH_o$ ,  $J=8.0$  Hz), 3.06 (s, 3H,  $-OCH_3$ ), 2.20 (m, 8H,  $ArCHCH_2-$ ), 1.39-1.17 (m, 32H,  $-CH_2-$ ), 0.84 (m, 12H,  $-CH_3$ ); **ESI-MS**:  $m/z$  1295  $[M+Na]^+$ ,  $m/z$  1311  $[M+K]^+$ .

**4-out**:  **$^1H$  NMR** ( $CDCl_3$ , 300 MHz)  $\delta$  = 8.24 (s, 2H  $ArH_{i, up}$ ), 7.86 (m, 2H,  $H_d$  part D of an ABCD system), 7.83 (m, 2H,  $H_e$  e  $H_{e'}$  part AA' of an AA'BB' system), 7.66 (m, 2H,  $H_a$  part A of an ABCD system), 7.53-7.41 (m, 6H,  $H_b$  and  $H_c$  part B e C of an ABCD system, and  $H_f$  and  $H_{f'}$  part BB' of an AA'BB' system), 7.23 (s, 2H,  $ArH_{i, up}$ ), 7.19 (s, 2H,  $ArH_{h, down}$ ), 7.17 (s, 2H,  $ArH_{g, down}$ ), 5.66 (m, 3H,  $ArCH_n$ ,  $ArCH_m$ ), 4.67 (t, 1H,  $ArCH_o$ ,  $J=7.9$  Hz), 4.34 (s, 1H,  $H_{in}$ ), 3.83 (s, 3H,  $-OCH_3$ ), 2.22 (m, 8H,  $ArCHCH_2-$ ), 1.58-1.22 (m, 32H,  $-CH_2-$ ), 0.89 (m, 12H,  $-CH_3$ ); **ESI-MS**:  $m/z$  1295  $[M+Na]^+$ ,  $m/z$  1311  $[M+K]^+$ .

### TriquinoxalineCOOH-bridged Cavitands (**5-in** and **6-out**)

A suspension of 3-in and 4-out cavitands (0.74 g, 1.50 mmol) and NaH (0.04 g, 1.50 mmol) in distilled THF (6.40 mL) and water (0.75 mL) was heated in a microwave oven (maximum power 200W, rump time 10 min, hold time 1 h at 90 °C). The reaction was quenched by adding 15 mL of acidic water. The aqueous layer was extracted with  $CH_2Cl_2$ . The crude product was purified by column chromatography ( $SiO_2$ , gradient from 95/5 to 90/10,  $CH_2Cl_2$ / EtOH, v/v) affording **5-in** (434 mg, 23 %) and **6-out** (471 mg, 25 %) as a white solid.

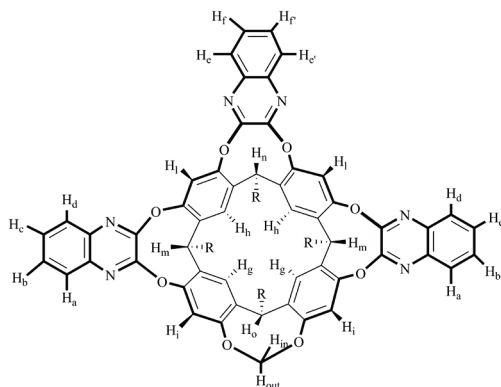


**5-in:**  $^1\text{H NMR}$  ( $\text{CDCl}_3$ , 600 MHz)  $\delta$  = 8.15 (s, 2H  $\text{ArH}_{l, up}$ ), 7.93 (m, 2H,  $H_d$  part D of an ABCD system), 7.85 (m, 2H,  $H_a$  part A of an ABCD system), 7.79 (m, 2H,  $H_e$  and  $H_{e'}$  part AA' of an AA'BB' system), 7.57 (s, 2H,  $\text{ArH}_{i, up}$ ), 7.52-7.47 (m, 6H,  $H_f$  and  $H_{f'}$  part BB' of an AA'BB' system,  $H_b$  and  $H_c$  parts B and C of an ABCD system), 7.12 (s, 2H,  $\text{ArH}_{h, down}$ ), 7.09 (s, 2H,  $\text{ArH}_{g, down}$ ), 5.60 (m, 4H,  $\text{ArCH}_n$ ,  $\text{ArCH}_m$ ,  $H_{out}$ ), 4.60 (t, 1H,  $\text{ArCH}_o$ ,  $J=7.8$  Hz), 2.20 (m, 8H,  $\text{ArCHCH}_2-$ ), 1.47-1.23 (m, 32H,  $-\text{CH}_2-$ ), 0.83 (m, 12H,  $-\text{CH}_3$ ); **Exact mass:**  $m/z$  calculated for  $\text{C}_{78}\text{H}_{77}\text{O}_{10}\text{N}_6$   $[\text{M}-\text{H}]^-$ : 1257.57012, found: 1257.57030

**6-out:**  $^1\text{H NMR}$  (DMSO, 600 MHz)  $\delta$  = 8.16 (s, 1H,  $\text{COOH}$ ) 8.11 (s, 2H,  $\text{ArH}_{i, up}$ ), 8.06 (m, 2H,  $H_e$  and  $H_{e'}$  part AA' of an AA'BB' system), 7.96 (m, 2H,  $H_d$  part D of an ABCD system), 7.77 (m, 2H,  $H_f$  and  $H_{f'}$  part BB' of an AA'BB' system), 7.73 (s, 2H,  $\text{ArH}_{i, up}$ ), 7.65 (m, 6H,  $H_a$  and  $H_c$  parts A and C of an ABCD and  $\text{ArH}_{h, down}$ ), 7.54 (t, 2H,  $H_b$  part B of an ABCD system,  $J=7.8$  Hz), 7.04 (s, 2H,  $\text{ArH}_{g, down}$ ), 5.58 (t, 1H,  $\text{ArCH}_n$ ,  $J=8.4$  Hz), 5.48 (t, 2H,  $\text{ArCH}_m$ ,  $J=8.1$  Hz), 4.56 (t, 1H,  $\text{ArCH}_o$ ,  $J=8.1$  Hz), 4.21 (s, 1H,  $\text{CH}_{in}$ ), 2.36 (m, 8H,  $\text{ArCHCH}_2$ ), 1.44-1.19 (m, 32H,  $-\text{CH}_2-$ ), 0.84 (m, 12H,  $\text{CH}_3$ ); **Exact mass:**  $m/z$  calculated for  $\text{C}_{78}\text{H}_{77}\text{O}_{10}\text{N}_6$   $[\text{M}-\text{H}]^-$ : 1257.57012 found: 1257.56939

### TriquinoxalineMe-bridged Cavitand (7)

To a stirred solution of triquinoxaline resorcinarene **2** (0.19 g, 0.16 mmol) and  $\text{K}_2\text{CO}_3$  (0.13 g, 0.96 mmol) in dry DMF (12 mL),  $\text{CH}_2\text{ClBr}$  (0.62 mg, 4.80 mmol) was added. The mixture was heated at  $80^\circ\text{C}$  for 3 h. The solvent was removed under vacuum and the solid was dissolved in  $\text{CH}_2\text{Cl}_2$  and washed with water to afford product **7** as a white solid in quantitative yield (195 mg).



$^1\text{H NMR}$  ( $\text{CDCl}_3$ , 600 MHz)  $\delta$ = 8.20 (s, 2H  $\text{ArH}_{l, up}$ ), 7.83 (m, 2H,  $H_d$  part D of an ABCD system), 7.80 (m, 2H,  $H_e$  and  $H_e'$  part AA'BB' of an AA'BB' system), 7.62 (m, 2H,  $H_a$  part A of an ABCD system), 7.48-7.44 (m, 4H,  $H_c$  part C of an ABCD system,  $H_f$  and  $H_f'$  part BB' of an AA'BB' system), 7.39 (m, 2H,  $H_b$  part B of an ABCD system), 7.15 (s, 2H,  $\text{ArH}_{i, up}$ ), 7.14 (s, 2H,  $\text{ArH}_{h, down}$ ), 7.13 (s, 2H,  $\text{ArH}_{g, down}$ ), 5.61 (m, 3H  $\text{ArCH}_n$  e  $\text{ArCH}_m$ ), 5.57 (d, 1H,  $H_{out}$ ,  $J=7.2$  Hz), 4.63 (t,  $\text{ArCH}_o$ ,  $J=8.1$  Hz), 3.92 (d, 1H,  $H_{in}$ ,  $J=7.2$  Hz), 2.19 (m, 8H,  $\text{ArCHCH}_2$ ), 1.36 (m, 32H,  $-\text{CH}_2-$ ), 0.87 (m, 12H,  $-\text{CH}_3$ ), **ESI-MS**:  $m/z$  1254  $[\text{M}+\text{K}]^+$ .

### Traps preparation and conditioning:

The traps were prepared by introducing 60 mg of each cavitand (**1**, **5-in**, **6-out** and **7**) in glass tubes ( $l=16$  cm,  $d.i.=4$  mm). Fiberglass was put at the edges and the tubes were closed with Swagelock caps.

The traps were conditioned in the injector of the gas chromatograph at  $140^\circ\text{C}$  for about 14 hours under nitrogen.

### Samples preparation:

Solutions of nitrobenzene, 2-nitrotoluene, and toluene at the concentration of 100 mg/L were obtained from pure compounds in 1 mL vials using methanol as solvent. Solutions of octane, decane, at the concentration of 100 mg/L were obtained from pure compounds in 1 mL vials using n-pentane as solvent. Working solutions at the concentration of 1 mg/L were obtained by dilution from the stock solutions.

## **DHS Sampling:**

### Pre-concentration of the analytes:

The analytes were purged for 10 minutes with a flow of nitrogen ( 60 mL/min) from the headspace of a 50 mL flask containing stirred solution at 50°C.

### Thermal desorption:

The analytes were desorbed in the GC injector using a thermal desorber. (Tekmar, TD800, Fisons Instruments, MI, Italy)

The desorption process has required four steps:

- pre cooling: the cryogenic trap was cooled down using liquid nitrogen at -120°C;
- desorption: the carrier gas (He, 10 mL/min) was flown into the trap kept at the temperature of 50°C or 250°C and the desorbed analytes were transported into the cryogenic trap;
- injection: the cryogenic trap was quickly heated and the analytes were injected into the GC in 0.6 minutes through a transfer line kept at high temperature;
- bake: the cryogenic trap was heated and cleaned by flowing carrier gas in the opposite way as before.

## **GC-MS analysis:**

Gas-chromatograph GC 8000:

- Column: Supelcowax-10<sup>TM</sup> (l= 30m, d.i.= 0.25 mm, d.f.= 0.25 µm, Supelco);
- Carrier gas: helium
- Carrier gas flux: 1 mL/min
- Carrier gas pressure: 70 KPa.
- Injector Temp: 200°C
- Injection mode: splitless

Mass Spectrometer MD800, Fisons Instruments, MI, Italy:

- Source Temperature: 200°C;
- Transfer Line temperature: 200°C;
- Ionization: E.I. (70 eV);



- Acquisition Mode: Full scan (40-200 amu);

The Mass Spectrometer has been tuned using Perfluorotributylamine and the analytes were identified on the base of the retention time of standards solution and the MS spectra reported in NIST Library (National Institute of Standards and Technology).

## 5.7 References

- <sup>1</sup> S. Singh, *Journal of Hazardous Materials*, **2007**, *144*, 15.
- <sup>2</sup> Environmental Protection Agency, Health Advisory for TNT, Criteria and Standard Division, Office of Drinking Water, Washington, DC, **1989**.
- <sup>3</sup> S.S. Talmage, D.M. Opresko, C.J. Maxwell, C.J.E. Welsh, F.M. Cretella, P.H. Reno, F.B. Daniel, *Rev. Environ. Contam. Toxicol.* **1999**, *161*, 1.
- <sup>4</sup> E.V. Anslyn, *J. Org. Chem.* **2007**, *72*, 687.
- <sup>5</sup> a) J.J. Lavigne, E.V. Anslyn, *Angew. Chem., Int. Ed.* **2001**, *40*, 3118; b) L. Pirondini, E. Dalcanale, *Chem. Soc. Rev.* **2007**, *36*, 695.
- <sup>6</sup> a) L. Zhang, L. Chen, X. Lu, C. Wu, Y. J. Chen, *Chromatogr., A* **1999**, *840*, 225; b) S.K. Panda, W. Schrader, J. T. Andersson, *J. Chromatogr., A* **2006**, *1122*, 88.
- <sup>7</sup> F. Bianchi, M. Mattarozzi, P. Betti, F. Bisceglie, M. Careri, A. Mangia, L. Sidisky, S. Ongarato, E. Dalcanale, *Anal. Chem.*, **2008**, *80*, 6423.
- <sup>8</sup> M. Vincenti, E. Dalcanale, P. Soncini, G. Guglielmetti, *J. Am. Chem. Soc.* **1990**, *112*, 445.
- <sup>9</sup> P. Soncini, S. Bonsignore, E. Dalcanale, F. Ugozzoli, *J. Org. Chem.* **1992**, *57*, 4608.
- <sup>10</sup> C. A. Hunter, K. R. Lawson, J. Perkins, C.J. Urch, *J. Chem. Soc., Perkin Trans. 2* **2001**, 651.
- <sup>11</sup> M. Vincenti, E. Dalcanale, *J. Chem. Soc., Perkin Trans. 2* **1995**, 1069
- <sup>12</sup> F. Bianchi, R. Pinalli, F. Ugozzoli, S. Spera, M. Careri, E. Dalcanale, *New J. Chem.* **2003**, *27*, 502.
- <sup>13</sup> S. Zampolli, P. Betti, I. Elmi, E. Dalcanale, *Chem. Commun.* **2007**, 279
- <sup>14</sup> E. Dalcanale, J. Hartmann, *Sens. Actuators, B* **1995**, *24*, 39; b) J. Hartmann, P. Hauptmann, S. Levi, E. Dalcanale, *Sens. Actuators, B* **1996**, *35*, 154.
- <sup>15</sup> E. B. Feresenbet, M. Busi, F. Ugozzoli, E. Dalcanale, D.K. Shenoy, *Sens. Lett.* **2004**, *2*, 186.
- <sup>16</sup> a) E. Dalcanale, G. Costantini, P. Soncini, *J. Inclusion Phenom. Mol. Recognit. Chem.* **1992**, *13*, 87; b) M. Ferrari, V. Ferrari, D. Marioli, A. Taroni, M. Suman, E. Dalcanale, *IEEE Trans. Instrum. Meas.* **2006**, *55*, 828.
- <sup>17</sup> P. Roncucci, L. Pirondini, G. Paderni, C. Massera, E. Dalcanale, V. A. Azov, F. Diederich *Chem. Eur. J.* **2006**, *12*, 4775-4784.
- <sup>18</sup> P.P. Castro, G. Zhao, G.A. Masangkay, C. Hernandez, L.M. Gutierrez-Tunstad, *Org. Lett.*, **2004**, *6* (3), 333.

- <sup>19</sup> a) J.R. Moran, S. Karbach, D.J. Cram, *J. Am. Chem. Soc.*, **1982**, *104*, 5826; b) J.R. Moran, J. L. Ericson, E. Dalcanale, J.A. Bryant, C.B. Knobler, D.J. Cram, *J. Am. Chem. Soc.*, **1991**, *113*, 5707; c) D.J. Cram, H-J. Choi, J. A. Bryant, C.B. Knobler, *J. Am. Chem. Soc.*, **1992**, *114*, 7748.
- <sup>20</sup> C.F. Poole, and S.K. Poole, *Chromatography Today*, Elsevier, Oxford, **1991**, p. 818.
- <sup>21</sup> F. St-Germain, O. Mamer, J. Brunet, B. Vachon, R. Tardif, T. Atribat, C.D. Rosiers, J. Montgomery, *Anal. Chem.*, **1995**, *67*, 4536.
- <sup>22</sup> J. Namiesnik, T. Gorecki, M. Biziuk, and L. Torres, *Anal. Chim. Acta*, **1990**, *237*, 1.



# Active metal template synthesis of hard-to-access mechanically interlocked molecules

# 6

## *6.1 Introduction*

Unlike classical molecular structures, mechanically interlocked molecules contain two or more discrete components which are not connected by traditional chemical bonds (i.e. covalent), but are intrinsically linked to the other by a so-called “mechanical bond”. These structures fulfilling the definition of a single molecule are not considered supramolecular species. Indeed, they required the cleavage of at least one covalent bond to allow the molecules component to dissociate, one from the other.<sup>1</sup>

The simplest mechanically interlocked molecules are [2]rotaxanes and [2]catenanes, where the bracketed numeral preceding the name indicates the number of individual molecules which compose the assembly (Figure 6.1).<sup>2</sup>

Catenanes in general consist of two or more interlocked macrocyclic rings whereas, rotaxanes contain a linear component (the “thread”) encircled by one or more macrocyclic rings. The two bulky substituents, (the “stoppers”), attached at the end of the thread must be large enough to trap the macrocycle(s) mechanically, preventing the dissociation of the system.

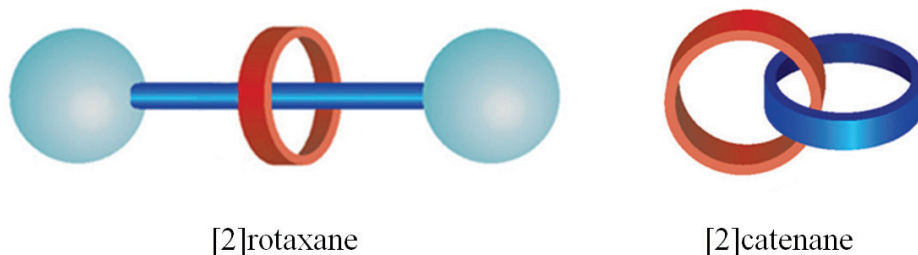


**Figure 6.1.** Cartoon representations of a [2]rotaxane (left), (2) [2]catenane (right).

In addition to catenanes and rotaxanes a wide variety of molecules containing mechanical bonds, such as trefoil knots and Borromean rings, have been identified and synthesized (Figure 6.2).<sup>1</sup>

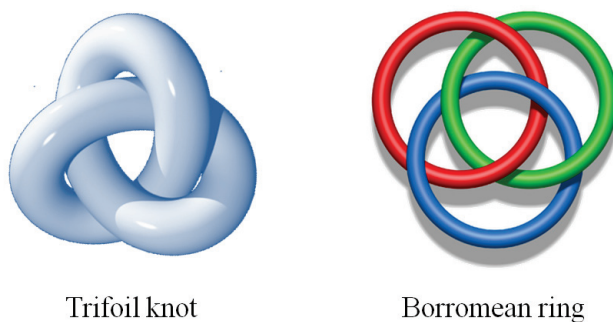


**Figure 6.2.** Cartoon representations of trifoil knot (left) and Borromean ring (right).

Interlocked molecules can be synthesized without any preorganization of their precursors by statistical methods but, these are generally lower yielding. The first example of synthetic interlocked molecule was described in the literature by Wasserman in 1960.<sup>3</sup> He showed a statistical methodology for the synthesis of the first [2]catenane. In this statistical process, less than the 1% of the starting materials react in a mechanically interlocked co-conformation, leading to the isolation of a very small quantity of the catenane. The statistical method was used again in 1967 for the synthesis of the first wholly synthetic rotaxane by Harrison and Harrison.<sup>4</sup> In order to obtain the rotaxane in good quantities they attached the macrocycle to a resin and passed a solution containing the thread

and the stopper over the resin no less than 70 times. Despite the 70 repetitions of the process they were able to report only a 6% yield.

The introduction of noncovalent template-directed strategies has greatly increased the efficiency of the synthesis of interlocked molecules.

These strategies involve the formation of supramolecular assemblies in which the components are mutually interwoven. Post-assembly covalent modification leads to the desired mechanically bonded species. Template complexes among the components are obtained by means of coordinative or noncovalent bonding interactions that include: (i) donor-acceptor forces; (ii) metal-ligand coordination; (iii) hydrogen-bonding; (iv)  $\pi$ - $\pi$  stacking; (v) solvophobic repulsion; and/or (vi) electrostatic forces. These new template strategies allow to prepare mechanically interlocked molecules in high yield.<sup>1</sup>

The traditional template-directed strategies are the classical metal template-directed synthesis reported by Sauvage and coworkers<sup>5</sup> and the donor/acceptor-based template-directed synthesis reported by Stoddart and coworkers.<sup>6</sup>

## ***6.2 Active metal template synthesis of interlocked molecules***

Classical metal template strategies to mechanically bonded molecules generally involve in the first step the complexation of two or more components to one or more metal ions.<sup>7</sup> This coordination to the metal centre allows to hold together and in the right orientation all the components that a subsequent covalent bond forming reaction can link one to the other, generating a new mechanical bond. Apart from the roles it plays in holding the ligands in the right position, the metal ion is passive during formation of the mechanically bonded molecules.<sup>8</sup>

The new “active metal template (AMT) approach” developed in the group of professor Leigh, differs from the classical “passive template” process because the metal acts both as the template and the catalyst for the formation of the covalent bond(s).<sup>9</sup>

The active metal template process is based on the use of a macrocycle which can bind a metal ion endotopically within its cavity. The metal ion is chosen such that it is capable of mediating covalent bond formation between two suitably functionalized “half-thread” units in the case of the rotaxane synthesis

or to effect ring enclosure of a precursor to a macrocycle in the case of catenane synthesis. The metal ion immobilized within the cavity, promotes the formation of new covalent bond through the macrocycle and leads to the formation of the mechanical bond (Figure 6.3).

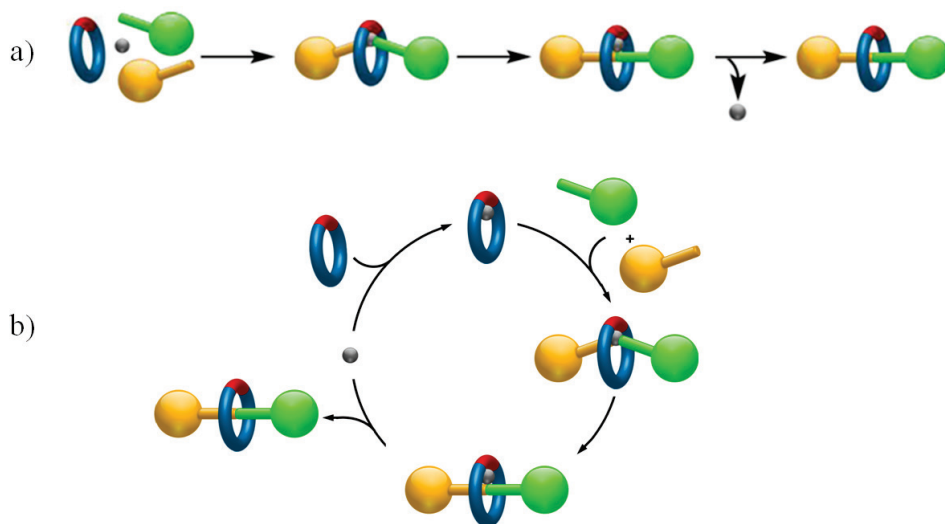


**Figure 6.3.** Scheme of the active metal template process in a) stoichiometric, b) catalytic variants.

There are many advantages of such a synthetic approach to mechanically interlocked molecules: (i) the inherently efficiency and flexibility in having the macrocycle-metal complex perform multiple functions during the reactions; (ii) the lack of requirement for permanent recognition elements on each component of the interlocked product which increase the structural diversity in catenanes and rotaxanes and enables their formation to be “traceless”; (iii) in some cases only sub-stoichiometric quantities of the active template may be required; (iv) the strategy could be applicable to many different types of well-known transition metal-catalysed reactions; (v) reactions that only proceed through a threaded intermediate could allow access to several currently inaccessible mechanically linked macromolecular architectures; and, finally, (vi) the coordination requirements during key stages of the catalytic cycle of active

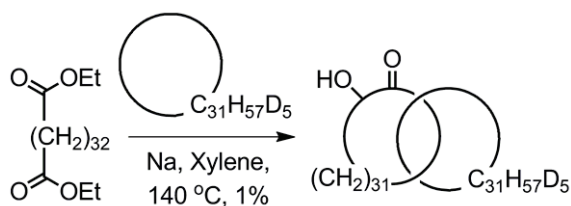


template reactions could provide insight into the mechanisms of the metal catalysed reactions.<sup>9</sup>

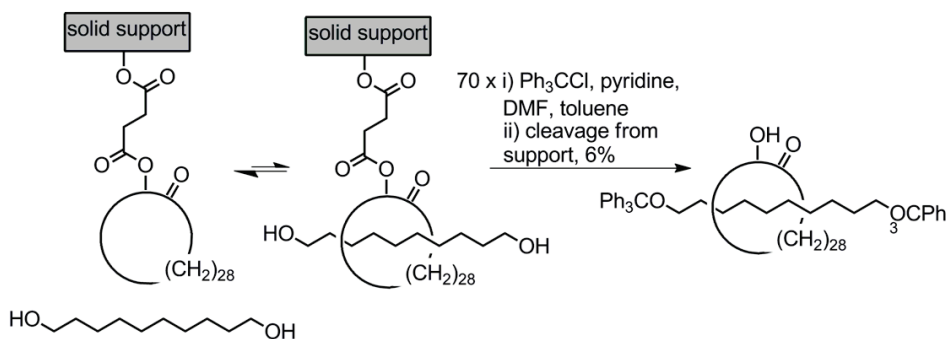
In this chapter we exploited the advantages of this active metal template process for the synthesis of a hydrocarbon [2]rotaxane.

### 6.3 Introduction to hydrocarbon interlocked molecules

Interlocked molecules close to hydrocarbon ones were synthesised by statistical methodologies and were obtained in very low yield. The first two examples were: the statistical synthesis of a [2]catenane reported by E. J. Wasserman and co-workers in 1960 (Scheme 6.1)<sup>3</sup> and the Harrison and Harrison [2]rotaxane (Scheme 6.2)<sup>4</sup>.



**Scheme 6.1.** Statistical synthesis of the first [2]catenane.



**Scheme 6.2.** Statistical synthesis of the first [2]rotaxane.

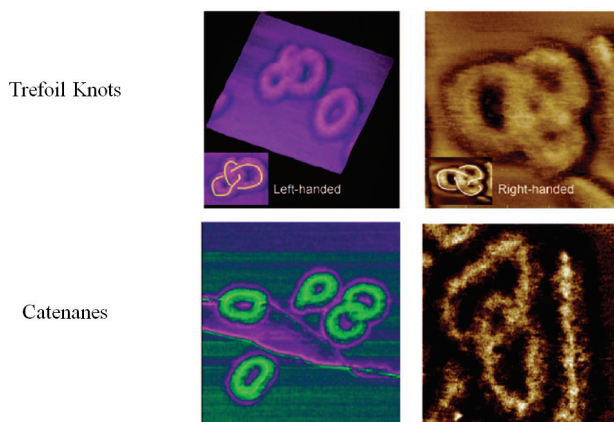
The first evidence of the presence of a hydrocarbon interlocked system was obtained simultaneously by Wolovsky and Wasserman in 1970. They got mass

spectroscopic evidence of the formation of hydrocarbon interlocked molecules as products of the enlargement of cyclododecene using the metathesis reaction.<sup>10</sup>

So far, the use of new template strategies have not allow to obtained hydrocarbon interlocked systems, because the non covalent binding motifs used to template the synthesis of these architectures are generally retained in the final products.<sup>11</sup>

The synthesis of hydrocarbon interlocked systems is interesting mainly for two reasons. The first one concerning the preparation of fast molecular shuttle. The non covalent interactions (typically 12-30 kcal mol<sup>-1</sup>) used to maximize the rotaxane yield and localize the position of the ring on the thread also provided the major contribution to the activation energy to shuttling.<sup>12</sup> To achieve faster moving rotaxane-based molecular machines, it will be necessary to make them with much weaker intercomponent interactions, therefore in this context the synthesis of a hydrocarbon interlocked rotaxane is of great interest.

The second reason is related to the studies of catenated and knotted polymers. During polymerization of neutral polymers as polyethylene, secondary molecular structures, like catenanes and knots can be generated (Figure 6.4).<sup>13</sup> The influence of this secondary structure on the properties of the polymer is an interesting topic, but difficult to study because the formation of this system cannot be controlled.



AFM studies on poly(chloroethyl vinyl ether) demonstrated the presence of non-trivial rings.

**Figure 6.4.** Imaging of catenated and knotted rings in neutral polymers.

The preparation of hydrocarbon interlocked systems might provide a model for studying the influence of these secondary structure on the properties of neutral polymers.

For the above reasons, in this chapter we exploited the AMT process to prepare a hydrocarbon [2]rotaxane.

#### 6.4 Design and synthesis of a hydrocarbon [2]rotaxane

The preparation of a hydrocarbon rotaxane with no strong inter-component interactions or recognition sites, has required an accurate design of the system and of the synthetic project. The synthetic project reported schematically in figure 6.5, involves the synthesis of a macrobicyclic system containing a suitable recognition site necessary for promoting the AMT process of the macrobicyclic [2]rotaxane. This recognition unit must be removed after the formation of the mechanical bond giving the final hydrocarbon [2]rotaxane.

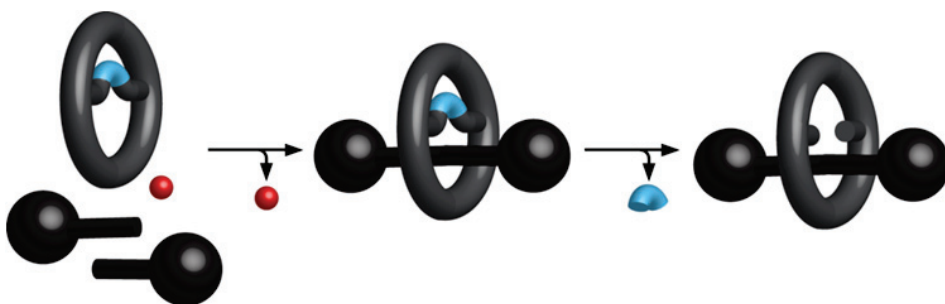
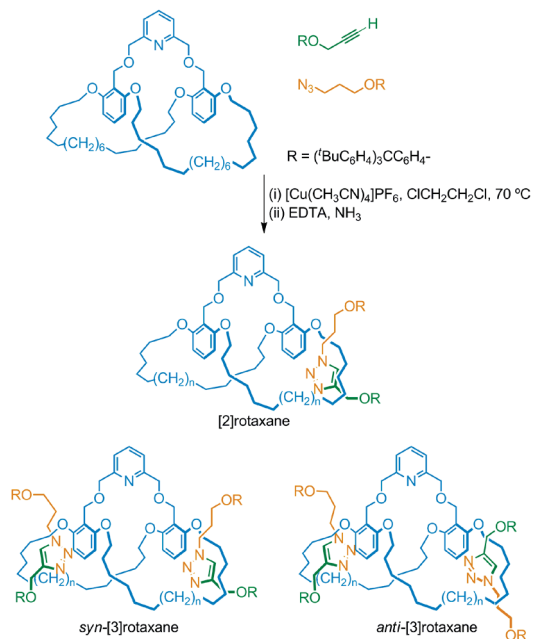


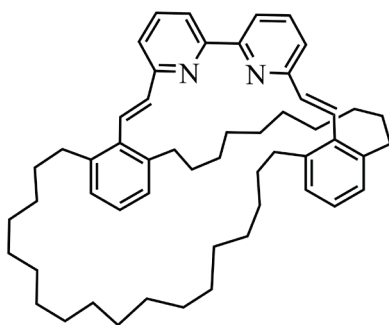
**Figure 6.5.** Scheme of the active metal template process for the synthesis of a hydrocarbon rotaxane.

This idea was based on a previous work published by the group of D.A. Leigh<sup>14</sup> concerning the synthesis of the macrobicyclic [3]rotaxane shown in scheme 6.3. The use of a macrobicyclic system for the synthesis of the hydrocarbon [2]rotaxane is necessary, because it allows to preserve the mechanical bond even after the excision of the recognition moiety.



**Scheme 6.3.** Active metal template process for the synthesis of a hydrocarbon rotaxane.

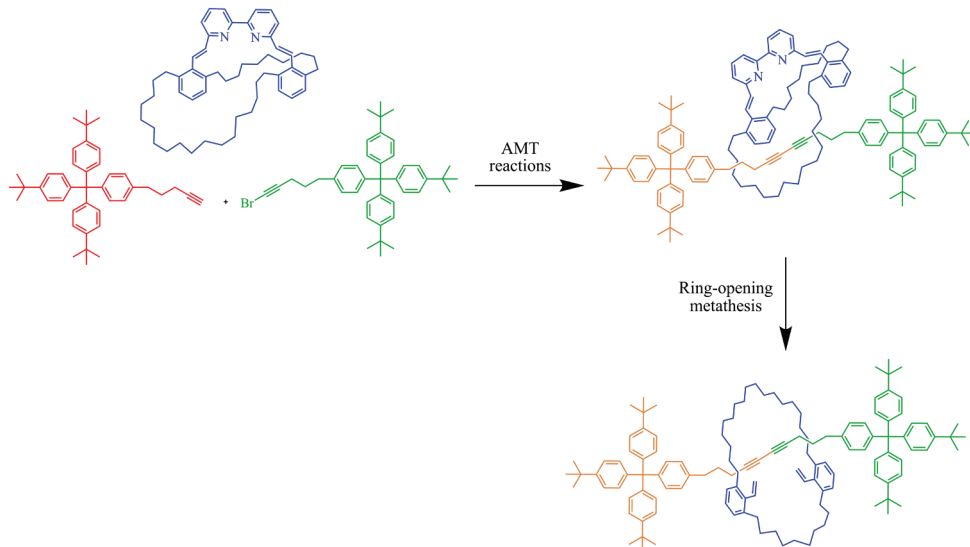
After an accurate design of the macrobicyclic system, the best candidates resulted to be macrobicycle **1** (Figure 6.6). It contains a 2,2'-bipyridine unit connected to the remaining part of the system via two double bonds.



**1**

**Figure 6.6.** Structure of the target macrobicycle **1**.

The bipyridine unit has been chosen because it can be exploited in different AMT reactions and, thank to the presence of the two double bond, it can be removed after the formation of the mechanical bond via a ring opening metathesis reaction (Scheme 6.4).



**Scheme 6.4.** Synthesis of the target [2]rotaxane.

Before starting the synthesis of the target macrobicyclic and [2]rotaxane, a model macrocycle **2** (Figure 6.7) was designed and synthesised in order to optimize the synthetic procedure with particular attention to (i) the Horner-Wadsworth-Emmons olefination, (ii) the AMT reaction and (iii) the ring opening metathesis.

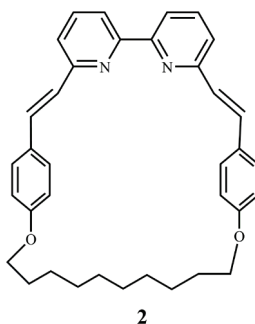
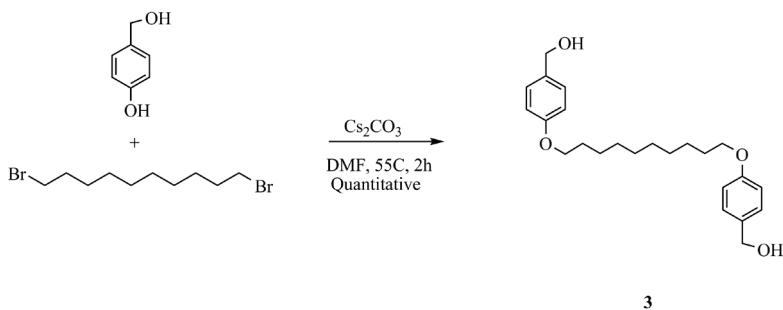


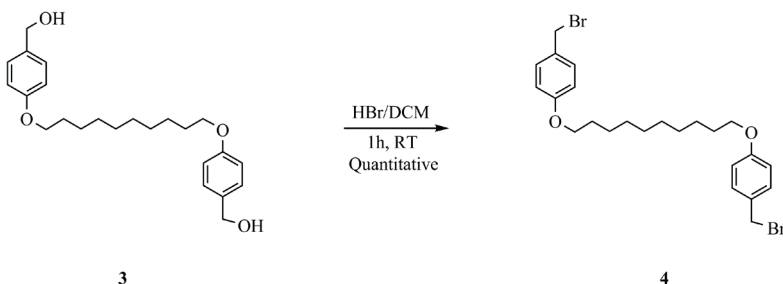
**Figure 6.7.** Structure of the model macrocycle **2**.

The preparation of the model macrocycle involved a five steps process. The first one was a Williamson reaction between 1,10-dibromodecane and 4-hydroxybenzyl alcohol in the presence of  $\text{Cs}_2\text{CO}_3$  as base, that led to the formation of the dibenzyl alcohol **3** in quantitative yield (Scheme 6.4).



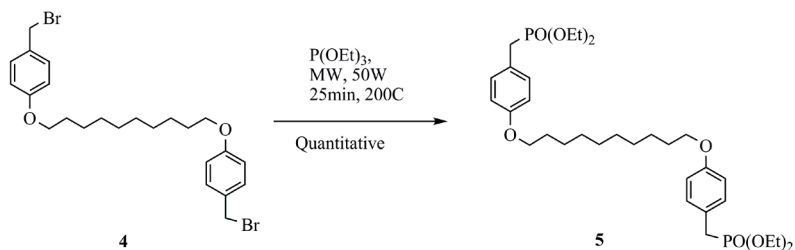
**Scheme 6.4.** Synthesis of the dibenzyl alcohol **3**.

In the following step, dibenzyl alcohol **3** was converted quantitatively into dibromide **4** via a  $\text{S}_{\text{N}}1$ -type reaction with HBr (scheme 6.5).



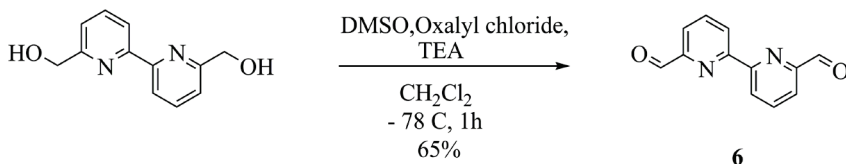
**Scheme 6.5.** Synthesis of the dibenzyl bromide **4**.

Then a microwave assisted Arbuzov reaction was performed to converted quantitatively dibromide **4** into diphosphonate **5** (Scheme 6.6). This reaction was performed using a microwave reactor to improve the yield.



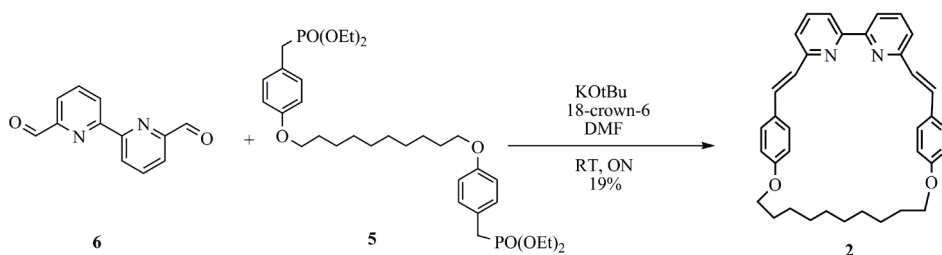
**Scheme 6.6.** Synthesis of the diphosphonate **5**.

At the same time a Swern oxidation of 2,2'-bipyridine-6,6'-diyl dimethanol was done to obtain the 2,2'-bipyridine-6,6'-dicarbaldehyde **6** (scheme 6.7) necessary for the following step.



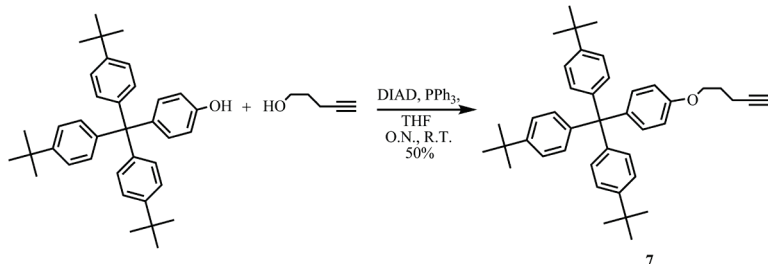
**Scheme 6.7.** Synthesis of the 2,2'-bipyridine-6,6'-dicarbaldehyde **6**.

The last step was the macrocyclization reaction via Horner-Wadsworth-Emmons olefination between the diphosphonate **5** and the dialdehyde **6** that led to macrocycle **2**. The optimization of this reaction required several attempts to choose the right working conditions, concentration and base. In the end, the best result was obtained working at room temperature, over night at 1 mM concentration of the two starting materials and using 10 eq. of KOTBu as base (Scheme 6.8).



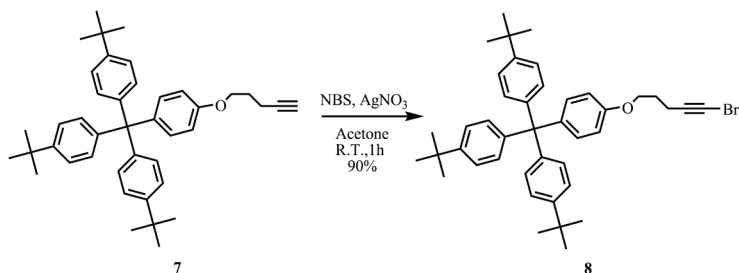
**Scheme 6.8.** Synthesis of the model macrocycle **2**.

Once the macrocycle was ready, appropriately “stoppered” alkyne and alkyne bromide, necessary for the rotaxane forming reactions, were synthesised. The alkyne stopper **7** was obtained in good yield via a Mitsunobu reaction between 4-pentyn-1-ol and 4-[tris-(4-tert-butylphenyl)methyl]phenol (scheme 6.9).



**Scheme 6.9.** Synthesis of the alkyne stopper **7**.

Alkyne stopper **7** was then treated with N-bromosuccinimide (NBS) in the presence of AgNO<sub>3</sub> leading to alkyne bromide **8** (Scheme 6.10).



**Scheme 6.10.** Synthesis of the bromo alkyne stopper **8**.

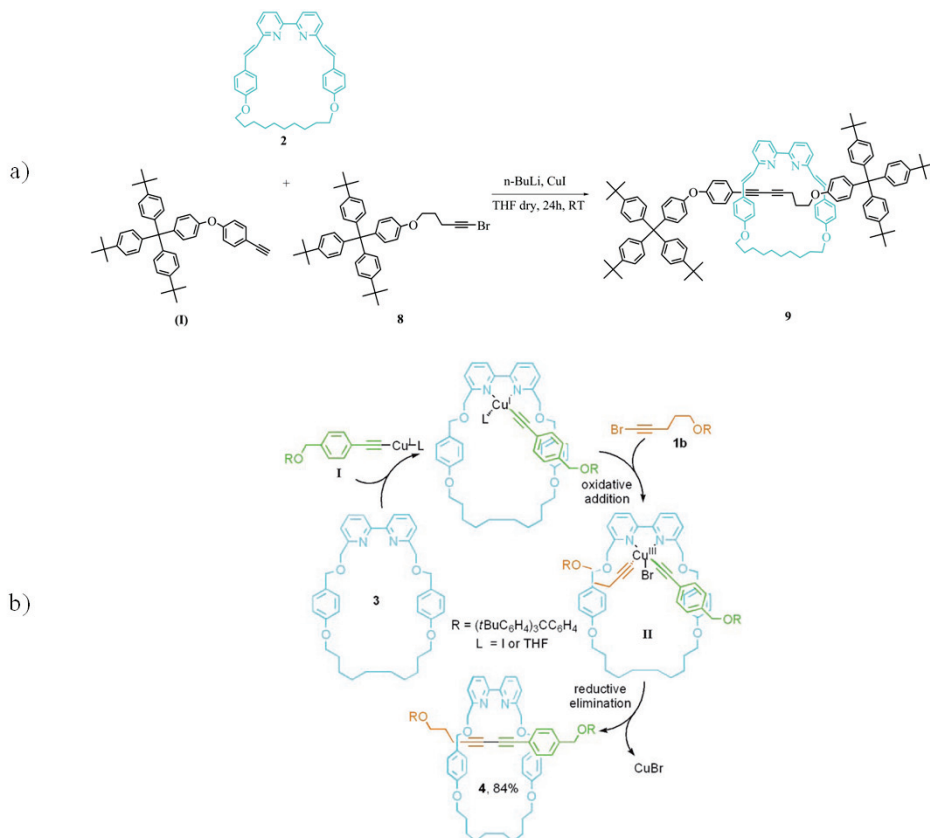
The rotaxane forming reaction was performed trying three different AMT synthesis: (i) Cadiot-Chodkiewicz active metal template reaction<sup>12</sup>; (ii) Nickel-Copper-mediated alkyne homocoupling<sup>15</sup>; (iii) Palladium active metal template reaction<sup>16</sup>.

These three AMT reactions were chosen because in all the case the bipyridine unit has already been proved to be a suitable ligand for promoting these processes.

The Cadiot-Chodkiewicz active template reaction was performed using the model macrocycle **2**, the “stoppered” alkyne bromine **8** and a “stoppered” aryl



alkyne (**I**) previously synthesised in the Leigh group. This reaction required the use of CuI as catalyst and n-BuLi as base (Scheme 6.11) and led to the formation of model rotaxane **9**, as demonstrated by the mass spectrum and the  $^1\text{H}$  NMR of the crude. Unfortunately this system had a low stability and decomposed overnight, not allowing its purification and better characterization.

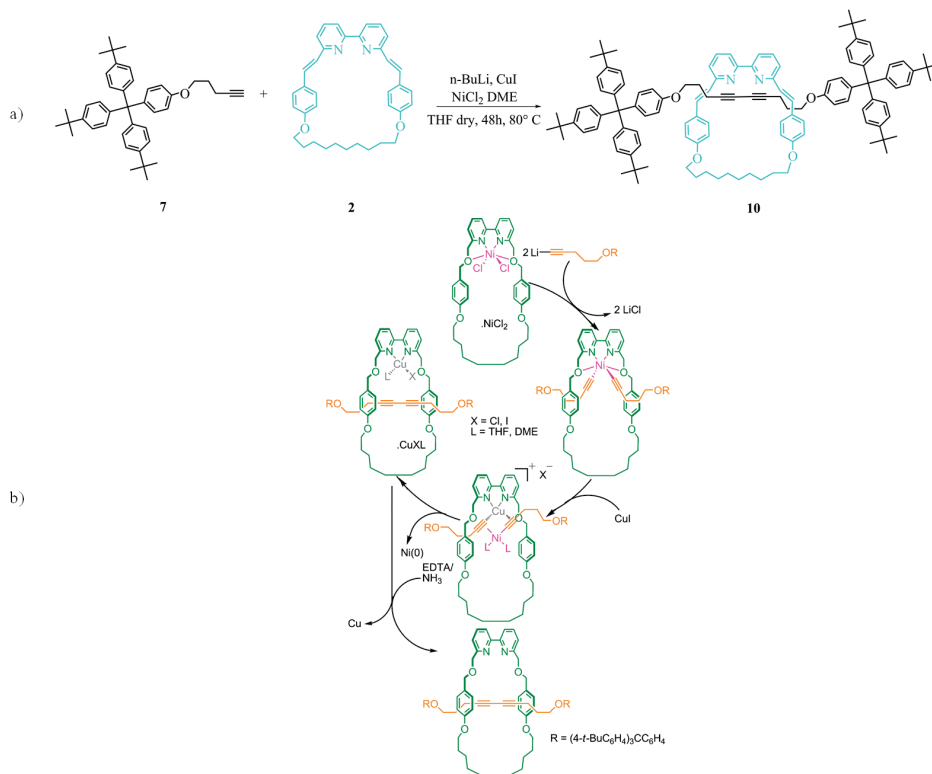


**Scheme 6.11.** Cadiot-Chodkiewicz active metal template process: (a) synthesis of model [2]rotaxane **9**; (b) general proposed mechanism for the formation of [2] rotaxane.

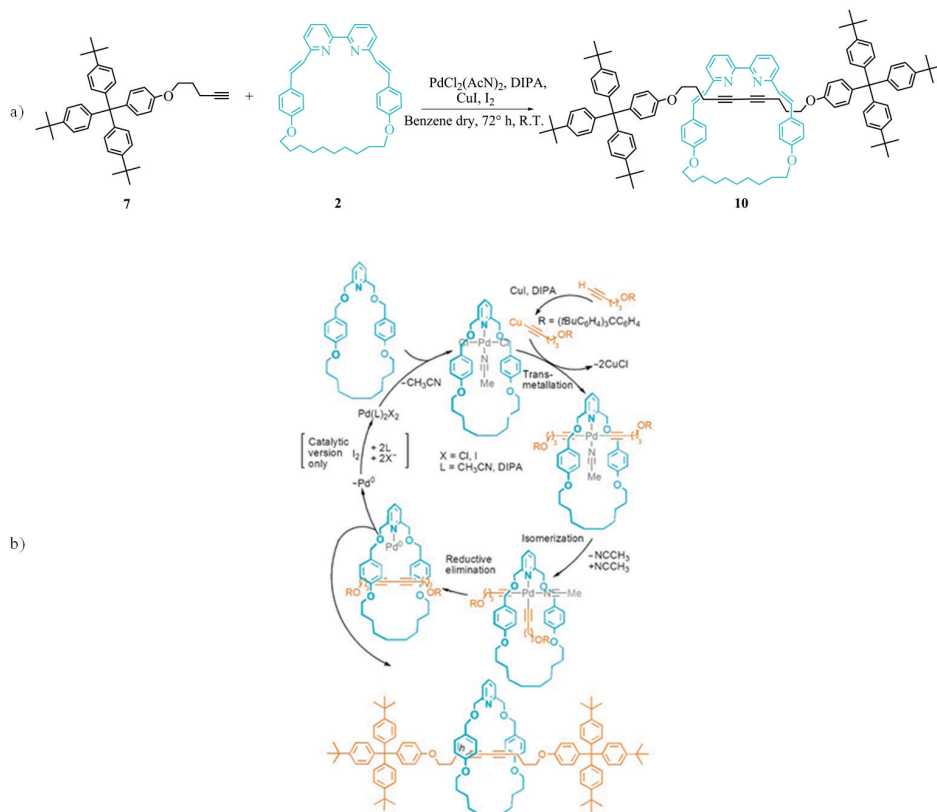
Then the Nickel-Copper-mediated alkyne homocoupling (Scheme 6.12) and then Palladium active metal template reaction (Scheme 6.13) were performed to synthesis model [2]rotaxane **10**. They has been both performed starting from the model macrocycle **2** and the alkyne stopper **7** in the presence of  $\text{NiCl}_2\text{DME}$ , CuI as catalysts and n-BuLi in the case of nickel-copper homocoupling, whereas

the palladium active metal template reaction has required the use of  $\text{PdCl}(\text{ACN})_2$  as catalyst in the presence of  $\text{CuI}$ ,  $\text{I}_2$  and DIPA.

As for the Cadiot-Chodkiewicz active template reaction, the final product **10** could not be isolated because it quickly decomposed but, the mass spectrum and the  $^1\text{H}$  NMR of the crude proved its formation.

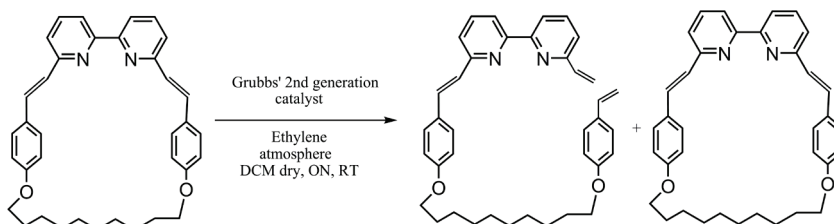


**Scheme 6.12.** Nickel-Copper-mediated alkyne homocoupling: (a) synthesis of model [2]rotaxane **10**; (b) general proposed mechanism for the formation of [2] rotaxane.



**Scheme 6.13.** Palladium active metal template reaction: (a) synthesis of model [2]rotaxane **10**; (b) general proposed mechanism for the formation of [2] rotaxane.

Because of the low stability of the two systems it has not been possible to test the ring opening metathesis on the final rotaxane. A test reaction was done anyway directly on model macrocycle **2** observing by mass spectroscopy the break of only one double bond. The reaction was performed using Grubb's 2<sup>nd</sup> generation catalyst in ethylene atmosphere (Scheme 6.14).

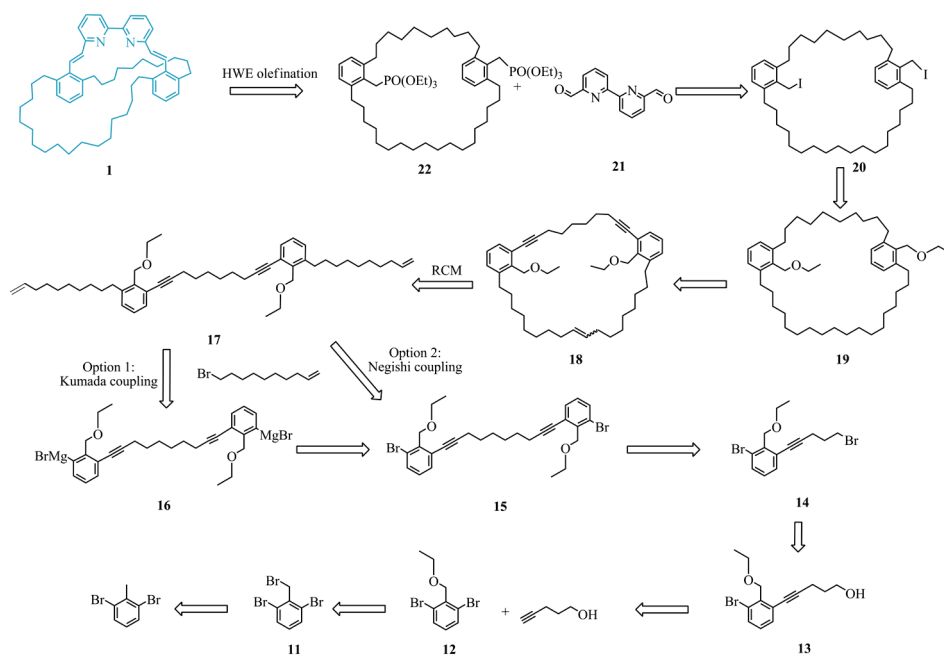


**Scheme 6.14.** Ring opening metathesis reaction.

These first test reactions on the model system allow us to optimize the strategy for the synthesis of the target system. Even if the model rotaxanes were not stable, we demonstrated that it is possible to perform the above mentioned AMT reactions with this new macrocycle and so we decided to continue with the synthesis of the target [2] rotaxane.

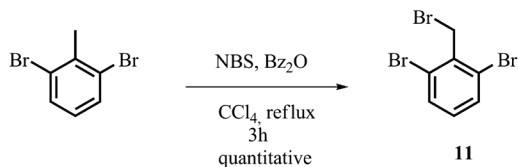
### 6.5 Synthesis of the target hydrocarbon [2]rotaxane

The synthesis of the target macrobicycle **1** requires several steps as shown in scheme 6.15.



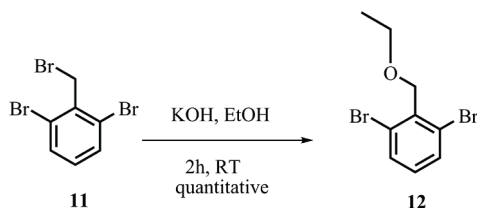
**Scheme 6.15.** Retrosynthetic scheme of the synthesis of the target macrobicycle **1**.

In the first step a Whole-Ziegler reaction was performed treating dibromotoluene with NBS in the presence of a catalytic amount of dibenzoyl peroxide leading to the formation of 1,3-dibromo-2-(bromomethyl)benzene **11** in quantitative yield (scheme 6.16).



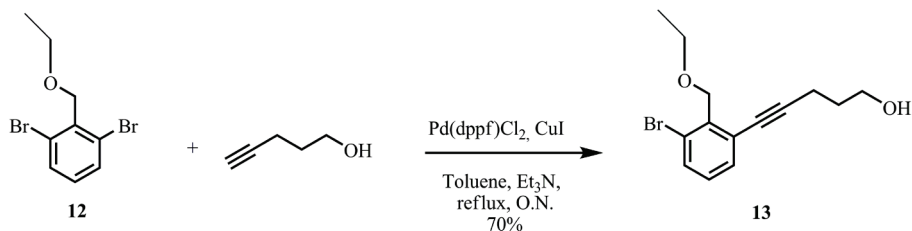
**Scheme 6.16.** Synthesis of 1,3-dibromo-2-(bromomethyl)benzene **11**.

In the following step bromomethyl benzene **11** was converted quantitatively into the ethyl ether **12** via a S<sub>N</sub>2-type reaction promoted by KOH (scheme 6.17).



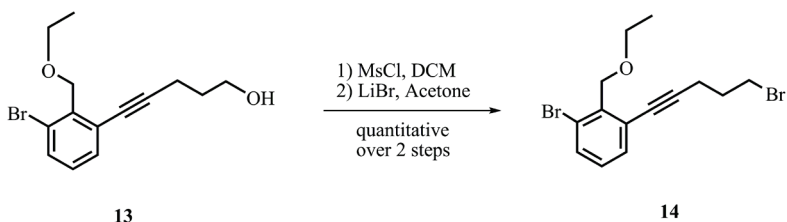
**Scheme 6.17.** Synthesis of ethyl ether **12**.

Then a Sonogashira coupling catalyzed by Pd(dppf)Cl<sub>2</sub> in the presence of CuI and triethylamine was performed starting from dibromide **12** to obtain 5-(3-bromo-2-(ethoxymethyl)phenyl)pent-4-yn-1-ol **13** (Scheme 6.18).



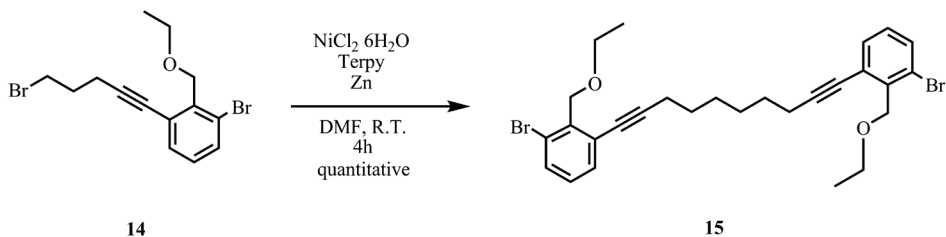
**Scheme 6.18.** Synthesis of bromo-2-(ethoxymethyl)phenyl)pent-4-yn-1-ol **13**.

In the next step the alcohol was converted into the mesylate by reaction with MsCl followed by the addition of LiBr that led to bromide **14** in quantitative yield (Scheme 6.19).



**Scheme 6.19.** Synthesis of bromide **14**.

Then following a procedure developed in the Leigh group for ligand-assisted nickel-catalysed  $sp^3$ - $sp^3$  homocoupling of unactivated alkyl bromides<sup>17</sup>, the dimerization of compound **14** was performed obtaining diarylbromide **15** in quantitative yield (Scheme 6.20).



**Scheme 6.20.** Synthesis of dibromide **15**.

The next step should have been the introduction of the terminal olefin to obtain compound **17** (Figure 6.8). This reaction has been performed following different procedure: (i) Negishi coupling and (ii) Kumada coupling but without obtaining the desired product.

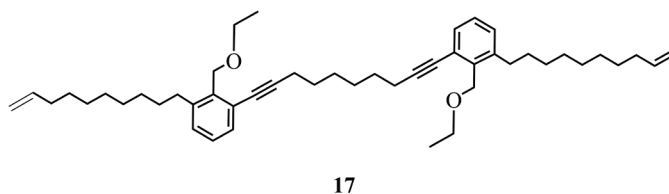


**Figure 6.8.** Structure of compound **17**.

Work is still in progress in this direction in order to find optimal condition for these coupling or to find an alternative way to synthesis **17** and go on with the synthesis of the target [2]rotaxane.

## 6.6 Conclusions

The synthesis of the model rotaxanes **9** and **10** have been performed obtaining the desired products. This has allowed to optimise the working conditions, and the synthetic project for the preparation of the target hydrocarbon [2]rotaxane even if the final rotaxanes **9** and **10** have shown a very low stability. Moreover it had proved the efficiency of the tested AMT reaction. Ongoing effort are made to synthesise the target hydrocarbon [2]rotaxane overcoming the synthetic problems.

## 6.7 Acknowledgements

Special thanks to Prof. David A. Leigh for this opportunity, to Dr. Paul McGonigal and Jhenyi Wu for their collaboration and precious help in each part of this work. Moreover, I would like to thank all the other members of the Leigh group, for their precious support.

## 6.8 Experimental section

### **(4,4'-(decane-1,10-diylbis(oxy))bis(4,1-phenylene))dimethanol (3)**

To a solution of 4-hydroxybenzyl alcohol (2 g, 16.11 mmol) in dry DMF (12 mL), Cs<sub>2</sub>CO<sub>3</sub> (5.21 g, 16.11 mmol) and dibromodecane (1.61 g, 5.37mmol) were added under nitrogen atmosphere. The solution was stirred for 3h at 55° C. Once complete, the reaction was diluted with chloroform and washed with water followed by washing with 1M solution of HCl, with 15% solution of NaOH and then with brine. The organic phase was dried affording product **3** as white solid in quantitative yield (2.0 g). <sup>1</sup>H-NMR(400 MHz, CDCl<sub>3</sub>): δ = 7.27 (d, 4H, ArH, J = 8.8 Hz), 6.88 (d, 4H, ArH, J = 8.8 Hz), 4.61 (s, 4H, ArCH<sub>2</sub>OH), 3.95 (t, 4H, ArOCH<sub>2</sub>-, J= 6.6), 1.77 (m, 4H, ArOCH<sub>2</sub>CH<sub>2</sub>-), 1.45

(m, 4H, ArOCH<sub>2</sub>CH<sub>2</sub>CH<sub>2</sub>-), 1.35 (m, 8H, ArOCH<sub>2</sub>CH<sub>2</sub>CH<sub>2</sub>CH<sub>2</sub>-ArOCH<sub>2</sub>CH<sub>2</sub>CH<sub>2</sub>CH<sub>2</sub>CH<sub>2</sub>-); **APCI-MS**: m/z 369.3 [M-H<sub>2</sub>O]<sup>+</sup>.

#### **1,10-bis(4-(bromomethyl)phenoxy)decane (4)**

To a 48% HBr solution (6 mL), **3** (1 g, 2.59 mmol) was added and the mixture was stirred rapidly for 1 h at room temperature. After extraction of the mixture with DCM the organic phase was washed with sat. NaHCO<sub>3</sub> solution and then with brine. The organic phase was dried affording product **4** as white solid in quantitative yield (1.28 g). **<sup>1</sup>H-NMR(400 MHz, CDCl<sub>3</sub>)**: δ = 7.30 (d, 4H, ArH, J = 8.8 Hz), 6.86 (d, 4H, ArH, J = 8.8 Hz), 4.50 (s, 4H, ArCH<sub>2</sub>Br), 3.94 (t, 4H, ArOCH<sub>2</sub>-, J = 6.6), 1.73 (m, 4H, ArOCH<sub>2</sub>CH<sub>2</sub>-), 1.44 (m, 4H, ArOCH<sub>2</sub>CH<sub>2</sub>CH<sub>2</sub>-), 1.35 (m, 8H, ArOCH<sub>2</sub>CH<sub>2</sub>CH<sub>2</sub>CH<sub>2</sub>-, ArOCH<sub>2</sub>CH<sub>2</sub>CH<sub>2</sub>CH<sub>2</sub>CH<sub>2</sub>-); **APCI-MS**: m/z 433.4 [M-HBr]<sup>+</sup>.

#### **Tetraethyl(4,4'-(decane-1,10-diylbis(oxy))bis(4,1-phenylene))bis(methylene)diphosphonate (5)**

Triethyl phosphite (2.4 mL, 13.61 mmol) and **4** (460 mg, 0.85 mmol) were heated in a microwave oven (maximum power 50 W, rump time 10 min, hold time 25 min at 200 °C). Once complete, triethylphosphite and ethylbromide were eliminated under vacuum at 180 °C, affording product **5** quantitatively (530 mg). **<sup>1</sup>H-NMR(400 MHz, CDCl<sub>3</sub>)**: δ = 7.30 (d, 4H, ArH, J = 8.4 Hz), 6.87 (d, 4H, ArH, J = 8.4 Hz), 4.50 (s, 4H, ArCH<sub>2</sub>PO(OEt)<sub>2</sub>), 3.94 (t, 4H, ArOCH<sub>2</sub>-, J = 6.4), 1.77 (m, 4H, ArOCH<sub>2</sub>CH<sub>2</sub>-), 1.43 (m, 4H, ArOCH<sub>2</sub>CH<sub>2</sub>CH<sub>2</sub>-), 1.32 (m, 8H, ArOCH<sub>2</sub>CH<sub>2</sub>CH<sub>2</sub>CH<sub>2</sub>-, ArOCH<sub>2</sub>CH<sub>2</sub>CH<sub>2</sub>CH<sub>2</sub>CH<sub>2</sub>-); **APCI-MS**: m/z 627.3 [M+H]<sup>+</sup>.

#### **2,2'-Bipyridine-6,6'-dicarbaldehyde (6)**

To a solution of oxalyl chloride (1.48 mL, 17.55 mmol) in CH<sub>2</sub>Cl<sub>2</sub> (10 mL) at -78° C a solution of DMSO (2.53 mL, 35.6 mmol) in CH<sub>2</sub>Cl<sub>2</sub> (10 mL) was added dropwise. The mixture was stirred for 10 min, 6,6'-bis(hydroxymethyl)-2,2'-dipyridine (500 mg, 2.31 mmol) was added and stirring was continued for an hour. Triethylamine (6.44 mL, 46.2 mmol) was then added at the same temperature. After 30 min., the mixture was warmed to 0° C, and 1/10 water/



CH<sub>2</sub>Cl<sub>2</sub> solution (15 mL) was added. The aqueous layer was extracted with DCM. The combined organic phases were washed with sat. NaHCO<sub>3</sub> solution and dried. The crude product was purified by column chromatography (SiO<sub>2</sub>, 99/1 DCM/MeOH, v/v) affording product **6** (318 mg, 65%). **<sup>1</sup>H-NMR(400 MHz, CDCl<sub>3</sub>):** δ = 10.21 (s, 2H, -COH), 8.35 (dd, 2H, ArH, J<sub>o</sub> = 7.6 Hz, J<sub>m</sub> = 1.6 Hz), 8.84 (t, 2H, ArH, J = 7.6 Hz) 7.27 (dd, 2H, ArH, J<sub>o</sub> = 7.6 Hz, J<sub>m</sub> = 1.6 Hz); **APCI-MS:** m/z 213.1 [M+H]<sup>+</sup>.

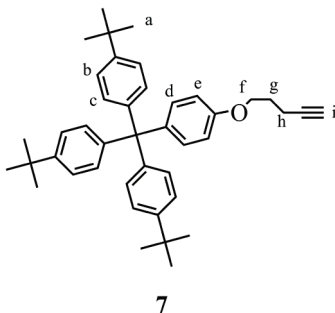
### Model macrocycle (2)

To a solution of KO<sup>t</sup>Bu (57 mg, 0.51 mmol) and 18-crown-6 (6 mg, 0.023 mmol) in dry DMF (48 mL) **5** (30 mg, 0.048) was added at room temperature. After 10 min. the mixture was cooled to 0 °C and **6** (10 mg, 0.048) was added. The mixture was stirred for 10 min at 0 °C, then warm to R.T. and stirred O.N. The solvent was concentrated and the crude was purified by column chromatography (SiO<sub>2</sub>, gradient: from 98/2 to 90/10 DCM/ ethyl acetate v/v) affording product **2** as yellow solid (4.8 mg, 19%).

**<sup>1</sup>H-NMR(400 MHz, CDCl<sub>3</sub>):** δ = 8.31 (d, 2H, H<sub>d</sub> or H<sub>e</sub>, J = 15.6 Hz), 7.76 (m, 4H, H<sub>a</sub> and H<sub>c</sub>), 7.62 (d, 4H, H<sub>f</sub> or H<sub>g</sub>, J = 8.8 Hz), 7.25 (m, 2H, H<sub>b</sub>), 7.10 (d, 2H, H<sub>d</sub> or H<sub>e</sub>, J = 15.6 Hz), 7.92 (d, 4H, H<sub>f</sub> or H<sub>g</sub>, J = 8.8 Hz), 3.89 (t, 4H, ArOCH<sub>2</sub>-, J = 6.8), 1.70 (m, 4H, ArOCH<sub>2</sub>CH<sub>2</sub>-), 1.38 (m, 4H, ArOCH<sub>2</sub>CH<sub>2</sub>CH<sub>2</sub>-), 1.29 (m, 8H, ArOCH<sub>2</sub>CH<sub>2</sub>CH<sub>2</sub>CH<sub>2</sub>-); **APCI-MS:** m/z 531.3 [M+H]<sup>+</sup>.

### Alkyne stopper (7)

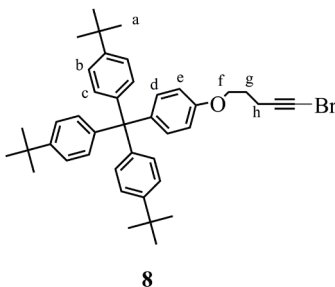
To a solution of 4-pentyn-1-ol (1g, 1.32 mmol) in dry THF (24 mL) at 0 °C 4-[tris-(4-tert-butylphenyl)methyl]phenol (1 g, 1.98 mmol) and PPh<sub>3</sub> (519mg, 1.98 mmol) were added under N<sub>2</sub>. Then DIAD (390 μL, 1.98 mmol) was added and the mixture was stirred at R.T. over night. The solvent was concentrated and the crude was purified by column chromatography (SiO<sub>2</sub>, petrol ether/DCM 7/3 v/v) affording product **7** as white solid (376 mg, 50%).



$^1\text{H-NMR}$ (400 MHz,  $\text{CDCl}_3$ ):  $\delta$  = 7.25 (d, 6H,  $\text{ArH}_b$ ,  $J$  = 8.4 Hz), 7.10 (d, 8H,  $\text{ArH}_c$  +  $\text{ArH}_d$ ,  $J$  = 8.8 Hz), 6.79 (d, 2H,  $\text{ArH}_e$ ,  $J$  = 8.8 Hz), 4.06 (t, 2H,  $H_f$ ,  $J$  = 6.0 Hz), 2.42 (td, 2H,  $H_h$ ,  $J_1$  = 7.0 Hz,  $J_2$  = 2.7 Hz), 2.01 (m, 2H,  $H_g$ ), 1.98 (t, 1H,  $H_i$ ,  $J$  = 2.8 Hz), 1.32 (s, 27H,  $H_a$ ); **APCI-MS**:  $m/z$  571.4  $[\text{M}+\text{H}]^+$ .

### Bromoalkyne stopper (8)

To a suspension of **6** (50 mg, 0.088 mmol) and NBS (17 mg, 0.096 mmol) in acetone (0.4 mL)  $\text{AgNO}_3$  (1.23 mg, 1.98 mmol) and  $\text{PPh}_3$  (519mg, 1.98 mmol) were added. The mixture was stirred at R.T. for 1h, then diluted with petrol ether and washed with water. The separated aqueous layer was extracted with diethyl ether and petrol ether. The combined organic phases were then concentrated affording product **8** as white solid.



$^1\text{H-NMR}$ (400 MHz,  $\text{CDCl}_3$ ):  $\delta$  = 7.14 (d, 6H,  $\text{ArH}_b$ ,  $J$  = 8.8 Hz), 6.99 (d, 8H,  $\text{ArH}_c$  +  $\text{ArH}_d$ ,  $J$  = 8.4 Hz), 6.67 (d, 2H,  $\text{ArH}_e$ ,  $J$  = 8.8 Hz), 3.92 (t, 2H,  $H_f$ ,  $J$  = 6.0 Hz), 2.33 (t, 2H,  $H_h$ ,  $J$  = 7.1 Hz), 1.89 (m, 2H,  $H_g$ ), 1.21 (s, 27H,  $H_a$ ) **APCI-MS**:  $m/z$  650.1  $[\text{M}+\text{H}]^+$ .

**Model [2]rotaxane (9) via Cadiot-Chodkiewicz active template reaction**

A solution of acetylene (**1**) (12.7 mg, 0.02 mmol) in THF (258  $\mu$ L) was cooled to  $-78^{\circ}$  C and nBuLi (13  $\mu$ L, 0.02 mmol, 0.1M in THF) was added. The resulting solution was allowed to warm to  $0^{\circ}$  C over 15 min. CuI was added (3.9 mg, 0.02 mmol), and the resulting yellow solution was allowed to warm to R.T. over 15 min. The reaction mixture was returned to  $-78^{\circ}$  C and a solution of the macrocycle **2** (10.9 mg, 0.02 mmol) and the brominated stopper **8** (13.3 mg, 0.02 mmol) in THF (386  $\mu$ L) was added. The resulting orange solution was allowed to stir at R.T. over night. The reaction was quenched by addition of a 17.5%  $\text{NH}_3(\text{aq})$  saturated with EDTA, and extracted with DCM.

**APCI-MS:**  $m/z$  1705.2  $[\text{M}+\text{H}]^+$ .

**Model [2]rotaxane (10) via Nickel-Copper-mediated alkyne homocoupling**

A solution of acetylene **7** (18.26 mg, 0.03 mmol) in THF (200  $\mu$ L) was cooled to  $-78^{\circ}$  C, and nBuLi (19  $\mu$ L, 0.02 mmol, 0.1 M in THF) was added. The resulting solution was allowed to warm to  $0^{\circ}$  C over 30 min. The reaction mixture was returned to  $-78^{\circ}$  C and a solution of macrocycle **2**  $\text{NiCl}_2\text{DME}$  (prepared by dissolving an equimolar quantity of macrocycle **2** [4.3 mg, 0.008 mmol) and  $\text{NiCl}_2\text{DME}$  (1.78 mg, 0.008 mmol) in THF (1 mL) at  $80^{\circ}$  C] was added. Then the reaction mixture was warmed to R.T. and after 5 min. CuI (3.04 mg, 0.016 mmol) was added, and the resulting yellow solution was allowed to warm to R.T. over 15 min. The resulting mixture was stirred at  $80^{\circ}\text{C}$  for 48h. The reaction was quenched by addition of a 17.5%  $\text{NH}_3(\text{aq})$  saturated with EDTA, and extracted with DCM. The crude was purified by column chromatography ( $\text{SiO}_2$ , 70/25/5 DCM/petrol ether/ ACN v/v/v) affording [2]rotaxane **10** as yellow solid that decomposed straight away. **APCI-MS:**  $m/z$  1670.9  $[\text{M}+\text{H}]^+$ .

**Model [2]rotaxane (10) via Palladium active metal template reaction**

To a solution of the macrocycle **2** (0.34 mg, 0.65  $\mu$ mol) in DCM (50  $\mu$ L) a solution of  $\text{PdCl}(\text{ACN})_2$  (0.16 mg, 0.650  $\mu$ mol l) was added. The mixture was allowed to stir at RT under  $\text{N}_2$  for 2.5h. The solvent was removed under

vacuum and the obtained palladium macrocycle complex was used in the next part of the reaction.

To a solution of the terminal alkyne **7** (223.3 mg, 0.39 mmol) in anhydrous benzene (2 mL) diisopropylamine (19.2  $\mu$ L, 0.14 mmol), copper iodide (4.6 mg, 0.024  $\mu$ mol), macrocycle **2** (6.5 mg, 0.123  $\mu$ mol) and iodine (1.7 mg, 6.54  $\mu$ mol) were added sequentially. The palladium macrocycle complex (0.65  $\mu$ mol) in anhydrous benzene (1 mL) was slowly added over a period of 12 h using a syringe pump. When addition was complete the reaction mixture was allowed to stir for a further 72 h at room temperature after which time the crude was taken into a partition of DCM and sat. Na<sub>4</sub>EDTA solution and stirred for 1 h. The layers were separated and the aqueous phase extracted with DCM. The combined organic phase was then washed with brine, dried with MgSO<sub>4</sub>, filtered and concentrated under reduced pressure. **APCI-MS**: *m/z* 1670.3 [M+H]<sup>+</sup>.

### **1,3-dibromo-2-(bromomethyl)benzene (11)**

To a solution of 2,6-dibromotoluene (700 mg, 2.8 mmol) in CCl<sub>4</sub> (5 mL), NBS (548 mg, 3.08 mmol) and a catalytic amount of Bz<sub>2</sub>O were added and the mixture was stirred at reflux for 3 h. Then it was washed with water and the organic phase was dried under vacuum. The crude was purified by column chromatography (SiO<sub>2</sub>, petrol ether) affording product **11** in quantitative yield (912 mg). **<sup>1</sup>H-NMR(400 MHz, CDCl<sub>3</sub>)**:  $\delta$  = 7.55 (d, 2H, ArH, J = 8.1 Hz), 7.01 (t, 1H, ArH, J = 8.1 Hz), 4.50 (s, 2H, ArCH<sub>2</sub>Br); **ESI-MS**: *m/z* 365.3 [M+K]<sup>+</sup>.

### **1,3-dibromo-2-(ethoxymethyl)benzene (12)**

To a solution of **11** (837 mg, 2.57 mmol) in EtOH (10 ml), KOH (144 mg, 2.57 mmol) was added. The resulting solution was stirred O.N at R.T. The reaction mixture was poured into an equal volume of brine and extracted with diethyl ether. The organic phase was dried under vacuum giving product **12** as a colourless oil in quantitative yield (752 mg). **<sup>1</sup>H-NMR(400 MHz, CDCl<sub>3</sub>)**:  $\delta$  = 7.54 (d, 2H, ArH, J = 8.0 Hz), 7.00 (t, 1H, ArH, J = 8.0 Hz), 4.79 (s, 2H, ArCH<sub>2</sub>O), 3.63 (q, 2H, OCH<sub>2</sub>CH<sub>3</sub>, J = 6.8 Hz), 1.26 (t, 3H, OCH<sub>2</sub>CH<sub>3</sub>, J = 6.8 Hz); **APCI-MS**: *m/z* 292.9 [M+H]<sup>+</sup>.

**5-(3-bromo-2-(ethoxymethyl)phenyl)pent-4-yn-1-ol (13)**

To a degassed solution of **12** (100 mg, 0.34 mmol) in toluene (3 mL) and Et<sub>3</sub>N (2 mL), Pd(dppf)Cl<sub>2</sub> (14 mg, 0.017 mmol), and CuI (6.5 mg, 0.034 mmol) were added. Directly after the solution turned black 5-pentyn-1-ol (23 mg, 0.27 mmol) was added and the mixture was stirred at reflux O.N.. The solvent was then concentrated and the crude was purified by column chromatography (SiO<sub>2</sub>, 98/2 DCM/MeOH, v/v) affording product **13** (57 mg, 71%). <sup>1</sup>H-NMR(400 MHz, CDCl<sub>3</sub>): δ = 7.50 (d, 1H, ArH, J = 8.0 Hz), 7.37 (d, 1H, ArH, J = 8.0 Hz), 7.08 (t, 1H, ArH, J = 8.0 Hz), 4.78 (s, 2H, ArCH<sub>2</sub>O), 3.83 (t, 2H, -CH<sub>2</sub>OH, J = 6.0 Hz), 3.59 (q, 2H, OCH<sub>2</sub>CH<sub>3</sub>, J = 6.8 Hz), 2.60 (t, 2H, C≡CCH<sub>2</sub>-, J = 7.2 Hz), 1.88 (m, 2H, C≡CCH<sub>2</sub>CH<sub>2</sub>-), 1.24 (t, 3H, OCH<sub>2</sub>CH<sub>3</sub>, J = 6.8 Hz); ESI-MS: m/z 283.2 [M-CH<sub>3</sub>+H]<sup>+</sup>.

**1-bromo-3-(5-bromopent-1-ynyl)-2-(ethoxymethyl)benzene (14)**

To a solution of **13** (171 mg, 0.57 mmol) in dry DCM (0.9 mL) at 0 °C, Et<sub>3</sub>N (160 μL, 1.15 mmol) and MsCl (66 μL, 0.86 mmol), were added. After being stirred at room temperature for 4h, a saturated solution of NH<sub>4</sub>Cl was added. The reaction mixture was extracted with DCM and the organic layer was evaporated.

To a solution of the resulting mesylate in acetone (18 mL), LiBr (490 mg, 5.7 mmol) was added. The mixture was stirred at reflux for 2 h, and then a saturated solution of NaHCO<sub>3</sub> was added. The reaction mixture was extracted with DCM and the organic layer was evaporated to afford **14** as a brown oil in quantitative yield (203 mg). <sup>1</sup>H-NMR(400 MHz, CDCl<sub>3</sub>): δ = 7.52 (d, 1H, ArH, J = 8.0 Hz), 7.36 (d, 1H, ArH, J = 8.0 Hz), 7.08 (t, 1H, ArH, J = 8.0 Hz), 4.76 (s, 2H, ArCH<sub>2</sub>O), 3.61 (m, 4H, OCH<sub>2</sub>CH<sub>3</sub>, -CH<sub>2</sub>Br), 2.66 (t, 2H, C≡CCH<sub>2</sub>-, J = 6.9 Hz), 2.15 (m, 2H, C≡CCH<sub>2</sub>CH<sub>2</sub>-), 1.25 (t, 3H, OCH<sub>2</sub>CH<sub>3</sub>, J = 6.8 Hz); ESI-MS: m/z 383.0 [M+Na]<sup>+</sup>.

**1,10-bis(3-bromo-2-(ethoxymethyl)phenyl)deca-1,9-diyne (15)**

To a solution of 2,2':6'2''-terpyridine (3.5mg, 0.15 mmol) and NiCl<sub>2</sub>6H<sub>2</sub>O (3.6 mg, 0.015 mmol) in DMF (600 μL) under N<sub>2</sub>, activated Zn (19.6 mg, 0.30 mmol) was added followed by the addition of **14** (110 mg, 0.30 mmol). The

suspension was stirred at room temperature for 4 h. The reaction mixture was diluted with EtOAc, extracted with 17.5%  $\text{NH}_{3(\text{aq})}$  solution saturated with EDTA, 1M HCl solution,  $\text{H}_2\text{O}$ , and brine. The organic layer was dried with  $\text{MgSO}_4$  and the solvent removed under pressure to give the homocoupled product **15** as brown oil in quantitative yield (168 mg).  $\delta = 7.48$  (d, 2H, ArH,  $J = 7.6$  Hz), 7.35 (d, 2H, ArH,  $J = 7.6$  Hz), 7.06 (t, 2H, ArH,  $J = 7.6$  Hz), 4.77 (s, 4H, ArCH<sub>2</sub>O), 3.60 (t, 4H, OCH<sub>2</sub>CH<sub>3</sub>,  $J = 7.2$  Hz), 2.47 (t, 4H, C≡CCH<sub>2</sub>-,  $J = 6.8$  Hz), 1.65 (m, 4H, C≡CCH<sub>2</sub>CH<sub>2</sub>-), 1.61 (m, 4H, C≡CCH<sub>2</sub>CH<sub>2</sub>CH<sub>2</sub>), 1.24 (t, 3H, OCH<sub>2</sub>CH<sub>3</sub>,  $J = 7.2$  Hz); **APCI-MS**:  $m/z$  561.1 [M+H]<sup>+</sup>.

---

## 6.9 References

- <sup>1</sup> J.-C. Olsen, K.E. Griffiths, J.F. Stoddart, *From Non-Covalent Assemblies to Molecular Machines*, (Ed. J-P Sauvage and P. Gaspard), W. VCH, Weinheim, **2001**, Chapter 8.
- <sup>2</sup> J.A. Wisner, B.A. Blight, *Modern Supramolecular Chemistry*, (Eds. F. Diederich, P.J. Stang, R.R. Tykwinski), Wiley VCH, **2008**, Weinheim, Chapter 10.
- <sup>3</sup> E. Wasserman, *J. Am. Chem. Soc.* **1960**, *82*, 4433.
- <sup>4</sup> I.T. Harrison, S. Harrison. *J. Am. Chem. Soc.* **1967**, *89*, 5723.
- <sup>5</sup> C.O. Dietrich-Buchecker, J.P. Sauvage. *Tetrahedron Lett.* **1983**, *24*, 5095.
- <sup>6</sup> (a) B.L. Allwood, N.Spencer, H. Shahriari-Zavareh, J.F. Stoddart, D.J. Williams. *J. Chem. Soc., Chem. Commun.* **1987**, 1061; (b) P.R. Ashton, A.M.Z. Slawin, N. Spencer, J.F. Stoddart, D.J. Williams. *J. Chem. Soc., Chem. Commun.* **1987**, 1066.
- <sup>7</sup> *Molecular Catenanes, Rotaxanes and Knots*, (Ed. J-P Sauvage and C.O. Dietrich-Buchecker) Wiley-VCH, Weinheim, **1999**.
- <sup>8</sup> J.CD. Crowley, S.M. Goldup, A.-L. Lee, D.A. Leigh, *Chem. Soc. Rev.* **2009**, *38*, 1530.
- <sup>9</sup> V. Aucagne, K.D. Hänni, D.A. Leigh, P.J. Lusby, D. B. Walker, *J. Am. Chem. Soc.* **2006**, *128*, 2186.
- <sup>10</sup> R. Wolovsky, *J. Am. Chem. Soc.*, **1970**, *92*, 2132; D.A. Ben-Efraim, C. Batich, E. J. Wasserman, *J. Am. Chem. Soc.* **1970**, *92*, 2133.
- <sup>11</sup> D.B Amabilinio, J.F Stoddart, *Chem. Rev.* **1995**, *95*, 2725.
- <sup>12</sup> J. Bernà, S.M. Goldup, A.-L Lee, D.A. Leigh, M.D. Symes, G. Teobaldi, F. Zerbetto, *Angew. Chem. Int. Ed.* **2008**, *47*, 4392.
- <sup>13</sup> M. Schappacher, A. Deffieux, *Angew. Chem. Int. Ed.* **2009**, *48*, 5930.
- <sup>14</sup> S.M. Goldup, D.A. Leigh, P.R. McGonigal, V.E. Ronaldson, A.M.Z. Slawin, *J. Am. Chem. Soc.* **2010**, *132*, 315.

<sup>15</sup> J.D. Crowley, S.M. Goldup, N.D. Gowans, D.A. Leigh, V.E. Ronaldson, A.M.Z. Slawin, *J. Am. Chem. Soc.* **2010**, 132, 6243.

<sup>16</sup> J. Bernà, J.D. Crowley, S.M. Goldup, K.D. Hänni, A.-L. Lee, D.A. Leigh, *Angew. Chem. Int. Ed.* **2007**, 46, 5709.

<sup>17</sup> S.M. Goldup, D.A. Leigh, R.T. McBurney, P.R. McGonigal, A. Plant, *Chem. Sci.* **2010**, 1, 383.



# Appendix A

## Materials and Methods

### *A.1 Materials*

All reagents and chemicals were obtained from commercial sources and used without further purification. Dry pyridine was distilled from KOH before use or purchased from Aldrich and used as received (Pyridine absolute, over molecular sieves,  $\text{H}_2\text{O} \leq 0.005\%$ ). Dry DMF (DMF purissim.  $\geq 99.5\%$ (GC), over molecular sieves) was provided by Aldrich and used as received. Silica column chromatography was performed using silica gel 60 (Fluka 230-400 mesh ASTM), or silica gel 60 (MERCK 70-230 mesh).

### *A.2 Methods*

#### **NMR Measurements**

(Ch. 2-3-4-5-6):  $^1\text{H}$  NMR spectra were obtained using a Bruker AC-300 (300 MHz), a Bruker AVANCE 300 (300 MHz), a Bruker AVANCE 400 (400 MHz) or a VARIAN INOVA 600 (600 MHz) spectrometer. All chemical shifts ( $\delta$ ) were reported in ppm relative to the proton resonances resulting from incomplete deuteration of the NMR solvents.  $^{31}\text{P}$  NMR spectra were obtained using a Bruker AMX-400 (162 MHz) or a Bruker AVANCE 400 (162 MHz) spectrometer. All chemical shifts ( $\delta$ ) were recorded in ppm relative to external 85%  $\text{H}_3\text{PO}_4$  at 0.00 ppm.

### **MS studies**

(*Ch. 2-3-4-5*): Electrospray ionization ESI-MS experiments were performed on a Waters ZMD spectrometer equipped with an electrospray interface. Exact masses were determined using a LTQ ORBITRAP XL Thermo spectrometer equipped with an electrospray interface. GC-MS analysis were performed using a (Hewlett Packard) HP 6890/5973 GC/MSD system.

(*Ch. 6*): ESI mass spectrometry was performed with a Micromass Platform II mass spectrometer.

### **Fluorescence Measurements.**

All fluorescent experiments were performed on a LS 55 Perkin-Elmer spectrofluorimeter.

# Appendix B

## X-Ray Data Analysis

### *B.1 X-Ray Crystallographic Studies of (±)-(AB)2PO<sub>ii</sub>1PS<sub>i</sub>Me[C<sub>2</sub>H<sub>5</sub>, H, Ph]•(±)-2-butanol complex.*

The crystal structure of (±)-(AB)2PO<sub>ii</sub>1PS<sub>i</sub>Me[C<sub>2</sub>H<sub>5</sub>, H, Ph]+2H<sub>2</sub>O+3C<sub>4</sub>H<sub>10</sub>O was determined by single crystal X-ray diffraction methods. Crystallographic and experimental details for the structures are summarized in Table 1. Intensity data and cell parameters were collected at the temperature of 100 K using *flash cooling* method. The structures was solved using the Denzo-SMN (Otwinowski et al., 1997) and SCALEPACK (Otwinowski et al., 1997) programs and refined using SHELXS (Sheldrick 1990) and SHELXS-97 (Sheldrick et al., 1997) programs and the SQUEEZE function of PLATON program (Spek 2003).

*Table 1. Crystallographic data and refinement details:*

Compound	(±)- (AB)2PO <sub>ii</sub> 1PS <sub>i</sub> Me[C <sub>2</sub> H <sub>5</sub> , CH <sub>3</sub> , Ph]+2H <sub>2</sub> O+ 3C <sub>4</sub> H <sub>10</sub> O
Formula	2C <sub>55</sub> H <sub>50</sub> O <sub>10</sub> P <sub>3</sub> S+2H <sub>2</sub> O+ 3C <sub>4</sub> H <sub>10</sub> O
Formula weight	4467.29
Temperature/K	100
Wavelength/ Å	1.54
Crystal system	monoclinic
Space group	P2 <sub>1/n</sub>
<i>a</i> /Å	24.15 (14)
<i>b</i> /Å	15.84(23)
<i>c</i> /Å	31.39(17)

$\alpha/^\circ$	85.98(15)
$\beta/^\circ$	96.99(19)
$V/\text{\AA}^3$	11926.6
$Z$	2
$D_c/\text{g cm}^{-3}$	1.244
$F(000)$	4698
Cube/ $\text{mm}^3$	0.2×0.2×0.1
$\mu/\text{mm}^{-1}$	1.738
Resolutions/ $\text{\AA}$	23.97-1.10
$I/\sigma(I)$ ( all data)	25.5
$I/\sigma(I)$ max resolution	3.3
Observed reflections	23805
Unique reflections	9333
Completeness (all data)	90.4%
Completeness (max resolution)	41.2%
Data/restr./param.	9333 / 24 / 1342
$R[I>2.0 \sigma(I)]$	0.0897
$R$ (all data)	0.0970
$wR2[I>2.0 \sigma(I)]$	0.2929
<i>Goodness of fit</i>	1.411

## ***B.2 X-Ray Crystallographic Studies of ( $\pm$ )-(AB)2PO<sub>ii</sub>1PS<sub>i</sub>Me[C<sub>2</sub>H<sub>5</sub>, CH<sub>3</sub>, Ph]***

The crystal structure of ( $\pm$ )-(AB)2PO<sub>ii</sub>1PS<sub>i</sub>Me[C<sub>2</sub>H<sub>5</sub>, CH<sub>3</sub>, Ph]+3H<sub>2</sub>O+2C<sub>2</sub>F<sub>3</sub>H<sub>3</sub>O was determined by single crystal X-ray diffraction methods. Crystallographic and experimental details for the structures are summarized in Table 2. Intensity data and cell parameters were collected at the temperature of 100 K under nitrogen. The collection of the diffraction data

required the use of a highly brilliant radiation source of the sincrotron of the Elettra laboratory in Trieste (diffraction line XRD1).

The structure was solved using the MOSFLM and SCALA programs belonging to CCP4 pack (CCP4, 1994, Leslie 1999) and refined using the SQUEEZE function of PLATON program ( Spek 2003).

**Table 2.** Crystallographic data and refinement details:

Compound	(±)- (AB) <sub>2</sub> PO <sub>ii</sub> 1PS <sub>i</sub> Me[C <sub>2</sub> H <sub>5</sub> , CH <sub>3</sub> , Ph]+3H <sub>2</sub> O+ 2C <sub>2</sub> F <sub>3</sub> H <sub>3</sub> O
Formula	C <sub>59</sub> H <sub>58</sub> O <sub>10</sub> P <sub>3</sub> S+3H <sub>2</sub> O+ 2C <sub>2</sub> F <sub>3</sub> H <sub>3</sub> O
Formula weight	2498.16
Temperature/K	100
Wavelength/ Å	1.0
Crystal system	tricline
Space group	<i>P</i> -1
<i>a</i> /Å	13.35(26)
<i>b</i> /Å	15.37(43)
<i>c</i> /Å	16.38(42)
<i>a</i> /°	85.98(15)
<i>β</i> /°	89.63(14)
<i>γ</i> /°	69.81(15)
<i>V</i> /Å <sup>3</sup>	3141.04
<i>Z</i>	2
<i>D<sub>c</sub></i> /g cm <sup>-3</sup>	1.321
<i>F</i> (000)	1302.0
Cube/mm <sup>3</sup>	0.05×0.1×0.1
<i>μ</i> /mm <sup>-1</sup>	0.47
Resolutions/ Å	0.92-16.34

---

I/ $\sigma$ (I) ( all data)	11.1
I/ $\sigma$ (I) max resolution	2.1
Observed reflections	16324
Unique reflections	6076
Completeness (all data)	72.5%
Completeness (max resolution)	15.9%
Data/restr./param.	6053 / 81 / 680
$R$ [ $I > 2.0 \sigma(I)$ ]	0.1538
$R$ (all data)	0.1669
$wR_2$ [ $I > 2.0 \sigma(I)$ ]	0.4516
<i>Goodness of fit</i>	2.070

---

## *Curriculum Vitae*

- 01/1983 Born in Parma, Italy.
- 07/2002 High School Diploma, Liceo Scientifico “G. Ulivi”,  
Parma Italy
- 09/2005 Bachelor in Chemistry, University of Parma, Italy.  
Referents: Prof. R. Marchelli and Prof. S. Sforza.
- 09/2007 Master in Chemistry, University of Parma, Italy.  
Referent: Prof. R. Marchelli and Prof. S. Sforza.
- 10/2007-12/2007 Post-Graduate Research, University of Parma, Italy.  
Advisor: Prof. R. Marchelli.
- 01/2008-12/2010 Doctoral Research with Prof. E Dalcanale  
University of Parma, Italy.
- 01/2008-12/2010 Research Exchange with Prof. D. A. Leigh  
University of Edinburgh, UK.

Parma, January 2011

Francesca Maffei